# IMPROVING GAS FLOODING EFFICIENCY

DOE CONTRACT NO. DE-FG26-04NT15532

New Mexico Petroleum Recovery Research Center
New Mexico Institute of Mining and Technology
801 Leroy Place
Socorro, NM 87801
(505) 835-5142

| | |
|---|---|
| Report Date: | May 1, 2006 |
| Contract Date: | April 1, 2005 |
| Completion Date: | September 30, 2007 |
| DOE Total Award: | $330,939 |
| Program Manager: | Reid B. Grigg |
| Principal Investigator: | Reid B. Grigg |
| Other Major Contributors: | Robert K. Svec |
| | Zheng Wen Zeng |
| | Baiojun Bai |
| | Yi Liu |
| | Alexander Mikhalin |
| | Guoqiang Yin |
| Contracting Officer's Representative: | Dan Ferguson |
| Reporting Period: | April 1, 2005–March 31, 2006 |

**DISCLAIMER**

This report was prepared as an account of work sponsored by an agency of the United States Government. Neither the United States Government nor any agency thereof, nor any of their employees, makes any warranty, express or implied, or assumes any legal liability or responsibility for the accuracy, completeness, or usefulness of any information, apparatus, product, or process disclosed, or represents that its use would not infringe privately owned rights. Reference herein to any specific commercial product, process, or service by trade name, trademark, manufacturer, or otherwise does not necessarily constitute or imply its endorsement, recommendation, or favoring by the United States Government or any agency thereof. The views and opinions of authors expressed herein do not necessarily state or reflect those of the United States Government or any agency thereof.

## ABSTRACT

This document presents the first year results from the project, "Improved Gas Flooding Efficiency," Department of Energy Contract No. DE-FC26-04NT15532. This study focuses on laboratory studies with related analytical and numerical models as well as work with operators for field tests to enhance our understanding of and capabilities for more efficient enhanced oil recovery (EOR).

Results presented in Chapter 1 determine plume size of the gas with injecting carbon dioxide into a brine saturation core and then brine injected into gas saturated or partially saturated core. The level of $CO_2$ saturation in the injected brine at reservoir pressure and temperature was varied from zero to over 90 % at two temperatures. These are used to determine the effect on the $CO_2$ saturation or plume size in the core during brine flow.

Chapter 2 reports surfactant adsorption/desorption kinetics and equilibrium onto Berea sandstone. Also, foam stability of the surfactant is compared before and after adsorption/desortion has occurred. Results show that surfactant adsorption and desorption in Berea sandstone took several days to reach equilibrium. Both are characterized by a short period of rapid adsorption/desorption followed by a longer period of slower adsorption/desorption. Both processes were best fit by a pseudo-second-order model. A method to predict equilibrium adsorption density using adsorption process data over a relative short period is proposed, which will save considerable in completing adsorption isotherms.

Chapter 3 gives some insight delivering surfactant as a higher concentration in a smaller volume versus a lower concentration at a higher volume. Indications are that the total available surfactant is more significant than the concentration in determining adsorption. This is a different approach then previously report and has significant ramification on reservoir predictions. Also the significance of adsorption into none-flow areas is demonstrated.

Chapter 4 describes the determination of gas mobility changes as a result of foam behavior and adsorption, in Indiana limestone at various surfactant concentrations, flow rates and foam quality. At a constant gas flow rate, gas mobility slightly decreases with increasing foam quality when below the critical foam quality ($f_g$*) and increases with increasing foam quality above $f_g$*. Increased surfactant concentration leads to the decrease of gas mobility. Comparing coinjected surfactant and gas (CSG) with coinjected water and gas (CWG) shows that the mobility of CSG is an order of magnitude lower than that of CWG.

Various studies have been carried out on surfactant adsorption to the rock and the flooding in CSG mode without the presence of an oil phase. Chapter 5 examines the effect of the presence of oil on two surfactants during the determination of unknown surfactant concentrations. This work demonstration that the concentrations can be determined if the proper care is taken for the light oils tested.

**TABLE OF CONTENTS**

DISCLAIMER ..... ii

ABSTRACT ..... iii

TABLE OF CONTENTS ..... iv

LIST OF TABLES ..... v

LIST OF FIGURES ..... vi

INTRODUCTION ..... 1

EXECUTIVE SUMMARY ..... 12

EXPERIMENTAL, RESULTS AND DISCUSSION ..... 14

Chapter 1: $CO_2$ Saturations and Transport Mechanisms in Sandstone ..... 14

Chapter 2. Adsorption and Desorption of a $CO_2$-Foam-Forming Surfactant onto Berea Sandstone ..... 26

Chapter 3. Study on Adsorption of Anionic Surfactant CD1045 ..... 41

Chapter 4. Foam Mobility and Adsorption in Carbonate Core ..... 45

Chapter 5: Partitioning of Surfactant in Oil and Aqueous phase ..... 59

CONCLUSIONS ..... 65

ACKNOWLEDGMENTS ..... 67

REFERENCES ..... 67

## LIST OF TABLES

Table 1. Frio Core Parameters .....20

Table 2. Frio Synthetic Brine Composition .....20

Table 3. Properties of Core Samples Used in This Study .....32

Table 4. Experimental Schedule of CD Adsorption and Desorption onto Berea Sandstone .....33

Table 5. Results of Modeling CD Adsorption Kinetics onto Sandstone Using a Pseudo-Second-Order Equation .....34

Table 6. Fitting Equations and R2 Using Pseudo-Second-Order Desorption Model .....34

Table 7. IFT and Foam Stability after Circulating through the Core .....34

Table 8. The Properties of Indiana Limestone .....52

Table 9. The Experimental Sequence for Adsorption and Desorption .....53

Table 10. The Core Experiment Strategy for fg* Determination .....53

Table 11. The Core Experiment Strategy for Determining Optimum fg at Constant Gas Flow Rate .....53

**LIST OF FIGURES**

Fig. 1. Schematic of the coreflood apparatus.....21

Fig. 2. Comparison of brine production during $CO_2$ injection of two tests both in Frio Core A. In each the 4.3 cc dead volume is subtracted. The points were the volumes by weight were determined are indicated for each as TW and compare well with the values determined by direct volume with the vapor trap values included. .....21

Fig. 3. Comparison of $CO_2$ production during brine injection for two tests in Frio Core A. In each the 4.3 cc dead volume is subtracted. .....22

Fig. 4. Comparison of $CO_2$ production (cc/min) from two brines saturated to about 50% $CO_2$ and one saturated to 90% $CO_2$; each at a flow rate of 20 cc/hr and 145°F.....22

Fig. 5. Production rate of $CO_2$ during the injection of brine into Frio Core B for three different tests, each at different concentrations of $CO_2$ in the injected brine. .....23

Fig. 6. Comparison of $CO_2$ production rates during brine injection into Frio Core B during from about 1 PV to 5 PV. .....23

Fig. 7. Comparison of the $CO_2$ production rate during the injection of 50% $CO_2$–brine at two different temperatures, 100° and 145°F. .....24

Fig. 8. Comparison of total $CO_2$ production at reservoir conditions and production rate from the separator at ambient conditions for $CO_2$ during the test at 100°F.....24

Fig. 9. Comparison similar to Figure Fig. 8 except the scale for $CO_2$ production rate is expanded to include the maximum production rate during production of the $CO_2$ phase.....25

Fig. 10. Comparison of $CO_2$ production of brine into the dry Frio Core A and injection of 50% $CO_2$ -brine into the core after being saturated with dead brine and then flooded with $CO_2$. .....25

Fig. 11. Kinetics of CD adsorption onto Berea sandstone, each performed at a flow rate of 15 cm3/hr. .....35

Fig. 12. Modeling CD adsorption kinetics onto sandstone using pseudo-second-order equation. 35

Fig. 13. Pseudo-second-order kinetic rate coefficient as a function of length-normalized initial concentration of the CD solution. .....36

Fig. 14. Pseudo-second-order kinetic rate as a function of the equilibrium concentration of the CD solution. .....36

Fig. 15. CD desorption from Berea sandstone at various flow rates. .....37

Fig. 16 Modeling CD desorption using a pseudo-second-order desorption model. .....37

Fig. 17. CD concentration effect on IFT before and after circulating CD through the core.....38

Fig. 18. Adsorption effect on foam stability. .....38

Fig. 19. Foam images comparing foam stability using CD solution after and before core contact during the adsorption tests. .....39

Fig. 20. CD concentration effect on foam stability before and after adsorption. .....39

Fig. 21. Desorption effect on foam stability. .....40

Fig. 22. Foam images comparing foam stability using CD solution after and before core contact during the desorption tests. .....40

Fig. 23. CD Adsorption density vs. initial CD concentration. .....43

Fig. 24. CD adsorption density vs. amount of CD available per 1 g of powdered limestone.....43

Fig. 25. Rate of CD adsorption onto powdered limestone.....44

Fig. 26. Comparison data for powdered limestone and cubes of limestone. .....44

Fig. 27. Schematic plot of core flooding setup. .....54

Fig. 28. Two foam-flow regime.[126,127] .....54

Fig. 29. CD adsorption profile. .....55

Fig. 30. Comparison of CD adsorption and desorption profiles for 500 mg/l CD solution.....55

Fig. 31. Determination of fg* at constant ug. .....56

Fig. 32. Permeability effect on fg*. .....56

Fig. 33. The relationship between foam quality and foam mobility at 10 cm3/hr total flow rate as a function of surfactant concentration. .....57

Fig. 34. Comparison of mobility obtained for Fig. 31 at constant qt=7 and 24.75 cm3/hr with mobility in Fig. 33 at qt=10 cm3/hr at 2500 mg/l CD. .....57

Fig. 35. CWG dp/ds contours (psi/ft) vs aqueous and gas phases Darcy velocity (ft/day). .....58

Fig. 36. CSG dp/ds contours (psi/ft) vs. surfactant solution and gas phase Darcy velocity (ft/day).....58

Fig. 37. CD concentration normalized versus decane in the original system. .....62

Fig. 38. Absorption of chloroform at two wavelengths with dissolved decane.....63

Fig. 39. Normalized CD concentration with light oil in the original system. .....63

Fig. 40. CLS concentration determinations with decane in the original mixture. .....64

## INTRODUCTION

The objectives of this study are to acquire the information required for and to subsequently develop adsorption/desorption models for reservoir rock at reservoir conditions, determine economic sweep efficiency/injectivity criteria for reservoir scale systems, expand foam gas flooding to shallow reservoirs, and develop models and modules for simulating $CO_2$ flooding mechanisms. This work will devote considerable energy to laboratory measurements to determine practical information for designing gas foam systems for a wide range of reservoir types; thus, through cost-effective and environmentally attractive means, adding to recoverable oil reserves in the US.

The sorption task comprises continuing laboratory work in determining adsorption/desorption isotherms for a number of pure minerals and several reservoir rocks, with additional tests under reservoir conditions for selected systems. An approach is under development to optimize foaming agent systems. Large-core tests are in progress to determine the dependent parameters of sweep efficiency, injectivity changes due to foam and injection fluid–rock interactions, and oil recovery. The pressure dependencies, below and above the minimum miscibility pressure (MMP), of gas-foam improved oil recovery parameters are being measured to determine the applicability to reservoirs that must be operated below the MMP. Finally, mechanistic models are being developed for sorption and efficiency and tested using DOE's and commercial reservoir simulators. Most of the numerical work will be related to testing models using existing programs with minimal new code development.

After primary and secondary oil recovery, two-thirds of the original oil in place in the US remains unrecovered, estimated to be 350 billion bbl of oil.[1] This oil is not recoverable without the application of enhanced oil recovery (EOR) technologies.[1] Among the available EOR methods, carbon dioxide ($CO_2$) flooding holds the greatest promise for additional oil recovery from light oil reservoirs in the US and will economically support carbon management goals of the US. $CO_2$ flooding is a proven EOR technology that prolongs the life of matured oilfields while managing carbon production. This is the only EOR method that has had a steady increase in project numbers and oil production over the last two decades,[2] and is economically viable in about 80% of projects to date.[3] With oil prices returning to relatively high levels and greenhouse gases a hot environmental issue, new $CO_2$ projects are being initiated and new sources of $CO_2$ are being identified each year.[4] Currently, the Permian Basin of west Texas and southeast New Mexico is the most active oil province for $CO_2$ flooding, producing over 80% of the nearly

200,000 barrels of oil per day (BOPD) of EOR in the US from $CO_2$ miscible projects. $CO_2$ full-field or pilot projects are also active in California, Colorado, Kansas, Michigan, Mississippi, Oklahoma, Utah, and Wyoming. In addition, there have been projects in Alabama, Louisiana, Montana, North Dakota, Pennsylvania, and West Virginia for at least 16 states spread across the lower 48 contiguous states, showing the viability of this process (contingent upon the availability of $CO_2$).[5] Recent projects, such as $CO_2$ from the Great Plains Coal Gasification Plant in North Dakota that is transported to Encana's Weyburn $CO_2$ flood in Saskatchewan, Canada provide an insight into the geographically wider application of $CO_2$ injection in the future.[6] It is expected that more $CO_2$ flooding projects will continue to be planned and implemented that will be economically beneficial while decreasing environmental concerns by storing greenhouse gases.[2]

The current status of $CO_2$ flooding technology is not satisfactory. Many $CO_2$ floods display poor sweep efficiency and/or inadequate injectivity; many reservoirs are not considered for $CO_2$ flooding because they are too shallow or extremely heterogeneous. Another concern that has not found widespread mention in the literature is the requirement for a minimum heterogeneity. There has been at least one case where the reservoir was relatively homogeneous with low permeability and the sweep was good—in fact, so good that the oil bank took so long to reach the production wells that the economics were poor.[5] Thus, a degree of heterogeneity is required for sufficiently early arrival of an oil bank to provide an acceptable return on investment. Many of the $CO_2$ flooding projects that have been economic failures have been the results of poorly understood sweep and displacement mechanisms, inadequate application of existing technology, and/or poor reservoir characterization. The work of this study will improve $CO_2$ efficiency by:

1. Developing adsorption/desorption models to minimize surfactant loss to the reservoir,
2. Determining foam sweep efficiency/injectivity criteria for reservoirs to maximize $CO_2$ sweep with economic benefits,
3. Verifying the validity of using foam systems for EOR in reservoirs that cannot reach the MMP, and
4. Developing models for experimentally established mechanisms and incorporating the models into related reservoir simulators.

Because of the importance of $CO_2$ flooding for EOR, the New Mexico Petroleum Recovery Research Center (PRRC), a research division of New Mexico Institute of Mining and

Technology (NMIMT), has maintained an active $CO_2$ flooding research program since the late 1970s.

**Related Internal Research:** A comprehensive review of recent accomplishments can be obtained from recent DOE Annual and Final Project Reports[5,7-13] and in over 50 publications on specific topics with the more recent work outlined below:

1. Injectivity has been a special concern for $CO_2$ projects in lower permeability reservoirs with a nominal economic injection rate. A review of injectivity outlined many of the early concerns of $CO_2$ flooding, and revealed that injectivity is one of the most significant lingering concerns.[14] Solution channels caused by dissolution in carbonate rock have been identified in laboratory tests. Also, core samples obtained from two San Andreas Permian Basin reservoirs under $CO_2$ flood show evidence of dissolution. This is a major source of increased permeability.[15-17] It has been subsequently shown that precipitation occurs downstream, resulting in decreased permeability and injectivity.[18,19] $CO_2$ residual saturation is not believed to be high enough to cause the 50% reduction in injectivity seen in the field.[5,20,21] Residual gas saturation values were determined using long-core experiments with limestone and dolomite core samples.[19] High flow rates in the near-wellbore regions represent another factor that should affect injectivity and productivity.[22-24] General equations under non-Darcy flow conditions for stress sensitivity have been developed.[22,25,26]
2. Phase behavior and multiphase flow studies have aided in understanding mechanisms of $CO_2$ flooding flow behavior and reservoir fluid/injectant interactions and their predictions.[27-29] EOR screening criteria have been proposed and revised for $CO_2$ flooding.[30-32]
3. Work comparing pressure effects from slim tube (minimum miscibility tests) and coreflood tests using reservoir fluids and rock show the similarities as well as the differences.[33] The limitations and use of the simpler slim tube tests are demonstrated.
4. Mobility control using foam has the potential for improving recovery efficiency of gas flooding and for adding recoverable oil reserves. The effects of fluid flow rate, foam quality, and surfactant concentration effects on resistance factor and foam properties are summarized in earlier work.[34,35] This laboratory has documented an interesting effect that we have referred to as selective mobility reduction, in which mobility is reduced a greater amount at higher than at lower permeabilities.[36] This is an interesting phenomenon, but is generally overwhelmed by problems related to the injectivity decrease (much higher pressure

gradients)[37] that must be addressed for foam injection. This phenomenon is not to be ignored but will come into focus only when injectivity is sufficient.[35]

5. A principal limitation of foam use is the cost of chemicals, thus use of sacrificial agents or co-surfactant systems has been proposed and tested.[37-40] This is the use of a second chemical to satisfy at least part of the adsorption requirement of the reservoir rock, which has been estimated to use over 90% of the available surfactant.[35] Co-surfactant systems have been tested, which use lower-cost chemicals to reduce the amount of foaming agent required to satisfy adsorption. This system also has a synergistic effect that reduces the amount of foaming agent required in solution in order to develop a stable foam.[35] Our current work is quantifying the effects of surfactant concentration (of both co-surfactants), brine salinity, brine pH, rock mineralogy, temperature, surfactant diffusion, and adsorption mechanism on chemical requirements for a stable foam.[5,41-45] Similar effects are also being studied for their influence on foam stability.[5,46,47]
6. There has been an ongoing effort to incorporate findings in the laboratory into reservoir simulators using history matching of field foam tests[48-52] to verify the mechanistic algorithm results[53,54] obtained using a modified version of the DOE pseudo-miscible reservoir simulator, MASTER. Several other field-related projects have investigated possible enhancements in present or future $CO_2$ field tests.[20,21,55] Finally, general reservoir simulation models have been considered using fuzzy logic and similar methods to converge on solutions.[56,57]

In summary, our section at PRRC has been involved in research on every major aspect of $CO_2$ flooding for EOR. The research has not only greatly improved our understanding of the complex process of $CO_2$ flooding, but also identified problems and enhanced our capabilities in experimental and numerical simulation for further investigation.

**Related External Research:** William Rossen's research group at University of Texas at Austin has conducted research on the generation, simulation, and application of foams for different purposes. They have focused on the fundamentals of the physical and chemical aspects of foams.[58,59] They are developing models and a numerical simulator to predict the complex process of foam transportation in porous media.[59-65] Compared to PRRC's focused research on developing $CO_2$ flooding technology for enhanced oil recovery, Rossen has studied general foams, for general purposes.[66-68] George Hirasaki's research team at Rice University has been

studying foam and wettability for a number of years. In recent years they have considered low pressure foams,[69-71] specifically for aquifer remediation.[72,73] In their EOR-related research, they are seeking surfactants to seal fractures.[71] In a related field, Robert M. Enick at University of Pittsburgh has been developing direct thickeners for $CO_2$.[74] However, there is still a long way to go before this technology can be used for hydrocarbon EOR, due to the high cost and volumes required for the identified additives.

**Field Trials:** There have been a number of field trials that indicate that $CO_2$ foam research has significant potential. In most cases, it was observed that gas production decreased, oil production increased, and injectivity decreased. Even though they were relatively small scale pilots, the economics on several of the trials were favorable.

***Pennzoil's Rock Creek Trial (1984-85).*** The US DOE, PRRC, and Pennzoil conducted a joint $CO_2$ foam field trial at Rock Creek, Roane County, West Virginia.[75] This was a trial on two 10-acre five-spots that had an average WAG (water alternating with gas injection) ratio of 1:1, using the surfactant Alipal CD128 both in SAG (surfactant solution alternating with gas injection) and preflush slug. No indication of an oil bank was found. Injectivity reduction was noted both during the preflush slug and the foam test.

***Chevron's Rangely Weber Sand Unit Trials (1988-1990).*** A foam field trial was conducted in the Rangely Weber Sand Unit, in northwestern Colorado.[76] The $CO_2$ flood was started at a 1:1 WAG ratio in October 1986. The major concern was early $CO_2$ breakthrough caused by thief zones between injectors and producers. The foam project began in April 1989. The treatment included a 12,000 bbl surfactant slug followed by 55,000 bbl of 79% quality foam. This was not a SAG test, but co-injection of surfactant solution and gas. Chaser™ CD1040 was used, with an average surfactant concentration in the injected brine of about 0.46 weight percent (wt %). Foam was placed in the reservoir in spite of a large hydraulic fracture in the injector. Performance improved in at least one offset producer, and the foam lowered $CO_2$ injectivity for two months during the $CO_2$ chase period. The test was a success because the foam treatment paid out in about two months.

***Chevron's North Ward-Estes Trial (1990-91).*** The second Chevron $CO_2$ foam field trial was in the North Ward-Estes field in Ward and Winkler Counties in west Texas.[77] The original $CO_2$ flood was initiated in 1989 with a project area of 3,840 acres and WAG ratio of 1:1. Over about two years, foam was injected into an injector using a four-cycle SAG process, followed by

continuous $CO_2$ injection after each. Chaser™ CD1040 was used as the surfactant. During the SAG cycles, $CO_2$ injectivity reduction by 40% to 85% was an indication of foam formation. Foam apparently diverted $CO_2$ from the thief zone regions, as indicated by a sharp decline in $CO_2$ production from the problematic producer and increased oil production at other offset producers. The most significant economic incentive was the reduction in $CO_2$ production and improved $CO_2$ utilization.

***Phillips' East Vacuum Grayburg San Andres Unit (EVGSAU) Trial (1991-93).*** The EVGSAU operators, in a joint project with the PRRC and the DOE, performed a $CO_2$ foam field trial in Lea County, New Mexico. While the $CO_2$ flooding was favorable, some wells showed excessive $CO_2$ breakthrough, thus increasing $CO_2$ recycling and compression costs. Laboratory results showed that Chaser™ CD1045 was an effective foaming agent at reservoir conditions for EVGSAU cores.[49] The field trial at EVGSAU confirmed these findings.[48,50-52] The surfactant showed great effectiveness as a $CO_2$ mobility reduction agent. For most of the trial a concentration of 0.25 wt% surfactant was used. A short test at 0.10 wt% was showing favorable results before mechanical problems ended the trial prematurely. Decreased gas production and increased oil production in the pilot area were indications of a successful project.

***Mobil's Slaughter and Greater Aneth Field Trials (1991-94).*** Mobil performed four pattern-scale $CO_2$-foam field trials.[78] Two trials were carried out at Slaughter Field in a San Andres reservoir (west Texas) and the other two at Greater Aneth Field in a platform carbonate reservoir (southern Utah). Two different surfactants, Rhodapex (formerly Alipal) CD128 and Chaser™ CD1045, and two injection methods, SAG and co-injection of $CO_2$ and surfactant solution were tested. Altogether, 160,000 lbs. of active surfactant was injected, with one well undergoing 18 months of foam treatment. The treatments resulted in a significant reduction in gas production with indications of increased oil production. Other research also found that foam significantly reduced $CO_2$ injectivity in all cases. Co-injection was operationally more difficult and reduced injectivity significantly more than did SAG.

***Unocal/Long Beach Oil Development Co. Wilmington Immiscible Trial (1984).*** Unocal and Long Beach Oil Development Co. reported an immiscible $CO_2$ foam trial in the Wilmington field in southern California in which Alipal CD128 was used as the surfactant.[79] The purpose of the foam emplacement field test was to divert the $CO_2$-$N_2$ gas mixture, injected in the immiscible flooding project, from the highly water-saturated high permeability zone to lower oil-containing zones. A total of about 21,000 bbl of 1 wt% Alipal CD128 solution was used with a volume of

gas mixture sufficient to provide foam quality of about 90%. About 70 ft of formation in the test well accepted fluid. A radial penetration of about 40 ft for the foaming solution was calculated, with a potential foam bank extending out to 110 ft around the wellbore. The project was successful in reducing in-depth permeability of the high permeability zone and diverting part of the injected gas mixture to the lower permeability zone. Skin damage in the well was greatly decreased, and gas injectivity was notably reduced.

**Previous PRRC Work on This Subject:** Surfactant-based mobility control in $CO_2$ flooding can effectively mitigate poor sweep efficiency that is normally associated with the miscible gas recovery process. Previous laboratory results indicate that the change of flow and displacement behavior of $CO_2$-foam reduces the mobility of $CO_2$ and increases the displacement efficiency.[80-82] Tests have shown improved mobility control with and without oil present.[80,83] Several surfactants have been identified as relatively good mobility control agents in heterogeneous rocks.[84-86] Previous work has shown the effect of foam on delaying $CO_2$ breakthrough time and improved oil recovery.[37,39,87] The decrease or elimination of foam formation in the presence of oil has been reported by several authors.[40,80,87-89]

***Mixed Surfactant Systems.*** To improve foam performance, a number of mixed surfactant systems have been tested.[11,40] Substantial mobility reduction was observed when mixed surfactants were coinjected with $CO_2$. The stability of mixed surfactant systems correlated well with their performance in mobility reduction and in mobility dependence on rock permeability. A few mixtures generated more stable foam than did either of their individual components at similar concentrations and yielded improved mobility reduction as well.

***Sacrificial Agents.*** Reservoir rock has a significant appetite for solution chemicals. In one field pilot test, it was estimated that 90% of the injected foaming agent (surfactant) was required to satisfy reservoir rock adsorption in order for the foam to propagate sufficiently in the reservoir to produce an oil bank.[35] For $CO_2$ foam to propagate through a reservoir at a satisfactory rate, minimizing the adsorption loss of the primary foaming agent is a critical factor. As a common practice, most foam applications involve preinjecting a sufficient amount of foaming agent into the reservoir to precondition the reservoir, which increases the required surfactant volume and consequently increases expense substantially. Therefore, the use of a lower-cost sacrificial agent is an economic necessity to minimize the loss of costly foaming agent and ensure a satisfactory foam displacement.

Calcium lignosulfonate, as an example, is an inexpensive byproduct of the paper industry that has been used as a sacrificial agent in surfactant flooding processes. Because of its preferential adsorption onto reservoir rock, significant reduction of surfactant loss was reported in several surfactant flooding applications where the lignosulfonate minimized the loss of primary surfactants due to adsorption.[90-93] We are examining lignosulfonate both as a sacrificial agent and co-surfactant. The economic appeal of lignosulfonate is its relatively low cost compared to that of the "good" foaming agents and its ready availability as a byproduct from the pulp and paper industry. It has also shown to act as a sacrificial agent and to allow the good foaming agents,[35,37] in our example CD1045, to have stable foam at concentrations 80% lower than with the single surfactant.

Adding chemicals to an oil recovery process increases cost, and thus must increase efficiency if they are to be used. In summary, there are two areas of concern that affect the required amount of chemical for an EOR foam process: the amount of chemicals required to create a foam bank, and the amount of chemicals lost due to reservoir adsorption.

**Expected Improvements over Existing Technologies:** Despite favorable features of $CO_2$ flooding for EOR,[94] $CO_2$ flooding frequently suffers from poor sweep efficiency, high $CO_2$ utilization rate and high cost in handling and recycling produced $CO_2$, low oil productivity due to lower-than-expected injectivity, and limited application in reservoirs that cannot be operated at pressures at or above the MMP.[95]

Poor sweep efficiency and high $CO_2$ utilization rate are results of a high mobility ratio caused by the low viscosity of $CO_2$ compared to that of water or oil. The effectiveness of WAG

for mobility control during $CO_2$ flooding is adversely influenced by gravity segregation between water and $CO_2$, and amplified by permeability contrasts. Foaming agents injected in the aqueous phase help control mobility. However, increased cost due to the adsorption of expensive chemicals onto reservoir rocks has limited the application of this technique. Foam quality, temperature, pressure, $CO_2$ injection rate and total injected volume each affects the ultimate oil recovery.[35,96,97] It is therefore advantageous to develop systems with lower concentrations of good foaming agents that will result in reduced cost. These systems are derived using a sacrificial agent; that is, a co-surfactant that reduce adsorption loss and/or concentration of the good foaming agent without reducing the effectiveness of the foam. In core tests the system of CD1045 with lignosulfonate reduces the pressure drop (increases the injectivity) while maintaining equally good sweep efficiency.[5,11,35] The combination of these two agents in small core tests appears to indicate that they could be tailored to vary injectivity, sweep efficiency, and sensitivity to oil saturation.[5,35]

To aid in predicting utilization of surfactant adsorption on pure minerals (silica, calcite, dolomite, kaolinite, and bentonite) that are common reservoir rock components, studies were performed to determine surfactant adsorption and desorption quantities, rates, mechanisms, and effects of physical parameters such as temperature, pressure, brine and surfactant composition and concentration, and pH on various rock components.[11,41-45] Work in this area will continue, particularly in determining adsorption values versus specific surface area of the mineral to determine sweep efficiency in a homogeneous system. These results are required to develop models to be used in numerical simulation to predict usage in a reservoir.

WAG often reduces injectivity more than expected and the addition of mobility control agents inherently increases the severity of this problem. Any resistance increases the pressure drop, and therefore decreases injectivity.[14,35] Improved mobility control will reduce injectivity; thus, for this purpose, it is critical that the two be optimized. Causes of injectivity reduction that have been identified in ascending order of severity and amenability to remediation are: contamination, gas saturation, dissolution, and precipitation.[5,11]

**Scientific and Technical Basis and Merit:** Previous laboratory and field tests have confirmed the effectiveness of $CO_2$-foam for mobility control and fluid diversion. Areas of progress in the past include:

- Identification of foam strength in high pressure $CO_2$ systems,[11,98]

- Identification of properties that affect foaming agent adsorption in a porous medium: rock type,[39] surfactant type,[98] surfactant concentration,[98] and co-surfactants,[11,40]
- Identification of co-surfactants and sacrificial agents,[11,35,39]
- Effects of heterogeneity with and without capillary contact,[36]
- Identification of a number of systems with varying degrees of selective mobility reduction,[36]
- Development of models to predict reservoir response to the identified foam systems, and
- Several successful field tests.[11,35,36,48-52,75-79]

**Benefits:** Project results will significantly benefit the future of gas injection EOR. Parameters will be determined that will result in improved sweep efficiency with better understanding of injectivity changes, assessing low pressure reservoir gas injection EOR potential, and some applicable simulation modules for incorporation into existing simulators. Anticipated benefits include:

- Surfactant cost reduction: optimizing sacrificial agent and high quality foaming surfactant mixtures, and decreasing primary foaming agent adsorption and required concentration,
- Extending the life of the petroleum reservoir, maintaining or increasing employment, and increasing oil recovery,
- Expanding $CO_2$ flooding to low pressure reservoirs,
- Delayed production of $CO_2$ and increased retention of $CO_2$ in the reservoir (carbon management),
- Improved injectivity of $CO_2$ and water,
- Enhanced $CO_2$ flooding predictions, and
- Decrease of $CO_2$ mobility during the alternate injection of brine and $CO_2$.

$CO_2$ flooding potential has been effectively demonstrated in the US, particularly in the Permian Basin of west Texas and southeast New Mexico. Much of the research on $CO_2$ flooding can be applied to other gas flooding processes. Today almost 350,000 BOPD are being produced by gas injection in the US; ~70% of this oil or nearly 240,000 BOPD is from $CO_2$ injection projects.[99] With oil prices above $60 per barrel recently, this oil production signifies over $7 billion less in imports each year, and provides a significant number of domestic jobs as well. Out of the 350 billion barrels remaining in US oil reserves, the amount of oil presently produced by $CO_2$ flooding barely scratches the surface of this resource. The potential recovery is at least an order of magnitude greater.

Moderately successful future research will maintain current production rates, whereas good to excellent success in research, expanding market availability of $CO_2$ and/or sequestration incentives have the potential of increasing $CO_2$ use in EOR by severalfold. The potential is easily several billion dollars each year in reduced foreign imports and maximization of US resources.

## EXECUTIVE SUMMARY

This is the First Annual Report from the project, "Improved Gas Flooding Efficiency," Department of Energy (DOE) Contract No. DE-FC26-04NT15532. This project focuses on laboratory studies with related analytical and numerical models to enhance our understanding and capabilities for more efficient enhanced oil recovery (EOR).

There is increasing pressure to inject gases into geological formation for greenhouse gas sequestration and to maximize hydrocarbon reserves using advanced techniques such as carbon dioxide ($CO_2$) injection. Thus a need exists to understand the formation and propagation of injected $CO_2$ plumes. The development of $CO_2$ plumes and subsequent dissolution into formation brine are essential mechanisms in most scenarios and are the subject of Chapter 1. This chapter describes laboratory tests on Frio sandstone, the first of several core types being tested that will include several sandstone and carbonate samples. Gas injection was performed into brine-saturated core to a pseudo-residual brine saturation with respect to gas, followed by brine injection to a pseudo-residual saturation gas with respect to brine. The level of $CO_2$ saturation in the injected brine at reservoir pressure and temperature was varied from zero to over 90 %. This variation in $CO_2$ saturation in the injected brine determined the effect on the $CO_2$ saturation or plume size in the core. The change in plume size was related to the ability to dissolve $CO_2$ into flowing brine.

Chapter 2 reports adsorption/desorption kinetics and equilibrium onto Berea sandstone for a surfactant, Chaser™ CD1045 (CD), used as a $CO_2$–water foaming agent. Also, foam stability of the surfactant was compared before and after adsorption/desortion occurred. Results show that this surfactant's adsorption onto Berea sandstone and desorption from Berea sandstone took several days to reach equilibrium. Both adsorption and desorption were characterized by a short period of rapid adsorption/desorption followed by a longer period of slower adsorption/desorption. Both adsorption and desorption processes were best fit by a pseudo-second-order kinetic model. A method to predict equilibrium adsorption density using adsorption process data over a relative short period is proposed, which will save considerable time to determine complete adsorption isotherms. Foam stability is affected by selective surfactant adsorption onto the rock, and the mechanisms or at least their relative importance for adsorption and desorption are not identical.

In the study presented in Chapter 3 an attempt is made to understand the process of adsorption of surfactant CD by looking at its adsorption behavior in adsorption experiments on

Indiana limestone and a solution of CD in 2% brine. In order to estimate CD adsorption density and adsorption kinetics onto limestone, surfactant solution and powdered limestone were added together in test tubes, varying mass ratios. It appears that the total available surfactant is more important then the concentration below 1250 ppm CD. If the CD mass for two samples were similar the adsorption onto sandstone from a higher concentration, lower volume sample would be similar to a lower concentration, higher volume sample. It was also found that adsorption into a no-flow zone of a core, though slow compared to powder minerals or a core flow-through test, it was as great.

Chapter 4 describes the use of foam to decrease the mobility of gas during coreflooding a reservoir rock sample at reservoir conditions. Foam behavior and adsorption, two of the mechanisms required to model surfactant requirements, are studied in this project. This study uses a commercial surfactant, nitrogen gas, and reservoir conditions of 10.34 MPa (1500 psi) and 40°C (104°F), and Indiana limestone. Variables are surfactant concentration, flow rate, and foam quality. At a constant gas flow rate, gas mobility slightly decreases with increasing foam quality when below the critical foam quality ($f_g$*) and increases with increasing foam quality above $f_g$*. Increased surfactant concentration leads to the decrease of gas mobility. Comparing coinjected surfactant and gas (CSG) with coinjected water and gas (CWG) shows that the mobility of CSG is an order of magnitude lower than that of CWG. Also, it took longer for CSG to reach steady state compared to CWG, even with a surfactant pad conditioning the core before surfactant and gas were coinjected.

Most foam studies at PRRC and elsewhere have been performed on surfactant adsorption onto rock without the presence of an oil phase. Chapter 5 covers some preliminary work to include oil. This work was performed to assess the effects of oil in the core system in determining unknown surfactant concentrations in the effluent. In the near future, our research project will focus on the foam behavior at reservoir condition in $CO_2$, surfactant solution and oil. To prepare for this, the partitioning analysis of the surfactant into the oil is required. In this chapter, two series of experiments were performed with three different light oils and two types of surfactant for this purpose. Results from these experiments show that if a mixture of surfactant and light oil is properly handled, the effect on surfactant concentration is negligible. Only single component oils were used and thus crude oil samples are yet to be tested.

## EXPERIMENTAL RESULTS AND DISCUSSION

### Chapter 1: $CO_2$ Saturations and Transport Mechanisms in Sandstone

### Introduction

Injectivity changes while injecting water alternating with gas (WAG) and the increasing pressure to inject gases into aquifers for greenhouse gases sequestration will undoubtedly increase carbon dioxide ($CO_2$) injection into geological formations for EOR and sequestration. The development of $CO_2$ plumes and subsequent dissolution into formation brine are essential mechanisms in most scenarios. This chapter describes laboratory tests on Frio sandstone, the first of several core types being tested. These will include sandstones and carbonate rock types. Several types of displacement tests were performed; gas injection to a pseudo-residual brine saturation with respect to gas, followed by brine injection to a pseudo-residual saturation gas with respect to brine. The level of $CO_2$ saturation in the injected brine at reservoir pressure and temperature was varied from zero to over 90%. This variation in $CO_2$ saturation in the injected brine was to determine the effect on the $CO_2$ saturation or plume size in the core.

It was desired to determine the saturation of $CO_2$ that was injected into a core originally saturated with brine until no water except that vaporized into the $CO_2$ phase vapor was being produced. This was followed with the injection of brine into the core to determine when brine was displacing free $CO_2$ versus where only $CO_2$ dissolved in the brine was produced. $CO_2$ is being injected into reservoirs nearing their waterflood economic limit and into aquifers; thus into geological formations containing high brine saturation. To aid in conformance control and to reduce the amount of $CO_2$ required for injection, $CO_2$ and water are alternately injected into oil reservoirs. Also, it is being proposed to inject $CO_2$ into innumerable aquifers for carbon sequestration. Thus tests are required for both the understanding of how brine and $CO_2$ streams flow through porous media and how their mutual solubilities change their saturations with time.

A Frio core was saturated with brine. High density $CO_2$ was injected into the brine-saturated core until brine production at a particular condition stopped. Brine was then injected into the system and $CO_2$ production recorded to determine amount of and time that the $CO_2$ was produced. This procedure was repeated several times. The objective was to obtain saturation conditions and movement of brine with time and whether the brine/water was in a free phase or dissolved in the $CO_2$ and similarly the movement of $CO_2$ with time and whether it was in a free phase or dissolved in the brine.

## Core Flooding Apparatus

The core flooding apparatus is located in a temperature-controlled air bath, with a piston pump and separator system outside the air bath (see Fig. 1). The dead volume of this system (non-flow path volume and non-core volume) was minimized by reducing the number of pressure control devices, pressure transducers and valves in the system. During the analysis care was taken to capture all the water using an ambient condition separator (liquid trap) to catch the brine/water and a salt breaker (vapor trap) to capture water vapor. For a volume check the liquid and vapor traps were weighed before and after each test and in a couple of cases at an intermediate point. The wet test meter was used to determine gas production at ambient conditions. Included in the gas calculations were corrections for gas displaced by brine/water in the separator.

## Material

Frio cores used in these tests were obtained from depths of 8179, 8191 and 8195 ft in the Felix Jackson # 62 Well, located in Chambers County, Texas. This is located south of the S. Liberty DOE $CO_2$ pilot site. These cores were selected because they were consolidated sandstone, see Frio Core Parameters listed in Table 1. The DOE carbon sequestration DOE test site south of Houston is at a shallower depth and the test horizon is in unconsolidated rock. These tests were performed in the consolidated core to minimize the difficulty while developing test procedures. Future tests, if the results are found applicable, will be performed on unconsolidated samples. Table 2 lists the composition of the synthetic brine used in these tests, which is intended to represent reservoir brine.

## Tests Procedures

All tests were performed at reservoir conditions of 145°F and 2200 psig; except for a couple of comparison tests at 100°F (these will be indicated). The overburden pressure was maintained at 4000 psi (always a minimum of 1000 psi above the pore pressure). The brine was prepared with the composition indicated in Table 2. In some cases the brine had $CO_2$ dissolved in it to represent brine that had been in contact with $CO_2$. The brine will be indicated as dead brine (no dissolved $CO_2$), 50% $CO_2$–brine (brine saturated to about 50% $CO_2$), and 90% $CO_2$–brine (brine saturated to about 90% $CO_2$). Brine saturated to 100% $CO_2$ was not used, to ensure no new free $CO_2$ would occur from $CO_2$ evolving out of the brine. Pressure drop across the core and dissolved solid changes in the brine due to dissolution of core material or water vaporizing into the $CO_2$

phase could cause an additional $CO_2$ phase to occur if brine 100% saturated with $CO_2$ was injected. In all but one case the coreflood was initially 100% saturated with dead brine. Dehydrated $CO_2$ was then injected into the core at least until no free brine was being produced for several pore volumes. $CO_2$ was stored outside the air bath at ambient temperature and injected at rates from 10 to 200 cc/hr (20 cc/hr was used unless otherwise indicated) at ambient temperature and about 2200 psig. The $CO_2$ injection volume at 145°F was about 65% higher than at ambient temperature; both at 2200 psig. The temperature of the air bath, core, and injection pump were recorded. The head and end volumes of the core system were 4.3 cc; thus in Figs. 2, 3 and 8–10 the volumes are shown starting at -4.3 cc.

**Discussion of Results**

Figure 2 compares two tests of $CO_2$ displacing brine in Frio Core A. In both about 7 cc of brine was produced before $CO_2$ breakthrough. After $CO_2$ breakthrough there was a small quantity of brine produced; then brine production stopped except for water dissolved in the $CO_2$. Normally over 95% of the brine production occurred before 1 pore volume (PV) of $CO_2$ had been injected. Any continued production after about 1 PV of $CO_2$ had been injected was from vaporized water. At the end of the test the salt vapor trap was weighed and this value was added evenly over the duration of the test versus injection rate to the brine/water production weight determinations. The time when the vapor was actually produced is not known. In Fig. 2 the first system showed an injection rate increase from 20 to 100 cc/hr after 200 cc of $CO_2$ had been injected. Note the increase in the rate of brine production for an interval following the injection rate increase. During the second test injection was continued overnight at a reduced injection rate of 10 cc/hr and then increased to 100 cc/hr for a short time period at the end of the test.

In each test after reaching what was considered a pseudo-end point. Stable saturation can be changed by increasing the flow rate, decreasing pressure, or by evaporating brine saturation, so there is no true end point. For this paper it will be referred to as a pseudo-end point. After completion of $CO_2$ injection, brine was injected into the core to displace the $CO_2$. For both tests shown in Fig. 2, dead brine was injected (see Figure 3). It is interesting that when about 4.3 cc of reservoir condition $CO_2$ was produced (the same as the end plate dead volume) the $CO_2$ production rate decreased significantly. After the production decrease, an additional 5 cc of $CO_2$ at reservoir condition were produced at a constant rate. Using values from Wiebe and Gaddy[100] adjusted for dissolved solids,[101] these rates are what would be expected from $CO_2$ dissolved in

Frio brine at the test conditions. The produced $CO_2$ after the dead volume was produced did not advance as a free phase. The final value of produced $CO_2$ from the system, including blowdown to ambient pressure, was equal to the brine produced during $CO_2$ injection, so a good material balance was obtained.

The second set of experiments was performed using Frio Core B. In this set the test procedure was similar to that used for Frio Core A, except that the $CO_2$ concentration in the injected brine was varied from 0 to 90% of full saturation. Figure 4 shows the production rate of $CO_2$ in cc/min at ambient conditions for three brines tested at a production flow rate of 20 cc/hr. Thus these values multiplied by three would be the dissolved $CO_2$ in a cc of brine at reservoir conditions. Figure 5 compares the production rate of $CO_2$ while injecting brine into Frio Core B during three different tests. Excluded in Figs. 5–7 was the $CO_2$ production rate during the early brine injection period where the production of the $CO_2$ phase was occurring. See the example in Figure 9 where the early $CO_2$ production rate is included in the plot. In all cases the rate of $CO_2$ phase production is in the 100 to 200 cc/min range with a brine injection rate at 20 cc/hr. Of the three tests shown in Fig. 5, each followed the injection of $CO_2$ into the core saturated with Dead brine. The three tests differ in the concentration of $CO_2$ in the injected brine. During the early time period of dissolved $CO_2$ production (see Fig. 6) the production rates are essentially equal for all three scenarios. The brine produced from this 2.4 in. core was saturated with $CO_2$ and did not depend on the $CO_2$ concentration of the injected brine. Thus the brine was saturated with $CO_2$ in a relatively short flow path. Also shown for comparison in Fig. 6 is the production rate of 50% $CO_2$-brine and 90% $CO_2$-brine.

The injection test using 90% $CO_2$–brine was not continued until free $CO_2$ was depleted in the core, as in the other two cases. Injection and production continued long enough to verify the production rate of $CO_2$ during the first part of the injection. From Fig. 5, $CO_2$ depletion in the core during the dead brine injection shows a rapid decline in the $CO_2$ production rate after most of the $CO_2$ had been produced. In the 50% $CO_2$-brine the drop is slower and as might be expected the system stabilizes at a rate of about 3 cc/min, which is the same as the content of the brine being injected, see Figs. 4 and 6. When the pressure was lowered to ambient pressure (blowdown) at the end of the 50% $CO_2$-brine test, the produced $CO_2$ was equal to what would be evolved from 1 PV of brine saturated to 50% $CO_2$, indicating that all the free $CO_2$ had been removed. Figure 7 compares the production of $CO_2$ during the injection of 50% $CO_2$–brine at two temperatures, 100° and 145°F. The production rates are similar but it appears that the $CO_2$

production rate is a little higher at 100°F. Literature values indicate that the solubility of $CO_2$ in brine is around 10–15% higher at the lower temperature.[100] Even though the data has scatter similar to the expected difference, the average for the first 200 min in Fig. 7 is 7.3 cc/min at 145°F and 8.3 cc/min at 100°F, which is a 14% increase in production at the lower temperature.

The results of the final set of tests reported in this paper were from Frio Core C (see Figs. 8–10. Figure 9 has an expanded production rate scale, compared to Figure 8, to demonstrate the rate comparison during free $CO_2$ production and production evolving from $CO_2$ dissolved in brine at reservoir conditions. In this series the first tests performed started with a dry core. The core was then saturated with 100% dehydrated $CO_2$ and followed with the injection of Dead brine into the core. In this system about 9 cc of $CO_2$ at reservoir conditions were produced before production stabilized at the rate evolved from brine saturated with $CO_2$ at 100°F and 2200 psig. About 11 cc of $CO_2$ at reservoir conditions were produced at a rate of about 8 cc/min at ambient conditions, thus a total of about 20 cc at reservoir conditions. From this subtract the 4.3 cc dead volumes, thus leaving 16 cc or almost 90% of the 18.1 cc core PV. Another 2 cc were produced during the remaining injection period and blowdown after injection was terminated. In this test it required about 4 cc of brine or just over 0.2 PV to establish a brine flow path. As soon as or soon after a brine flow path (brine breakthrough) was established, $CO_2$ phase production ended. Shortly after brine breakthrough it appears that only $CO_2$ dissolved in produced brine was produced.

After the pressure of Frio Core C was reduced to ambient pressure, dead brine was injected to remove any remaining $CO_2$. To compare to Frio Cores A and B the system was returned to reservoir pressure, but left at 100˚F. Again the dead volume and a few cc of additional brine were produced. When the production of free brine stopped 50% $CO_2$–brine was injected. Figure 10 compares the production rate and total production of $CO_2$ during the injection of the 50% $CO_2$–brine with the injection of dead brine into the dry $CO_2$ core. The results are different from Frio Cores A and B, in that $CO_2$ phase production terminated before the dead volume equivalence of $CO_2$ was produced. This had occurred once before and in both cases it appeared that brine had remained in the end plates of the core and/or in the lines and thus not as much brine injection was required to push out all the $CO_2$ phase. In one case, after $CO_2$ injection into the core ended and the lines isolated from the core about 1 cc of brine was blown out of the lines. In all the other tests the system lines had been brine/water free. The slope of the cumulative production for the second tests is about half that of the first tests because the $CO_2$

dissolved in the 50% $CO_2$–brine that was being injected was subtracted from the produced $CO_2$ when calculating the $CO_2$ production during brine injection.

**Summary and Conclusions**

These were relatively short cores (2.25 to 2.4 in.) about 1.5 in. in diameter; therefore care must be taken when extrapolating results to reservoir scale. Some of the conclusions are:

1. A range of 0.2 to 0.3 PV fraction of $CO_2$ phase saturation was required to establish a $CO_2$ flow path, after which there was little brine production except through evaporation. $CO_2$ saturation can be increased by increasing flow rate, reducing pressure, and water evaporation.
2. At the end of $CO_2$ injection, there was relatively low $CO_2$ saturation and high brine saturation in the core, and no apparent reduction in $CO_2$ saturation was required to return to establish brine flow path. In the case of a water-wet system this and the previous conclusion are not surprising.
3. Brine is equilibrated with $CO_2$ in minutes over a relatively short distance.
4. In the systems tested, once $CO_2$ injection stopped, the $CO_2$ phase did not migrate and did not change except to the extent that unsaturated brine was available to dissolve $CO_2$.
5. The injection of brine into a 100% $CO_2$ phase required less then 0.3 PV fraction saturation to establish a brine flow path.

This work is ongoing. We are presently looking at carbonate core and determining pore body and throat size distributions for each core type.

| Table 1. Frio Core Parameters | | | |
|---|---|---|---|
| **Core** | **A** | **B** | **C** |
| **Depth [ft]** | **8179** | **8191** | **8195** |
| **Diam [in]** | **1.47** | **1.44** | **1.47** |
| **Length [in]** | **2.393** | **2.4** | **2.25** |
| **Mass [g]** | **121.07** | **111.86** | **111.53** |
| **Bulk vol [cc]** | **66.6** | **64.1** | **62.6** |
| **PV [cc]** | **18.51** | **18.01** | **18.1** |
| **Por [%]** | **27.8** | **28.1** | **28.9** |

**Table 2. Frio Synthetic Brine Composition**

| Component | mg/L | Species | mg/L |
|---|---|---|---|
| **NaCl** | **82,753** | **Cl** | **57,460** |
| **$CaCl_2$** | **8,584** | **Na** | **32,603** |
| **$MgCl_2$** | **2,152** | **Ca** | **3,100** |
| **KCl** | **362** | **Mg** | **549** |
| **$NaHCO_3$** | **186** | **K** | **190** |
| | | **$HCO_3$** | **135** |
| **Total Dissolved Solids** | **94,037** | | **94,037** |

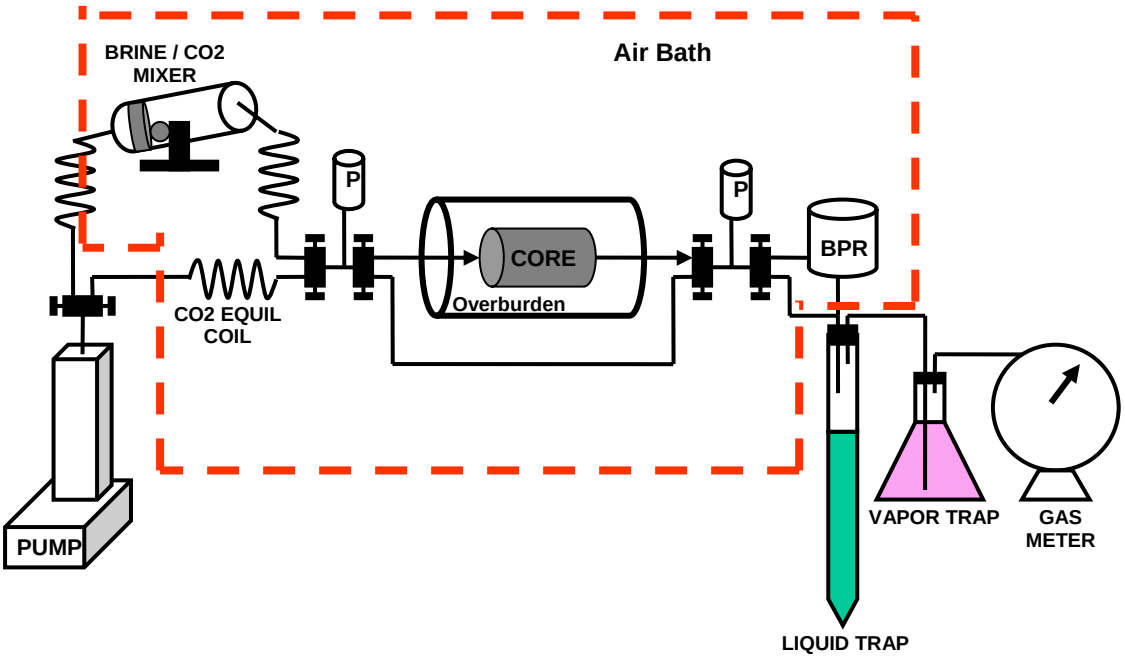


**Fig. 1. Schematic of the coreflood apparatus.**

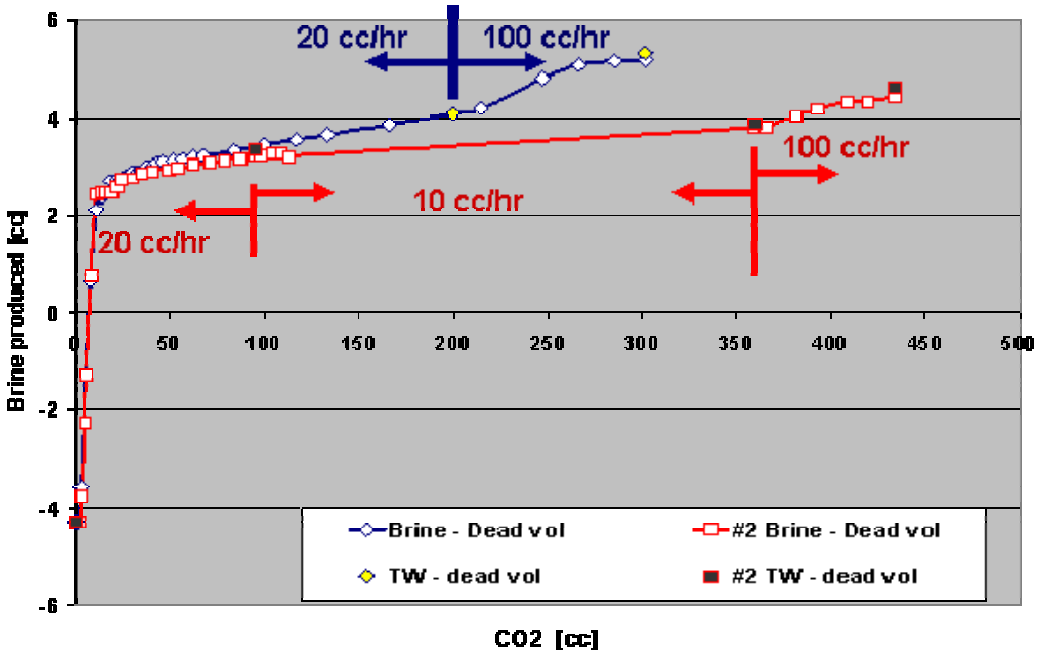


**Fig. 2. Comparison of brine production during $CO_2$ injection of two tests both in Frio Core A. In each the 4.3 cc dead volume is subtracted. The points were the volumes by weight were determined are indicated for each as TW and compare well with the values determined by direct volume with the vapor trap values included.**

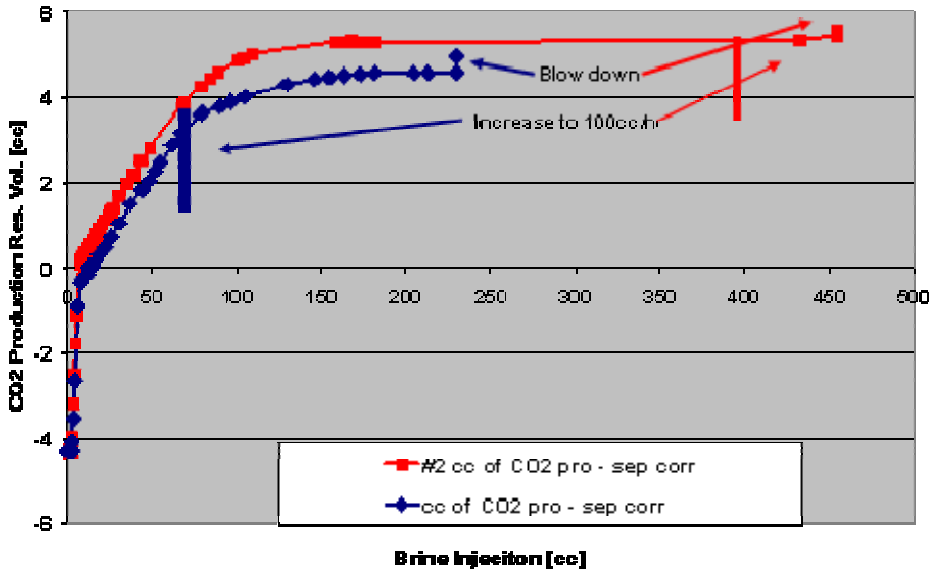


**Fig. 3. Comparison of $CO_2$ production during brine injection for two tests in Frio Core A. In each the 4.3 cc dead volume is subtracted.**

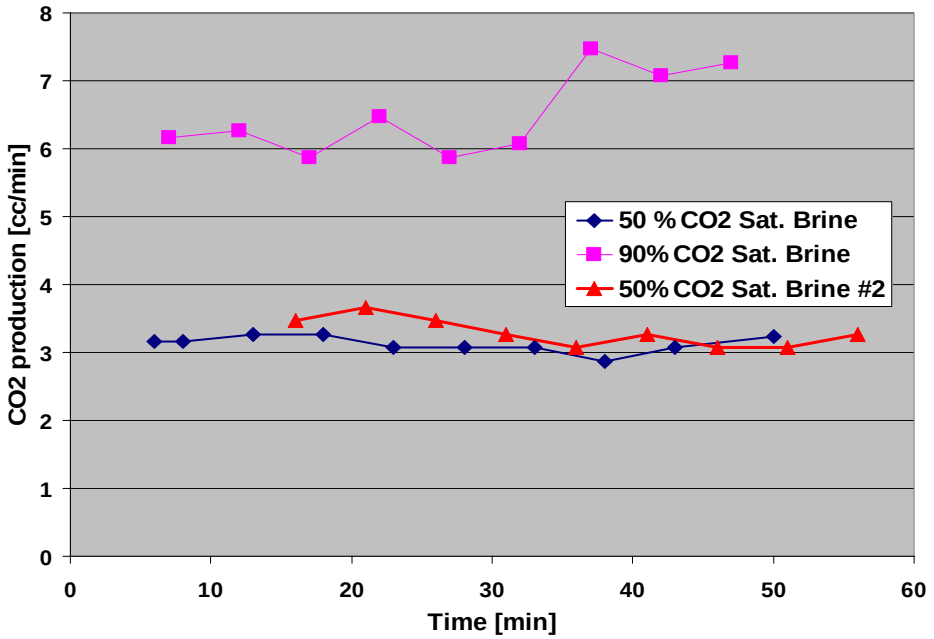


**Fig. 4. Comparison of $CO_2$ production (cc/min) from two brines saturated to about 50% $CO_2$ and one saturated to 90% $CO_2$; each at a flow rate of 20 cc/hr and 145°F.**

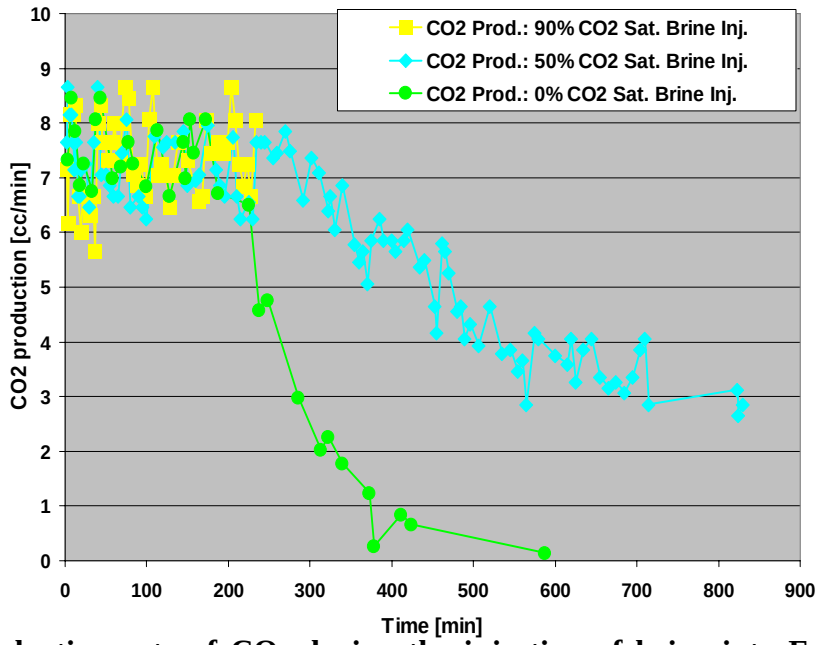


**Fig. 5. Production rate of $CO_2$ during the injection of brine into Frio Core B for three different tests, each at different concentrations of $CO_2$ in the injected brine.**

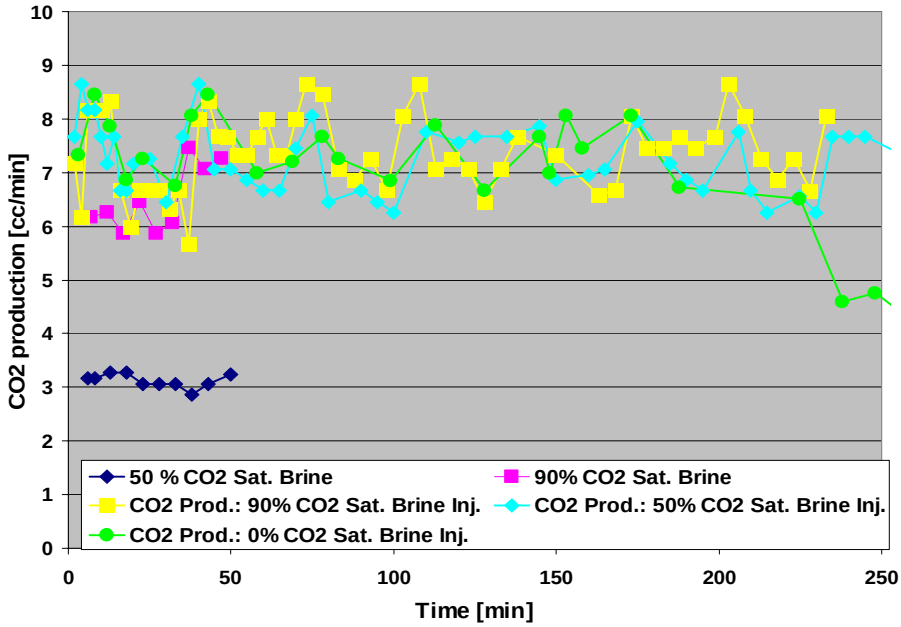


**Fig. 6. Comparison of $CO_2$ production rates during brine injection into Frio Core B during from about 1 PV to 5 PV.**

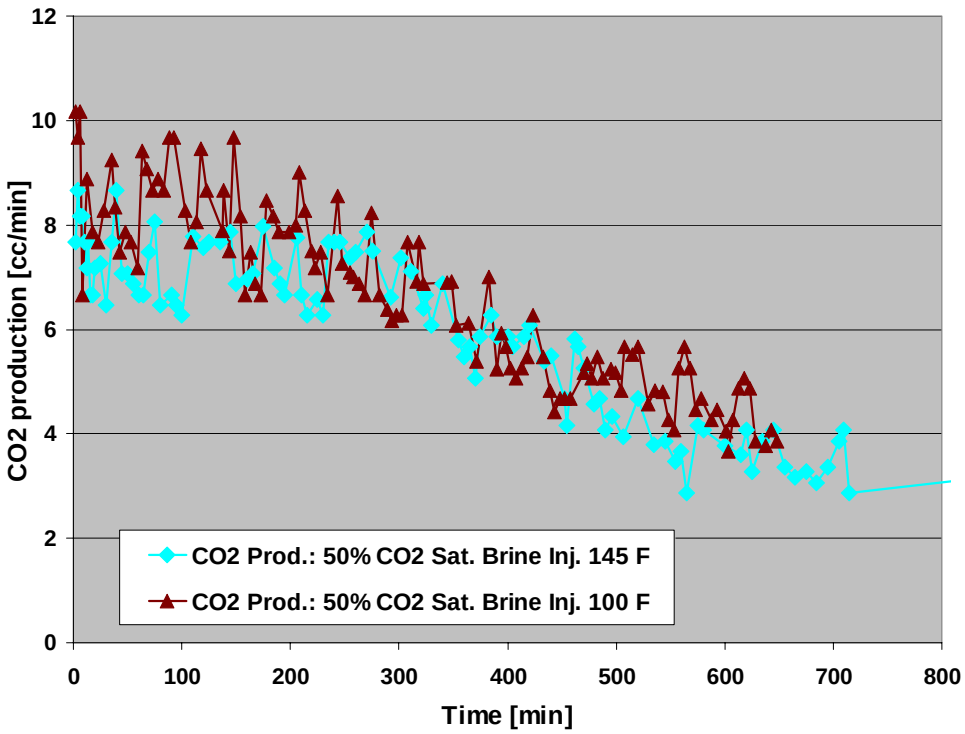


**Fig. 7. Comparison of the $CO_2$ production rate during the injection of 50% $CO_2$–brine at two different temperatures, 100°and 145°F.**

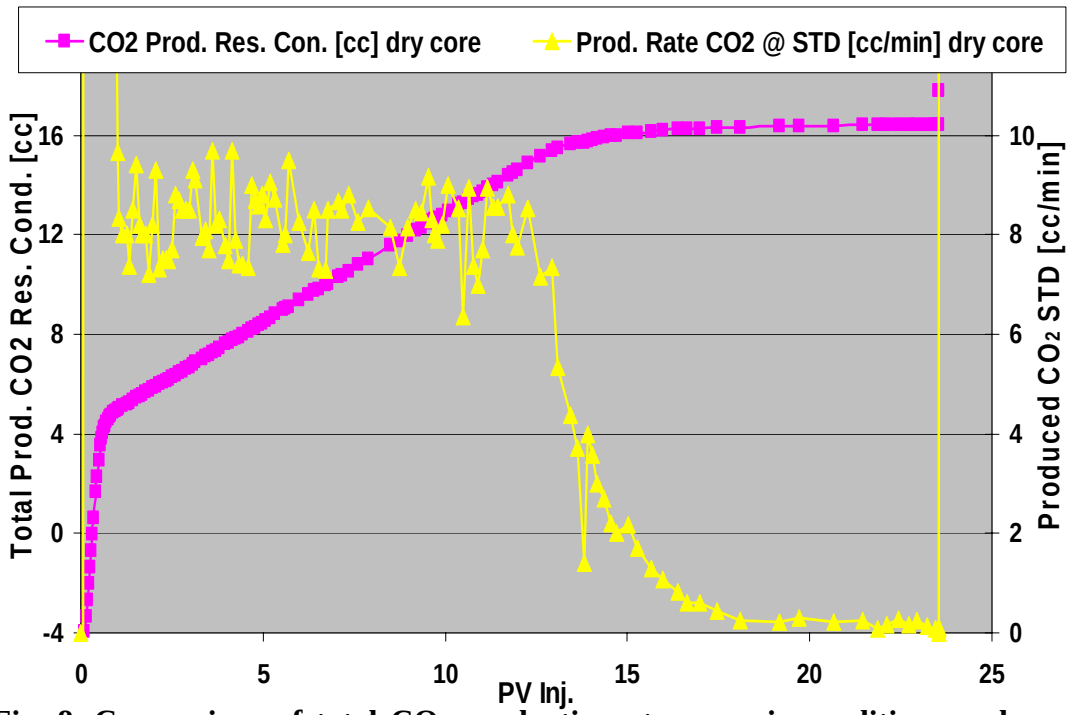


**Fig. 8. Comparison of total $CO_2$ production at reservoir conditions and production rate from the separator at ambient conditions for $CO_2$ during the test at 100°F.**

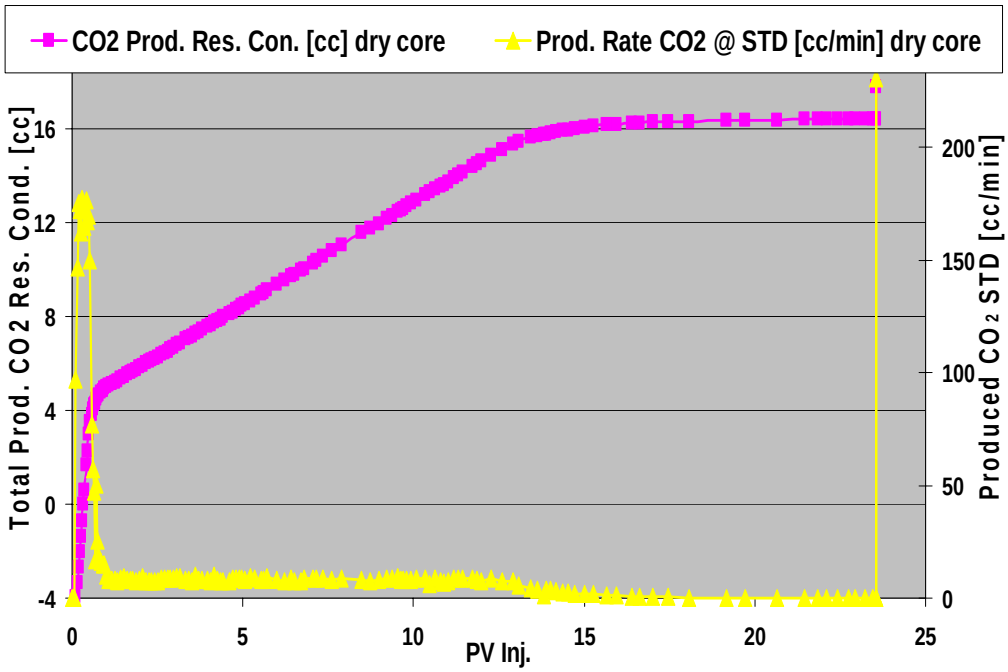


**Fig. 9. Comparison similar to Fig. 8 except the scale for $CO_2$ production rate is expanded to include the maximum production rate during production of the $CO_2$ phase.**

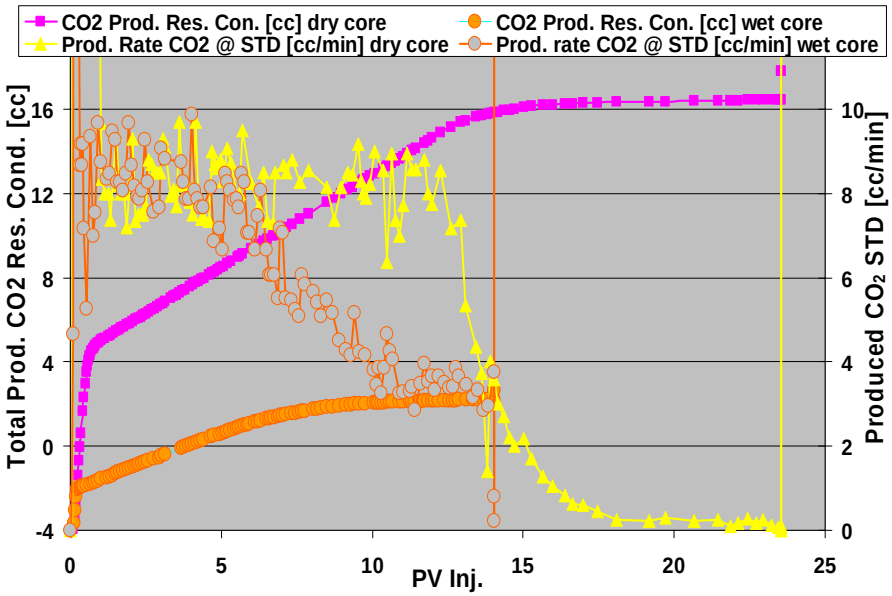


**Fig. 10. Comparison of $CO_2$ production of brine into the dry Frio Core A and injection of 50% $CO_2$–brine into the core after being saturated with dead brine and then flooded with $CO_2$.**

## Chapter 2: Adsorption/Desorption of a Surfactant onto Berea Sandstone

### Introduction

This chapter reports adsorption/desorption kinetics and equilibrium onto Berea sandstone for a surfactant used as a $CO_2$–water foaming agent. Also, foam stability of the surfactant is compared before and after adsorption or desorption has occurred. Results show that this surfactant's adsorption onto Berea sandstone and desorption from Berea sandstone took several days to reach equilibrium. Both adsorption and desorption were characterized by a short period of rapid adsorption/desorption followed by a longer period of slower adsorption/desorption. Both adsorption and desorption processes were best fit by a pseudo-second-order kinetic model. Coefficients of adsorption and desorption rate were determined. A method to predict equilibrium adsorption density using adsorption process data over a relative short period is proposed, which saves considerable time in comparing to determine complete adsorption isotherms. Surfactant concentration and temperature affect equilibrium density. Foam stability is affected by selective surfactant adsorption onto the rock, and the mechanisms for adsorption and desorption may be different.

Published EOR work on surfactant adsorption has focused on studying adsorption equilibrium with little mention of kinetics.[39,102,103] However, the kinetics of surfactant adsorption is important in determining the rate of adsorption onto the rock and the time required to reach equilibrium, and is thus useful in predicting the transport and fate of surfactant in the reservoir. This study focuses on adsorption equilibrium and kinetics for both adsorption and desorption of the surfactant Chaser CD1045™ intended for the application of mobility control and fluid diversion using $CO_2$-foam flooding. Foam stability will be investigated via testing effluents from the adsorption or desorption experiment at equilibrium state.

### Experimental

**Materials:** The surfactant used in this study was CD 1045 (CD), which was identified as a good foaming agent in earlier studies.[39,47,83,102,103] It was supplied by Chaser International as 46.7 wt % active aqueous solution. Dimidium Bromide-Disulphine Blue Indicator, used for anionic surfactant determination, supplied by BDH Laboratory Supplies, was used to detect CD; it is described in an earlier publication.[42] Chloroform, HPLC grade, containing approximately 0.75% ethanol as a preservative was used as part of the process to determine unknown CD

concentrations. Two weight percent synthetic brine composed of 1.5 wt% NaCl and 0.5 wt% $CaCl_2$ was used to prepare surfactant CD solution.

Berea sandstone was used as the adsorbent. The parameters of the two cores used in the study (B03 and B04) were listed in Table 3. During the testing process one end of B03 was broken. In order to eliminate the imperfection, the end was sliced off, thus changing the dimensions of B03 and creating B04.

## Experimental Methods

***Quantitative Analysis of CD Solution.*** A colorimetric method described previously was used to determine CD concentration in the study.[42,103] The absorbance of CD solution prepared by 2% brine was measured by spectrophotometer and found to have three absorbance peaks: 295 nm, 406 nm and 520 nm. The peak at 520 nm has been used because absorbance is linear versus CD concentration below 600 mg/l, and other surfactants used as co-surfactants have the minimum interference at this peak.

***CD Adsorption and Desorption onto Berea Sandstone.*** Two dynamic methods, circulation and flow-through experiments, were used to study surfactant adsorption/desorption onto the rock.[42-44] Eight experiments were carried out using core B03 and B04. Table 4 lists experimental procedures and conditions. All experiments were performed at 40°C, except for B04-A and Step 2 of B03-C. To achieve equilibrium, each circulation process took several days at a circulation rate of 15 $cm^3$/hr. After each circulation experiment, the core was flushed with 2% brine. Between experiment sets, about 400 $cm^3$ of tetrahydrofuran (THF) was flushed through the core to clean out all remaining surfactants.

***Foam IFT and Stability Determination.*** The calculation of interfacial tension (IFT) is analogous to that of the drop weight method.[47,83] The rate of introducing dense $CO_2$ is determined by the aqueous phase withdrawal rate. The number of produced bubbles per time period is recorded, from which the volume and radius of each bubble are calculated. The correction factor takes into account effects of attraction to the end of the needle and imperfections in the system.

Stability is determined using a sapphire visual cell.[47,83] In this study, the cell was first filled with the aqueous solution to be tested. The aqueous system was brought to the desired pressure by means of a positive displacement pump. The pressure difference between the $CO_2$ tank and the oil/surfactant-solution tank was determined and adjusted to zero. At this point $CO_2$ was

allowed to flow from the capillary tube into the surfactant solution. The dense $CO_2$ flowed upward through a needle at the lower end of the cell and kept flowing in the form of bubbles towards the top of the sapphire tube. Depending on the effectiveness of the surfactant, the bubbles either formed a layer of foam-like dispersion at the top of the sapphire tube or coalesced into a clear layer of dense $CO_2$. After a standard volume of $CO_2$ was introduced, the pump was stopped and the stability of foam was determined by measuring the change of the foam layer thickness within 90 minutes.

## Results and Discussion

**Kinetics of CD Adsorption onto Berea Sandstone:** Eight concentrations of CD solution prepared by 2% brine were circulated through Berea sandstone. Figure 11 shows the adsorption density as a function of circulation time. Each adsorption took more than 120 hours to reach equilibrium. Each adsorption curve is characterized by early rapid adsorption followed by a long period of slow adsorption. The rapid adsorption generally lasted less than 24 hours, and the slow adsorption continued for at least several days. Possible mechanisms controlling different stages were analyzed in an earlier publication.[42]

***Adsorption Kinetic Models.*** Models of adsorption kinetics were correlated with the solute adsorption rate. Selecting a correct model is important to predict surfactant transport and surfactant-based EOR process design. Three models: pseudo-first-order equation, pseudo-second-order equation, and interparticle diffusion, were tested to determine the best model for CD adsorption onto Berea sandstone.[104-110]

***Modeling Adsorption Using Pseudo-second-order Kinetic Model.*** The pseudo-second-order equation adsorption can be written as the following differential equation:

$$\frac{dq_t}{dt} = k_{a2}\left(q_e - q_t\right)^2 \quad \ldots\ldots\ldots\ldots\ldots\ldots\ldots\ldots\ldots\ldots\ldots\ldots 1$$

where $q_e$, CD adsorption density onto Berea sandstone at equilibrium, mg/g;

$q_t$, CD adsorption density onto Berea sandstone at time t, mg/g;

t = time, hr; and

$k_{a2}$, the pseudo-second-order kinetic coefficient of adsorption, g / (mg •hr).

Integrating Eq. 1 at the initial condition of $q_t|_{t=0} = 0$, the following equation is obtained:

$$\frac{1}{q_e - q_t} - \frac{1}{q_e} = k_{a2}t \quad \ldots\ldots\ldots\ldots\ldots\ldots\ldots\ldots\ldots\ldots\ldots\ldots 2$$

Rearranging Eq. 2, the following equation is obtained:

$$\frac{t}{q_t} = \frac{1}{q_e} t + \frac{1}{k_{a2} \cdot q_e^2} \quad \text{.....3}$$

where the plot of ($t/ q_t$) versus t should be a straight line with the slope of ($1/ q_e$) and the y-intercept of $1/(k_{a2} q_e^2)$. By measuring a series of adsorption density $q_t$ at different time t, a straight-line is defined, from which $q_e$ and $k_{a2}$ can be determined. Thus the adsorption density at any other time can be calculated using Eq. 3.

By rearranging Eq. 3, the adsorption density at different time can be calculated by:

$$q_t = \frac{t}{\frac{1}{q_e} t + \frac{1}{k_{a2} \cdot q_e^2}} \quad \text{.....4}$$

Figure 12 shows the fit result of CD adsorption onto Berea sandstone using the linear relationship between $t/q_t$ and t. Table 5 shows the corresponding fitting equations, $R^2$ and the calculation results of equilibrium adsorption density and the kinetic coefficient. Each of the eight adsorption tests is best fitted by a pseudo-second-order equation with $R^2$ over 0.99. Due to their relative high $R^2$, the equilibrated adsorption density can be predicted using the first few points from the circulation experiments, which would save considerable time to determine an adsorption isotherm.

A pseudo-first-order kinetic model and an intrapartical diffusion model were also checked using the experimental data, which resulted in very low $R^2$. This means that the adsorption can be best described by the pseudo-second-order kinetic model.

Comparing the adsorption kinetic coefficient $k_{a2}$ at 40°C in Table 5 shows that increasing the initial concentration decreases the adsorption kinetic coefficient. Comparing the adsorption coefficient of similar initial concentrations, 493 and 485 mg/l, at different temperatures, 40°C and 23°C respectively, the adsorption kinetic coefficient at the higher temperature is higher than that at the lower temperature. This result is consistent with the trend for the adsorption system of calcium lignosulfonate onto limestone reported in an earlier paper.[43]

Considering the adsorption coefficient at 40°C as a function of initial concentration $C_i$ and of equilibrium concentration $C_e$, their correlations are shown in Figs. 13 and 14, respectively. Azizian developed a model indicating that there should be a linear relationship between kinetic coefficient and initial concentration, but had no experimental result to support this theory.[104] The

trend of the experimental data in this paper can be best fitted with two different lines: one for low initial concentration, another for high initial concentration (Fig. 13).

These relationships are as follows:

$$\begin{cases} k_{a2} = -5.40E-3C_i + 1.3672 \;\; for \;\; C_i \le 205\,(\text{mg/l})/\text{cm} \\ k_{a2} = -4.39E-4C_i + 0.3387 \;\; for \;\; C_i > 205\,(\text{mg/l})/\text{cm} \end{cases} \quad \ldots\ldots 5$$

These results partly support Azizian's work.[103] Note that initial concentrations in Fig.13 are normalized with Berea core length.

Similarly, from Fig. 14, the relationship between the kinetic coefficient and equilibrium concentration $C_e$ can be obtained as follows:

$$\begin{cases} k_{a2} = -3.38E-3C_e + 1.2299 \;\; for \;\; C_e \le 287\,(\text{mg/l}) \\ k_{a2} = -1.57E-4C_e + 0.3387 \;\; for \;\; C_e > 287\,(\text{mg/l}) \end{cases} \quad \ldots\ldots 6$$

Figures 13 and 14 indicate that the kinetic coefficient shows bilinear correlations with both initial and equilibrium concentrations. This may indicate different mechanisms of adsorption at different states.

***Kinetics of CD Desorption from Berea Sandstone.*** An earlier publication[42] has shown that CD desorption is rate-dependent and does not reach equilibrium at tested flow rates in the core samples tested in this work. The remained adsorption density $q_t$ as a function of time during direct flow of brine is plotted in Fig. 15. The remaining adsorption density during desorption is characterized by a short, rapid desorption followed by a longer, slower desorption process.

***Modeling CD desorption from Berea Sandstone.*** The differential equation of the pseudo-second-order kinetic model during the desorption process can be defined as:

$$\frac{dq_t}{dt} = k_{d2}(q_t - q_r)^2 \quad \ldots\ldots\ldots\ldots\ldots\ldots\ldots\ldots\ldots\ldots\ldots 7$$

Integrating Eq. 7 at initial condition $q_{t|_{t=0}} = q_i$ during desorption gives

$$\frac{1}{q_t - q_r} = -k_{d2}t + \frac{1}{q_i - q_r} \quad \ldots\ldots\ldots\ldots\ldots\ldots\ldots\ldots\ldots 8$$

and the plot of $1/(q_t - q_r)$ versus t will be a straight line with the slope of $k_{d2}$ and the y-intercept of $1/(q_i - q_r)$ if the data fits the pseudo-second-order desorption model.

The plot of $1/(q_t - q_r)$ versus t shown in Fig. 16 indicates that CD desorption from Berea sandstone follows the pseudo-second-order desorption kinetic model for constant flow rate. All data except for the first one or two points show a fair fit. Table 5 lists the correlations and $R^2$ based on the assumption that complete desorption is zero.

**Foam stability.** In CD foam before the solution was circulated through the Berea sandstone core, the coalescence of bubbles was observed at CD concentration of only 50 mg/l (0.005 wt %).[47] This indicates that foam does not collapse except at a concentration of 50 mg/l, well below the critical micelle concentration (CMC), which is around 600 mg/l (Fig. 17). The foam stability of fresh CD solutions was insensitive to surfactant concentration over a wide range (from 100 to 10,000 mg/l).

Table 7 indicates that 50% or more of the injected CD was adsorbed or trapped onto the Berea sandstone core by comparing the CD concentration before and after circulation, which agrees with previous work.[42-44] When compared with a CD fresh solution of similar concentration, CD solution tested for foam stability after circulating through the Berea sandstone core developed a less stable foam (see comparison in Figs. 18 and 19). This indicates that a higher concentration of CD is needed to generate foam of similar stability after contacting with the reservoir rock (Fig. 20). This is an indication of selective adsorption. CD is a mixture of several surfactants with a wide range of molecular weight. The solution used for the foam stability test that was obtained from desorption demonstrated similar foaming properties (Figs. 21 and 22) when compared with a fresh CD solution of similar concentration. Thus at least some of the components adsorbed that decreased the foaming ability of the solution were desorbed and created a good foaming system during desorption.

## Conclusions

1. CD adsorption onto Berea sandstone took several days to reach equilibrium. The adsorption process is characterized by a short period of fast adsorption followed by a long period of slow adsorption.
2. CD adsorption onto Berea sandstone can be described well by a pseudo-second-order adsorption kinetic model.
3. Increasing CD concentration increased CD adsorption density onto Berea sandstone. No plateau was found even when surfactant concentration was above its CMC, which indicates some other physical mechanisms may influence CD solution transport through Berea sandstone.
4. CD desorption from Berea sandstone can be fit well by a pseudo-second-order kinetic model.
5. At a similar CD concentration, when compared with a CD solution before circulation, foam stability of CD solution after circulation decreased during adsorption, but remained at a

similar level during desorption. This indicates chromatographic separation when CD solution is transported through Berea sandstone and the mechanisms for adsorption and desorption are different.

**Nomenclature**

$C_e$ = CD equilibrium concentration, mg/l

$C_i$ = CD initial concentration, mg/l

$q_e$ = CD adsorption density at equilibrium, mg/g

$q_t$ = CD adsorption density at time t, mg/g

$q_r$= CD residual adsorption density at the end of the desorption process, mg/g

$k_{a2}$=adsorption kinetic coefficient, g / (mg • hr)

$k_{d2}$= desorption kinetic coefficient, g / (mg •hr)

t = time, hr

**Table 3. Properties of Core Samples Used in This Study**

| Test | Core | Length (cm) | Diameter (cm) | Weight (g) | Pore volume ( cm3)* | Porosity (%)* | Permeability (md)* |
|---|---|---|---|---|---|---|---|
| B03 | Sandstone | 6.20 | 3.81 | 142.21 | 14.88 | 21.05 | 224 |
| B04 | Sandstone | 5.20 | 3.81 | 123.41 | 12.48 | 21.05 | 224 |

* Values measured only for B04 and are extrapolated for B03.

**Table 4. Experimental Schedule of CD Adsorption and Desorption onto Berea Sandstone**

| Tests | Experiment Description |
|---|---|
| B03-A | 1. Adsorption: Circulate 493 mg/l CD through the core<br>2. Desorption: Inject 2% brine to flush the core at 30cm3/hr (direct flow) |
| B03-B | 1. Adsorption: Circulate 1034 mg/l CD through the core<br>2. Desorption: Inject 2% brine to flush the core at 30 cm3/hr (direct flow) |
| B03-C | 1. Adsorption: Circulate 1627 mg/l CD through the core<br>2. Adsorption: Effect of temperature on adsorption density (Circulation)<br>3. Desorption: Inject 2% brine to flush the core at 15 cm3/hr (direct flow) |
| B03-D | 1. Adsorption: Circulate 2114 mg/l CD through the core<br>2. Desorption: Inject 2% brine to flush the core at different flow rate(direct flow) |
| B04-A | Adsorption: Circulate 485 mg/l CD through the core at 23°C. Effluents from the adsorption experiment at equilibrium state was labeled as F5 and used to measure foam stability. |
| B04-B | 1. Adsorption: Circulate 3123 mg/l CD through the core at 40°C. Effluents from the adsorption experiment at equilibrium state was labeled as F1 and used to measure foam stability.<br>2. Desorption: Circulate surfactant-free brine through the core. Effluents from the desorption experiment at equilibrium state was labeled as F2 and used to measure foam stability.<br>3. Desorption: Inject 2% brine to flush the core at 15 $cm^3$/hr (direct flow) |
| B04-C | 1. Adsorption: Circulate 727 mg/l CD through the core at 40°C. Effluents from the adsorption experiment at equilibrium state was labeled as F3 and used to measure foam stability.<br>2. Desorption: Change the surfactant in the vial to brine and circulate the brine until desorption reaches equilibrium. Effluents from the desorption experiment at equilibrium state was labeled as F4 and used to measure foam stability.<br>3. Desorption: Direct flow at the flow rate of 15 $cm^3$/hr. |
| B04-D | 1. Adsorption: Circulate 196 mg/l CD through the core at 40°C. Effluents from the adsorption experiment at equilibrium state was labeled as F6 and used to measure foam stability.<br>2. Desorption: Inject 2% brine to flush the core at 15 $cm^3$/hr (direct flow) |

Note: All solutions were prepared with 2% brine.
All experiments were run at 40°C except for B04-A and Step 2 of B03-C.
All circulation experiments were run at the flow rate of 15 $cm^3$/hr.
All concentrations are the initial concentrations.

**Table 5. Results of Modeling CD Adsorption Kinetics onto Sandstone Using A Pseudo-Second-Order Equation**

| Initial Conc. (mg/l) | Correlations | $R^2$ | $q_e$ | $k_{a2}$ (g/(mg • hr)) | Temp (ºC) |
|---|---|---|---|---|---|
| 196 | $t/q_t = 6.9356t + 41.235$ | 0.9983 | 0.144 | 1.167 | 40 |
| 493 | $t/q_t = 3.9931t + 17.441$ | 0.9941 | 0.250 | 0.917 | 40 |
| 727 | $t/q_t = 2.3355t + 8.2148$ | 0.9999 | 0.428 | 0.664 | 40 |
| 1034 | $t/q_t = 1.7175t + 6.8383$ | 0.9992 | 0.582 | 0.431 | 40 |
| 1627 | $t/q_t = 1.3208t + 7.2674$ | 0.9996 | 0.757 | 0.240 | 40 |
| 2114 | $t/q_t = 1.0313t + 6.3496$ | 0.9995 | 0.970 | 0.168 | 40 |
| 3123 | $t/q_t = 0.7019t + 6.1476$ | 0.9978 | 1.425 | 0.080 | 40 |
| 485 | $t/q_t = 3.0273t + 13.2140$ | 0.9991 | 0.330 | 0.694 | 23 |

**Table 6. Fitting Equations and $R^2$ Using Pseudo-Second-Order Desorption Model**

| Initial Conc | Equation | $R^2$ | $k_{d2}$ (g/(mg • hr)) | Flow rate ($cm^3$/hr) |
|---|---|---|---|---|
| 196 | $\frac{1}{q_t} = 0.0547t + 10.922$ | 0.9802 | 0.0547 | 15 |
| 493 | $\frac{1}{q_t} = 0.0915t + 3.4766$ | 0.9812 | 0.0915 | 30 |
| 727 | $\frac{1}{q_t} = 0.0125t + 2.940$ | 0.9528 | 0.0125 | 15 |
| 1034 | $\frac{1}{q_t} = 0.0369t + 1.748$ | 0.9932 | 0.0369 | 30 |
| 1627 | $\frac{1}{q_t} = 0.0485t + 1.3489$ | 0.9713 | 0.0485 | 15 |
| 3123 | $\frac{1}{q_t} = 0.0098t + 1.0068$ | 0.9568 | 0.0098 | 15 |

**Table 7. IFT and Foam Stability after Circulating through the Core**

| Tests | Effluents | CD concentration (mg/l) | | IFT (mN/m) | Foam stability (%) | Experiments |
|---|---|---|---|---|---|---|
| | | Before circulating | After circulating | | | |
| B04-B | F1 | 3123 | 1500 | 4.86104 | 100 | Adsorption |
| | F2 | | 470 | 7.29932 | 100 | Desorption |
| B04-C | F3 | 727 | 192 | 13.2940 | 49 | Adsorption |
| | F4 | | 50 | 15.2170 | 62 | Desorption |
| B04-A | F5 | 485 | 165 | 14.6628 | 0 | Adsorption |
| B04-D | F6 | 196 | 24 | 19.5647 | 0 | Adsorption |

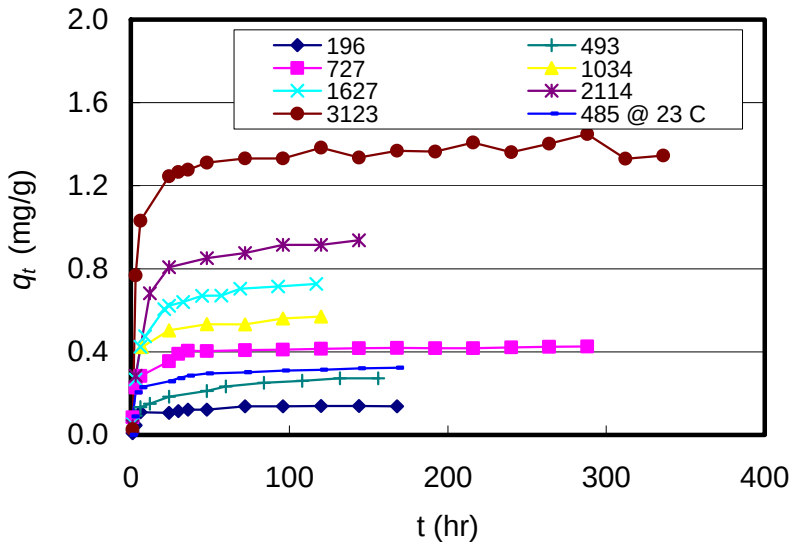


**Fig. 11. Kinetics of CD adsorption onto Berea sandstone, each performed at a flow rate of 15 cm$^3$/hr.**

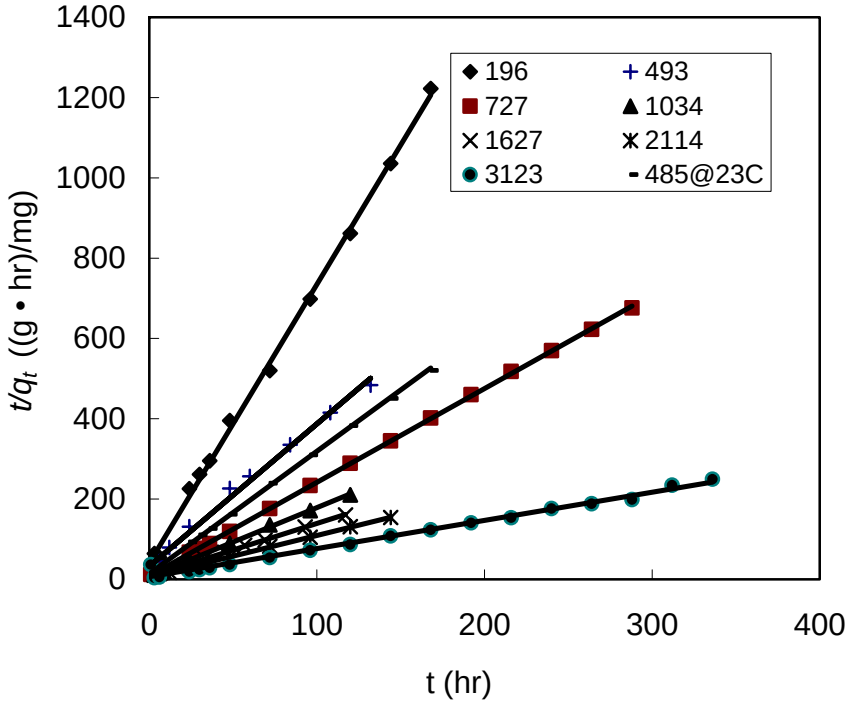


**Fig. 12. Modeling CD adsorption kinetics onto sandstone using pseudo-second-order equation.**

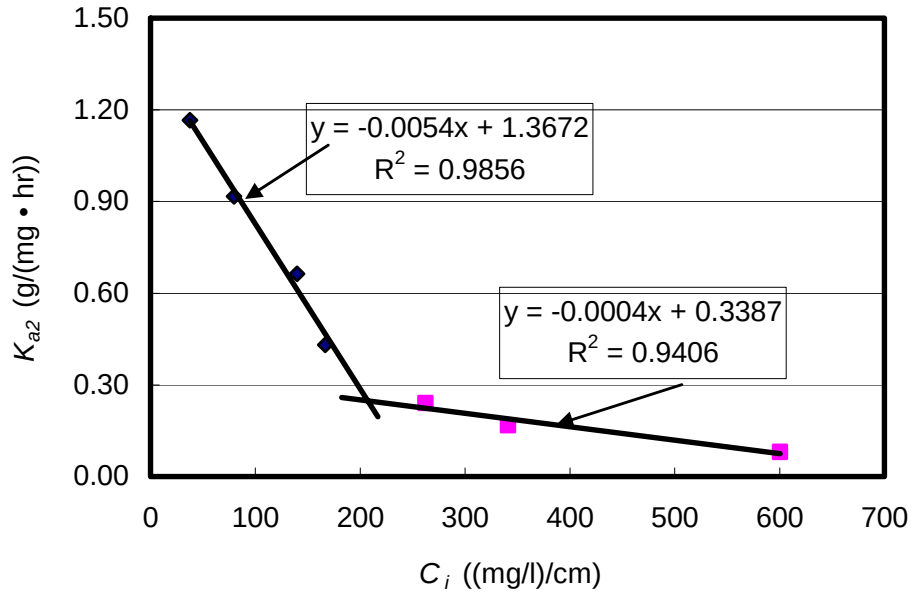


**Fig. 13. Pseudo-second-order kinetic rate coefficient as a function of length-normalized initial concentration of the CD solution.**

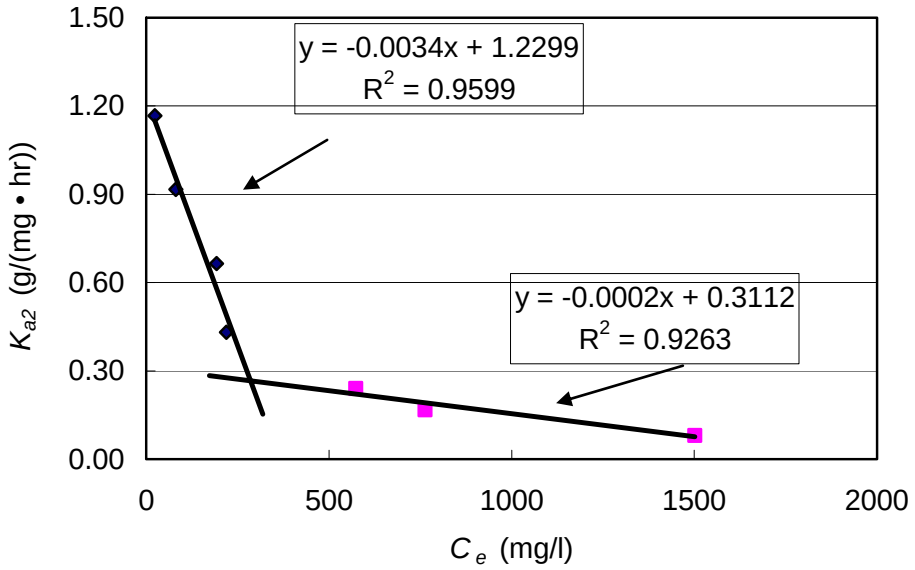


**Fig. 14. Pseudo-second-order kinetic rate as a function of the equilibrium concentration of the CD solution.**

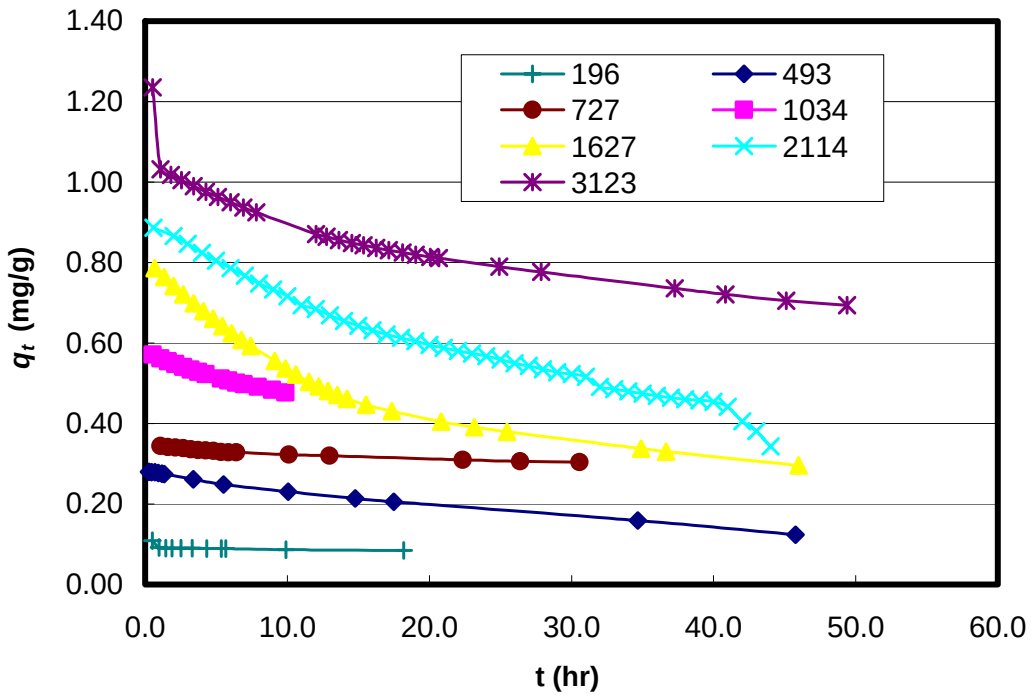


**Fig. 15. CD desorption from Berea sandstone at various flow rates.**

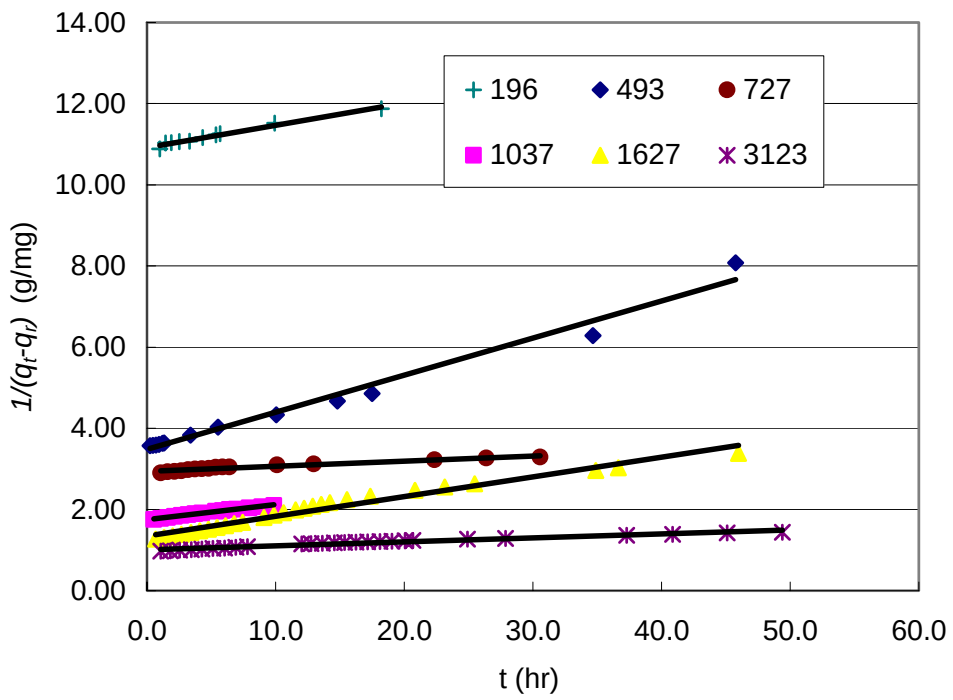


**Fig. 16 Modeling CD desorption using a pseudo-second-order desorption model.**

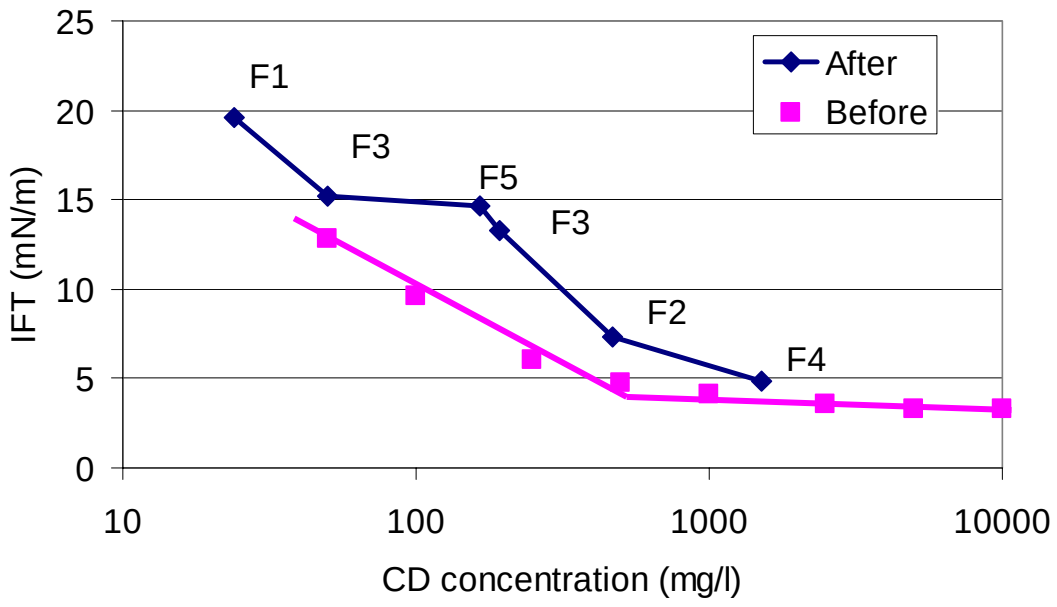


**Fig. 17. CD concentration effect on IFT before and after circulating CD through the core.**

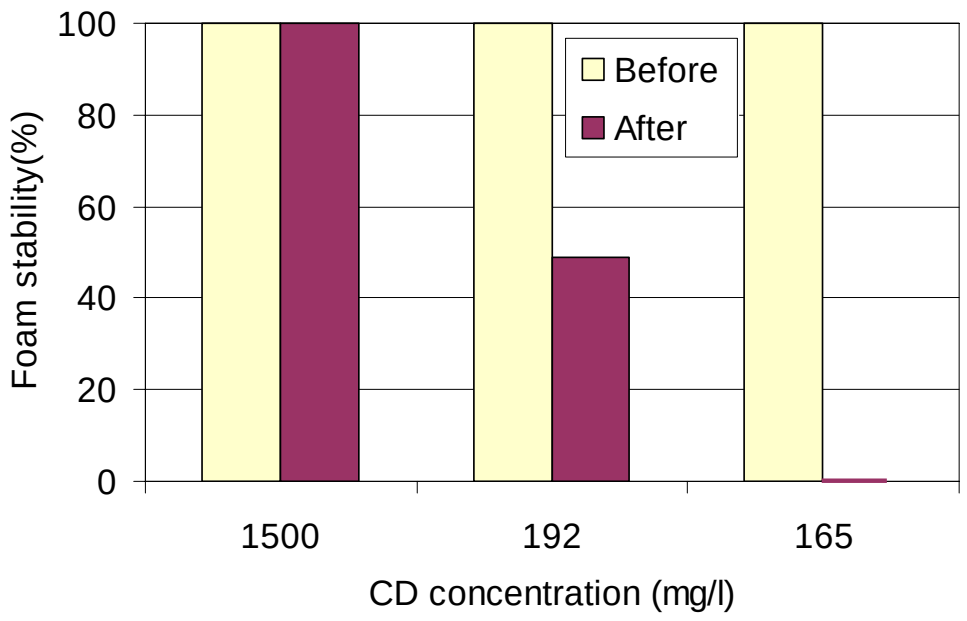


**Fig. 18. Adsorption effect on foam stability.**

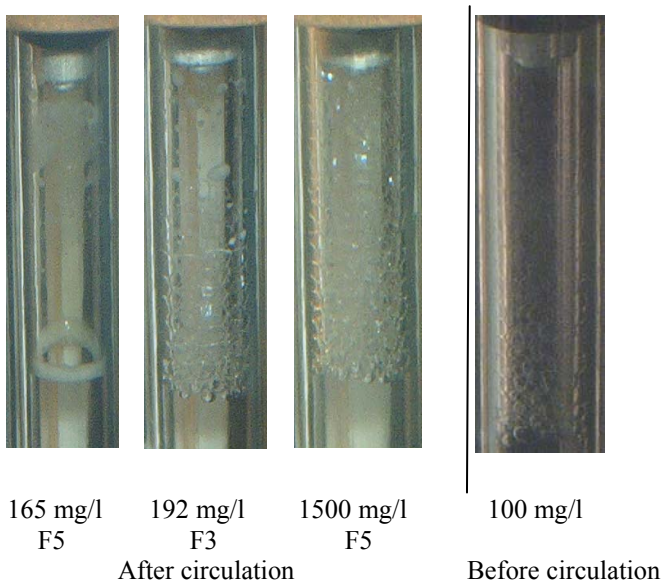


**Fig. 19. Foam images comparing foam stability using CD solution after and before core contact during the adsorption tests.**

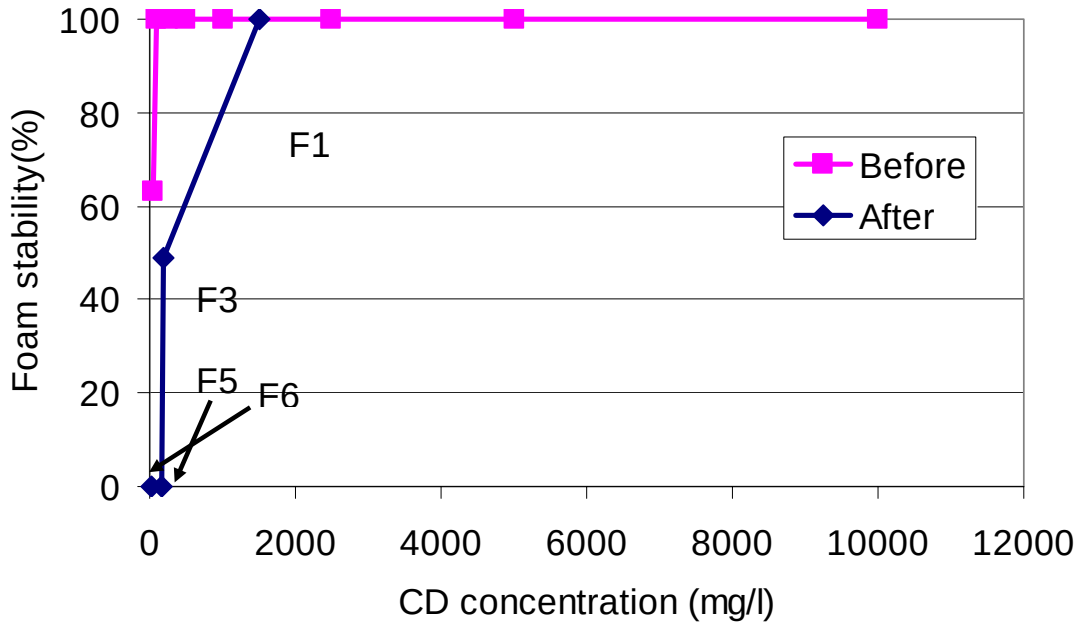


**Fig. 20. CD concentration effect on foam stability before and after adsorption.**

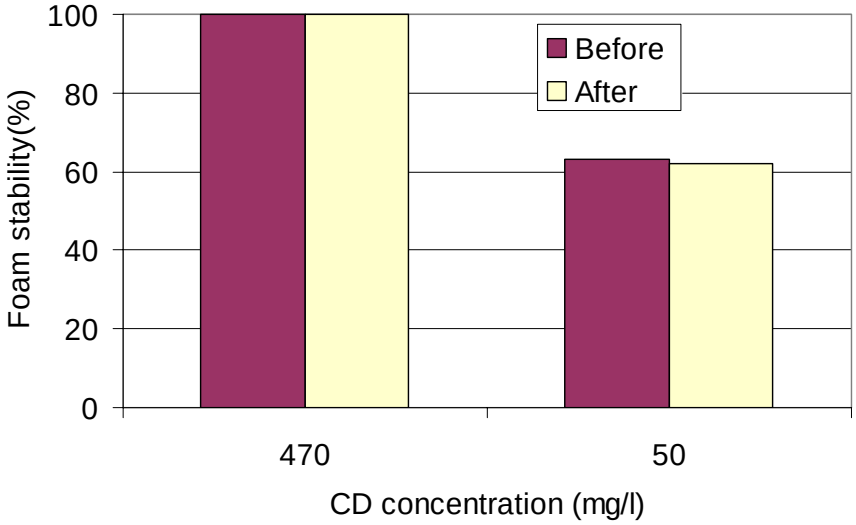


**Fig. 21. Desorption effect on foam stability.**

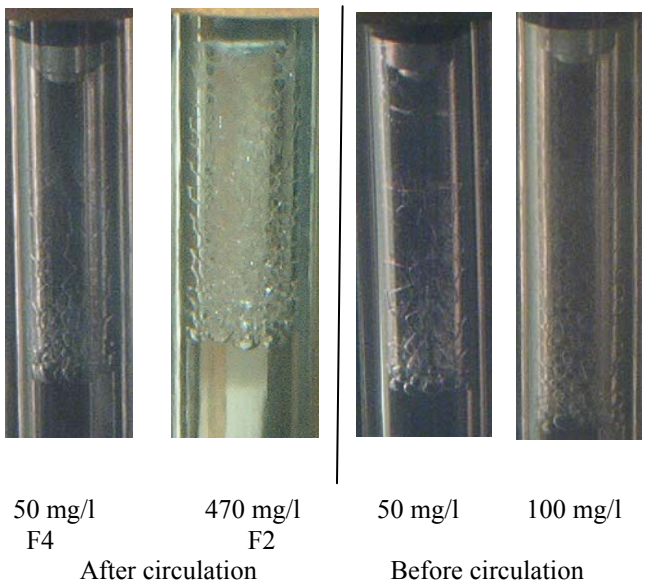


**Fig. 22. Foam images comparing foam stability using CD solution after and before core contact during the desorption tests.**

## Chapter 3: Study on Adsorption of Anionic Surfactant CD1045

### Introduction

This chapter covers current progress in understanding the adsorption behavior of CD solution prepared from 2% brine in relationship to the availability of surfactant. All the experiments were performed at atmospheric pressure and a temperature of 40°C. To estimate CD adsorption density and adsorption kinetics onto limestone, surfactant solution and powdered limestone were added together in test tubes. Then, the test tubes were set in a shaker and placed in an air bath. Samples of surfactant solution were taken from the test tubes over time to determine residual CD concentrations.

CD concentration was measured by using a spectrophotometer. Since CD does not absorb light in the range of 200–700 nm, indicator solution dimidium bromide disulphine blue was used to convert CD into a pink complex that has the characteristic absorbance in chloroform at 297 nm. Adsorption density was calculated by the following formula:

$$Ads = (Ci - Cf)*Ms/(Mc*1000), \quad \ldots\ldots\ldots\ldots\ldots\ldots\ldots\ldots \quad 9$$

Ads – CD adsorption density, mg/g

Ci, Cf – initial and final CD Concentration, ppm

Ms – mass of the surfactant solution, g

Mc – mass of the core sample, g

The final CD concentration is the residual CD concentration in the test tube when adsorption is finished and no change in surfactant concentration is observed over time. The adsorption experiments with weight ratio between surfactant solution and powdered limestone 1:1 showed that with the linear increase of surfactant concentration the surfactant adsorption density increases linearly over the range of 500 to 1250 ppm, as indicated in Fig. 23.

It was found that an increase in available volume of surfactant solution holding the initial CD concentration unchanged makes CD adsorption density increase. For crushed limestone, varying the CD concentration from 500 to 1250 ppm and the solution to rock ratios from 1:1 to 5:1 provides a fairly consistent relationship between the density of CD adsorbed on limestone and available mass of CD in the solutions (see Fig. 24).

From these CD concentrations and ratios, it can be concluded that CD adsorption density depends on the amount of CD available in the system—not the initial concentration of the surfactant. In order to estimate the rate of CD adsorption onto powdered limestone, samples of the CD solution were taken from test tubes at different time intervals to measure residual CD concentration. As shown in Fig. 25, CD adsorption ended about 10 minutes after CD solution was added to the powdered limestone. However, the majority of the surfactant was adsorbed almost immediately after the surfactant solution and the powdered rock were mixed.

To estimate CD adsorption density by its diffusion into limestone rock, cubes of limestone with the mass of approximately 130 g were used. Epoxy was applied over four sides of each cube leaving the two opposite sides of the cube uncovered. Each cube was saturated with surfactant-free brine and one of the uncovered sides was put in contact with the surfactant solution. The weight ratio between surfactant solution and limestone was 1 : 1 as it was in the initial adsorption experiments with powdered limestone. Samples of the surfactant solution were taken at different times to measure residual CD concentration until the system reached equilibrium. The data is summarized in Fig. 26.

The adsorption experiment with limestone cubes and powdered limestone showed that CD adsorption behavior is similar in both cases. However, the time it took to reach equilibrium concentration of CD in a test tube with powdered limestone was short (several minutes) compared to the time required in the no-flow case of limestone cubes (up to four weeks). This phenomenon can be explained by the slow diffusion of surfactant molecules towards the adsorption sites through the porous media. CD adsorption density on powdered limestone is probably higher compared to that on cubes, due to the larger surface area.

**Conclusion:**

1. CD adsorption in porous media is obviously a diffusion-controlled process.
2. CD adsorption density depends on the total amount of CD available in the system rather than the initial CD concentration.
3. The next stage of this research is to study the effect of the addition of calcium lignosulphonate into the system on the equilibrium CD concentration and CD adsorption density.

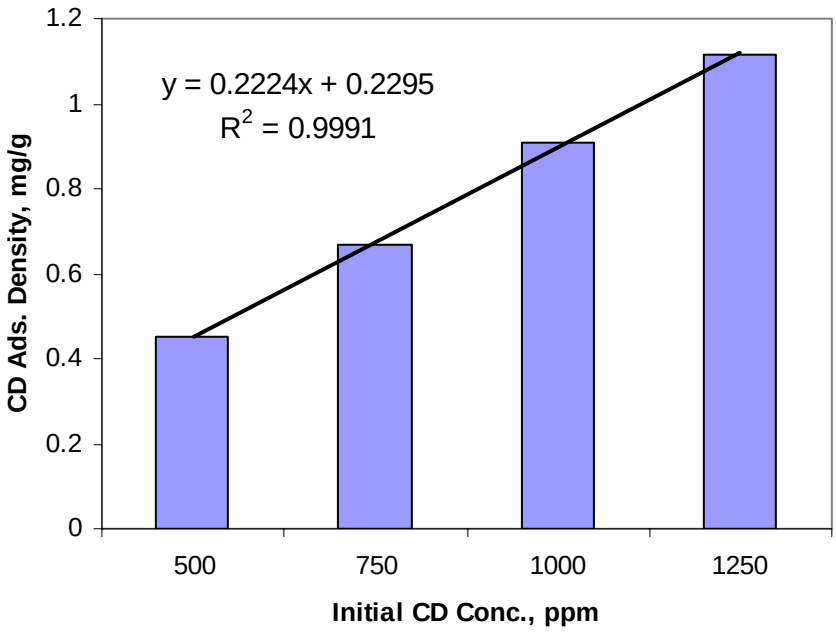


**Fig. 23. CD Adsorption density vs. initial CD concentration.**

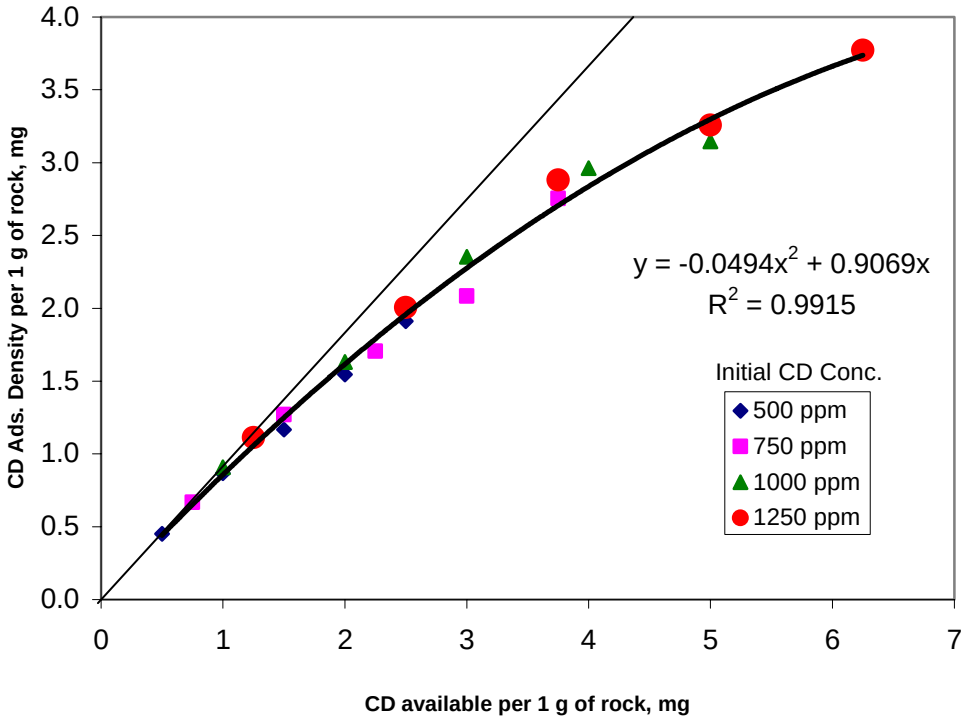


**Fig. 24. CD adsorption density vs. amount of CD available per 1 g of powdered limestone.**

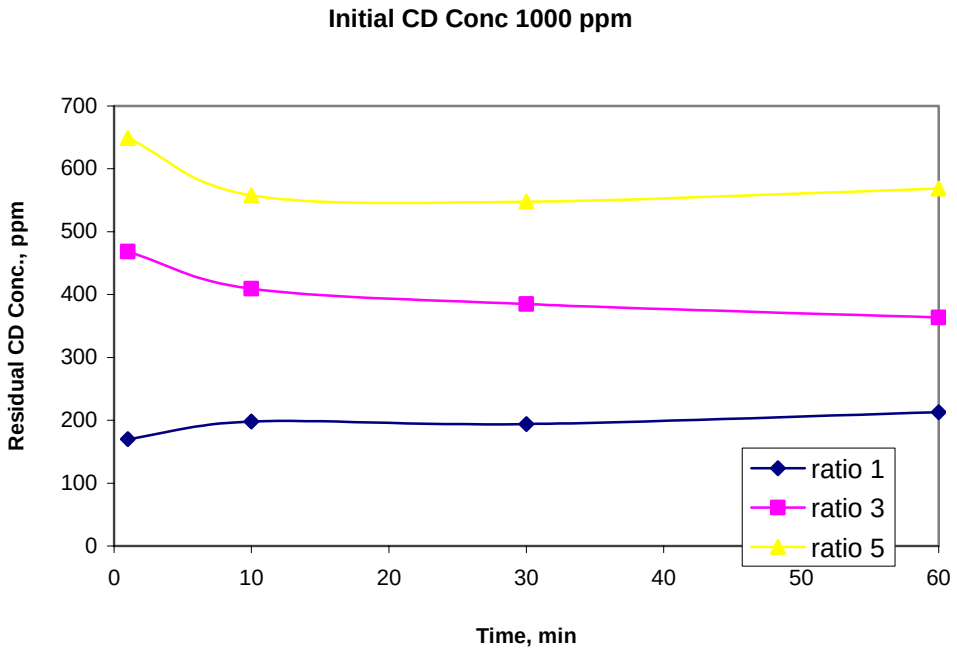


**Fig. 25. Rate of CD adsorption onto powdered limestone.**

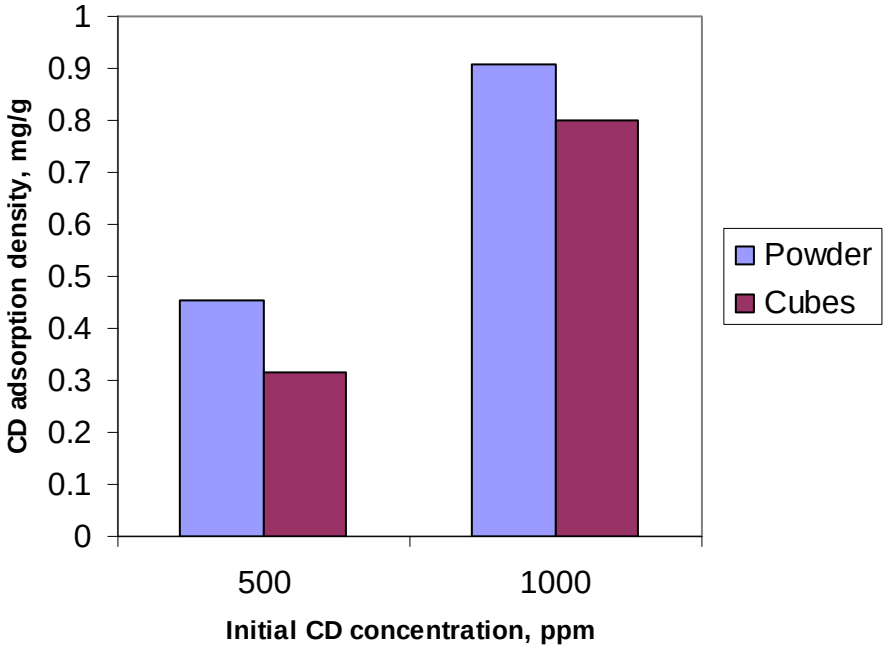


**Fig. 26. Comparison data for powdered limestone and cubes of limestone.**

## Chapter 4: Foam Mobility and Adsorption in Carbonate Core

### Introduction

Foam behavior and adsorption, presented in this chapter, are the two mechanisms that are required to model surfactant behavior in reservoirs. This study uses a commercial surfactant, nitrogen gas, and Indiana limestone, all at reservoir conditions of 10.34 MPa (1500 psi) and 40°C (104°F). Variables are surfactant concentration, flow rate and foam quality. At a constant gas flow rate, gas mobility slightly decreases with increasing foam quality when below the critical foam quality ($f_g$*) and increases with increasing foam quality above $f_g$*. Increased surfactant concentration leads to the decrease of gas mobility. Comparing co-injected surfactant and gas (CSG) with co-injected water and gas (CWG) shows that the mobility of CSG is an order of magnitude lower than that of CWG. Also, it took more time for CSG to reach steady state compared to CWG, even with a surfactant pad conditioning the core before surfactant and gas were co-injected.

There are no reservoirs that are really homogeneous. Porous media in the reservoir are characterized by size distribution of pores and pore throats, which leads to non-uniform displacement. The mobility of a single phase in porous media is inversely proportional to its viscosity (Darcy's law). Gases used in gas flooding (such as carbon dioxide, hydrocarbons, nitrogen, etc…) are normally less viscous (more than one order of magnitude less) and less dense than both water and crude oil, which results in gas channeling through the high permeability zones and gravity override. Thus, gas flooding normally has poor volumetric sweep efficiency, especially in an immiscible displacement, with the displacing phase being a lower viscosity.[111] Even in a homogeneous system, preferred channels are developed, as seen in glass bead laboratory systems and etched-glass micromodels. A need for mobility control in gas flooding has led to the study of foam flooding.

Foam is a colloidal dispersion in which a gas is dispersed in a continuous liquid phase.[112] Surfactants are added to the solution to stabilize foam by reducing interfacial tension. Many studies[83,86,113-119] demonstrated that surfactant-stabilized foam could drastically reduce gas mobility in porous media, consequently improving volumetric sweep efficiency and oil recovery.[118-124] In foam flooding, surfactant propagation is critical to foam propagation. A surfactant consists of both hydrophilic and hydrophobic parts. This unique characteristic of a surfactant molecule makes it vulnerable to adsorption onto rock. The total chemical loss in the porous medium is defined as system surfactant retention. Normally we think of the primary

contributor to retention being adsorption. In this work, adsorption will be considered as the *only* contributor to retention.

The objectives of this chapter are:

1. To study foam behavior in the carbonate core,
2. To analyze foam durability, adsorption and desorption at high pressure and temperature, and
3. To discuss their significance.

The results will be used to optimize foam quality and injection design for various applications in the petroleum industry, including brine or surfactant solution alternating gas (WAG or SAG) injection in the field.

## Experimental Setup and Procedures

**Materials.** Indiana limestone is a bioclastic grainstone that is rather uniform and homogeneous. In this paper, Indiana limestone was used in coreflooding experiments. A detailed description of the Indiana limestone is found in a previous publication.[125] The core is 5 in. long with diameter of 1.98 in. (see Table 8). Nitrogen is injected as the gas phase and surfactant solution or water is injected as the aqueous phase in our core flooding experiments. The surfactant used in this study was CD1045™ (CD), supplied by Chaser International as 46.7 wt% active aqueous solution. The critical micelle concentration of the CD is approximately 0.06 wt%.[46,47] Dimidium bromide-disulphine blue indicator, used for anionic surfactant determination, supplied by BDH Laboratory Supplies, was used to determine unknown CD concentrations and was described earlier.[39] Chloroform, HPLC grade, containing approximately 0.75% ethanol as a preservative was used as part of the process to determine CD concentrations.

**Apparatus.** The core flooding apparatus (Fig. 27) was designed and built to obtain the required information while varying foam quality, flow rate and surfactant concentration. A sapphire observation cell, 2.095 in. long, 0.315 in. ID and 0.375 in. OD, was placed at the end of the core to observe foam texture at test pressure and temperature. Three filters were placed in front of the core and acted as a foam generator and filter, the final and smallest aperture being 0.5 um. The coreholder can accommodate a core up to 2 in. in diameter and 24 in. long, with a maximum

working pressure of 10,000 psi and internal pressure taps. Four Honeywell pressure transducers were incorporated in the design to measure differential pressures across core segments.

**Experimental procedures.** All flooding tests were carried out at 40°C and 1500 psig core outlet pressure with 3100 psig overburden pressure. Pressure taps were set at 1 in. and 4 in. from the beginning of the core respectively. The entire core (5 in.) pressure drop (dp) and segment differential pressures across the inlet (a 1-in. segment (A, $dp_A$), the middle 3-in. segment (B, $dp_B$), and the final 1-in. segment (C, $dp_C$)) were recorded by four differential transducers. Two static pressure transducers were used to measure the core inlet and outlet pressures ($P_{in}$ & $P_{out}$, respectively), which could also be used as a backup for the entire core pressure drop.

The CD solution and $N_2$ injection were controlled by two ISCO syringe pumps, each through an accumulator. The core was evacuated and the water permeability was determined. The aqueous solution was filtered and degassed. To start the experiment, the desired gas and aqueous solution flow rates were set, and the computerized data-acquisition system started to collect pressure data of $P_{in}$ and $P_{out}$, pressure drop data of dp, $dp_A$, $dp_B$ and $dp_C$ and temperatures in the airbath, core holder and room.

Normally, each test interval stopped after the pressure drop through the core leveled out and the steady state of the flow was established. Next, either the solution conditions, gas to liquid injection ratio, or total flow rate was changed. At the end of a series of CD tests, the core was flushed with CD-free water until the pressure drop through the core was close to the core initial conditions at the same flow rate. The effluent from the core was collected to analyze the concentration of CD to determine the adsorption and desorption at reservoir conditions in the foam systems.

**Calculations.** The gas fraction ($f_g$) and foam quality are defined by the following equations:

$$f_g = \frac{q_g}{q_{g+w}} \quad \ldots\ldots\ldots\ldots\ldots\ldots\ldots\ldots\ldots\ldots\ldots\ldots 10$$

$$foam\ quality\ (\%) = f_g \times 100\% \quad \ldots\ldots\ldots\ldots\ldots\ldots\ldots\ldots\ldots 11$$

where $q_g$ is the gas flow rate in $cm^3$/sec, and $q_{g+w}$ is the total flow rate in $cm^3$/sec.

Many published studies[114,126-130] confirmed that the presence of foam did not affect the wetting-phase relative permeability. Darcy's law can be applied to calculate water relative permeability. Steady-state water saturations are different between foam and surfactant-free two-

phase flow under identical flow rate conditions, while the relation between the aqueous phase relative permeability, $k_{rw}$, and the aqueous saturation remains the same. But the non-wetting gas phase's relative permeability will be drastically reduced when foam is present in the porous media. Therefore, the gas mobility can be used as a measure for foam flow resistance in the porous media. Also, steady-state pressure gradients in the wetting phase and the non-wetting phase are the same. Thus, the gas mobility, $\lambda_g$, in md/cp can be calculated using Eq. 12 and is defined as the ratio of the gas Darcy (or superficial) velocity, $u_g$, or volume per time period per cross-sectional area of the core, $q_g/A$, in cm/sec divided by the average pressure gradient, dP/ds across the core in atm/cm after reaching a steady state as shown in Eq. 12,

$$\lambda_g = \frac{q_g/A}{dp/ds} \qquad \text{.....12}$$

**Two foam-flow regimes.** Figure 28 is a schematic plot for two foam-flow regimes.[130,131] The vertical dp/ds contours define the high foam quality regime, which is also known as the coarse foam regime. The horizontal contours define the low foam quality regime or stable foam regime. The mechanism behind Fig. 28 is the increase in capillary pressure with foam quality at constant gas flow rate. However, the capillary pressure, $P_c$, will increase up to a limiting value as $f_g$ increases. This limiting value is defined as the limiting capillary pressure, $P_c$*. The foam texture becomes coarser because the capillary pressure cannot exceed its $P_c$* with further $f_g$ increase.[133,134] In the high foam-quality regime, the pressure drop is independent of gas flow rate at constant liquid flow rate, which is controlled by $P_c$*. In the low foam-quality regime, the pressure gradient remains constant with changing liquid flow rate at constant gas flow rate. The transition zone between the two regimes is characterized by a specific value of the gas fraction, $f_g$*, which corresponds to the critical foam quality.

## Results and Discussion

**Surfactant adsorption and desorption at reservoir conditions.** Two series of experiments were carried out to study gas and surfactant concentration effects on surfactant adsorption (see Table 9). Co-injected surfactant and gas (CSG) without a CD pad injection mode is defined as surfactant and gas co-injected into 100% water-saturated core, while CSG with a CD pad injection mode is defined as surfactant and gas co-injected into a core where CD adsorption has been satisfied by an initial CD solution slug. Desorption was determined by injecting surfactant-free solution after CSG. The relation between effluent CD concentrations normalized to the

injecting CD solution concentration versus pore volumes (PV) of injected CD solution is shown in Fig. 29. The high initial concentration CD (2500mg/l) propagated through the core faster than the low initial concentration CD (500 mg/l). The high concentration CD front traveled faster, driven by diffusion force due to higher concentration gradient, and the increased availability of CD satisfied adsorption demand faster than the lower concentration solution. Each CD concentration had a test with and without gas present. During the initial adsorption part of each test at 500 mg/l CD concentration both with and without a CD pad, the results were within experimental accuracy (Fig. 29). The systems at 2500 mg/l also showed similar adsorption behavior. Therefore, with or without the presence of gas, CD adsorption behavior at reservoir conditions are similar (Fig. 29). Thus, the determination and study of surfactant adsorption with foam can be performed by surfactant solution only, which requires a simpler apparatus and less expense and time.

The behavior of CD desorption and adsorption for the 500 mg/l system are compared in Fig. 30. The effluent CD concentration drops rapidly after switching to the injection of CD-free solution. This rapid drop in produced CD with the long tail of low concentration corresponds to earlier studies in which desorption was seen to be slower than adsorption and not 100% reversible, at least in a comparable time frame to the adsorption.[42]

**Critical foam quality determination.** In order to determine critical foam quality $f_g$*, a series of coreflooding experiments were carried out at a constant gas flow rate of 22 cc/hr while varying the 2500 mg/l CD aqueous phase flow rate from 0.11 to 1000 $cm^3$/hr. The experiment sequence is outlined in Table 10. The relationship between gas mobility, $\lambda_g$, and the gas/liquid fractional flow, $f_g/1-f_g$, at constant gas Darcy gas velocity ($u_g$) of 22cc/hr is shown in Fig. 31. The plot is characterized by two straight lines intersecting at critical foam quality, $f_g$*. At lower values of $f_g$, gas mobility slightly decreases or remains constant with increasing $f_g$, while at higher $f_g$ the foam mobility increases with increasing $f_g$. The solid lines in Fig. 5 represent the trend obtained from experimental data, while the dashed lines represent the estimated trends from limited experimental data at lower constant gas Darcy velocities. Each data line represents a different constant $u_g$. The dashed lines were plotted based on the relation between mobility and $f_g$ at $u_g$ and assuming that $f_g$* has negligible change with $u_g$ and $f_g$* is a function of the characteristic surfactant formulation in the same rock. Therefore, the shape of mobility versus $f_g/(1-f_g)$ curve will be similar at different $u_g$. The experimentally determined $f_g$* is approximately 0.85$\pm$ 0.05.

In field applications, a high fg* surfactant system is desirable. When designing foam flooding for field application, higher foam quality will reduce the total amount of surfactant injected, thereby reducing operating cost. For CD solution, 85% foam quality must be considered maximum; however more surfactant would be required in a field application to ensure foam properties remain in the preferred strong foam regime (lower quality foam).

Critical foam quality for the entire core is compared with core segments in Fig. 32. Permeability and mobility values were determined for each of the core segments. The values for $f_g$* were 0.84, 0.85, and 0.85 for 21 md (the middle segment-B), 29md (the entire core), 53 md and (the ending segment-C) core, respectively (Fig. 32). Segment A (inlet) values are scattered (Fig. 32). Permeability of segment A increased over time presumable due to erosion and/or dissolution. The increased scatter in $\lambda_g$ for segment C at high $f_g/(1-f_g)$ is probably due to end effects at low $u_w$.

**Surfactant concentration effect on foam mobility.** Experiments were performed at a constant flow rate of 10 $cm^3$/hr while varying CD concentrations and foam qualities. The experimental strategies are listed in Table 11. Surfactants can lower the interfacial tension between gas and water, lower the surface energy, and increase the membrane strength. These factors contribute to improved foam stability with the characteristics of higher apparent viscosity and flow resistance in the porous media.

The curve of the gas mobility versus $f_g$ at a constant flow rate of 10 $cm^3$/hr and varying surfactant concentrations are plotted in Fig. 33. The results show that at a constant total flow rate, the gas mobility increases with $f_g$. The same trend was found in Fig. 34. The 24.75 and 7 cc/hr constant total flow rate data are derived from the different constant gas flow rate data shown in Fig. 31. This agreement again supports the previously outlined assumptions for determining $f_g$*.

The results plotted in Fig. 33 also demonstrate that increased surfactant concentration decreases foam mobility. When comparing CSG with co-injected water and gas (CWG), the mobility of CSG is an order of magnitude lower than that of CWG. This agrees with the foam theory and published results.[83,86,113-119] The time required to reach steady state was several times longer for CSG than for CWG. This is believed to be due both to the time required to reach equilibrium for surfactant adsorption and a larger displacement cross-sectional flow channel due to the higher apparent viscosity of the CSG system. Even with the longer time it took the CSG

solution to reach steady state, the system reached a pressure-differential steady state long before the effluent CD concentration was equal to the injection CD concentration. For example, differential pressure across the core reached a steady state when the effluent concentration was only about 9 mg/l compared to an injection concentration of 500 mg/l. Thus mobility steady state was reached before the adsorption plateau was achieved. This result is compatible with static foam stability experiments previously reported.[46] At 1500 psi and 40°C, the static foam durability tests demonstrated that weak foam can exist even at CD concentrations as low as 50 mg/l.[46] In foam flow tests in a porous medium, coalescence and regeneration are occurring, so even a foam of relatively short life span can be regenerating rapidly enough to result in significant mobility control. Again, this is a good implication for field applications.

The surfactant-free water and gas co-injection (CWG) experimental data was plotted into the contour plot (Fig. 35) and it was found that the $f_g$* in CWG is 0.1 compared to $f_g$* for CSG of 0.85 shown on a similar plot in Fig. 36. Values from the 1, 3, and 5 cc/hr gas flow tests shown in Fig. 5 were used to calculate the contours for the two flow regimes in Fig. 36 The value of $f_g$* in the surfactant system again demonstrates the advantage of foam flooding over surfactant-free gas, CWG or WAG floods.

**Summary**

1. At a constant gas flow rate, gas mobility slightly decreases with increasing foam quality when below the critical foam quality (fg*) and increases with increasing foam quality above $f_g$*.
2. Low gas mobility can be found over a wide range of foam qualities.
3. Increased surfactant concentration leads to the decrease of gas mobility. Comparing co-injected surfactant and gas (CSG) with co-injected water and gas (CWG) shows that the gas mobility of CSG is an order of magnitude lower than that of CWG.
4. Surfactant adsorption with gas present can be determined using surfactant solution alone, which lowers the expense due to simpler experimental setup and less time required.

**Nomenclature**

| | | |
|---|---|---|
| CD | = | surfactant Chaser CD1045™ |
| CSG | = | co-injection of surfactant solution and gas |
| CWG | = | co-injection of water and gas |
| SAG | = | surfactant solution alternating gas injection |
| WAG | = | water alternating gas injection |
| A | = | cross-sectional area of the core, $cm^2$ |
| dp/ds | = | pressure gradient, psi/cm |
| $f_g$ | = | gas fraction, fraction |
| $f_g$* | = | critical gas fraction, fraction |
| K | = | permeability, md |
| $P_c$ | = | capillary pressure |
| $P_c$* | = | limiting capillary pressure |
| Q | = | flow rate, $cm^3$/sec |
| $u_g$ | = | gas Darcy velocity, cm/sec |
| $u_w$ | = | aqueous Darcy velocity, cm/sec |
| $\lambda_g$ | = | gas mobility, md/cp |

**Table 8. The Properties of Indiana Limestone**

| Core | OD, in | Length, in | Pore Volume, cc | Porosity, % | Initial water permeability, md |
|---|---|---|---|---|---|
| 1 | 1.98 | 5.02 | 37.75 | 14.84 | 61.66 |
| 2 | 1.98 | 5.03 | 41.53 | 16.36 | 25.61 |

**Table 9. The Experimental Sequence for Adsorption and Desorption**

| Displacing fluid sequence | Determination | Injection strategy |
|---|---|---|
| (1)500mg/l CD | CD adsorption | CSG with CD pad |
| (2)500mg/l CD and $N_2$ | CD adsorption with $N_2$ presents | |
| (3)CD free water | Desorption | |
| (1)500mg/l CD and $N_2$ | CD adsorption with $N_2$ presents | CSG without CD pad |
| (2)CD free water | Desorption | |
| (1)2500mg/l CD | CD adsorption | CSG with CD pad |
| (2)2500mg/l CD and $N_2$ | CD adsorption with $N_2$ presents | |
| (3)CD free water | Desorption | |
| (1)2500mg/l CD and $N_2$ | CD adsorption with $N_2$ presents | CSG without CD pad |
| (2)CD free water | Desorption | |

**Table 10. The Core Experiment Strategy for fg* Determination**

| Running sequence | Gas flow rate, $cm^3/hr$ | 2500 mg/l CD flow rate, $cm^3/hr$ | fg |
|---|---|---|---|
| 1 | 22 | 0.11 | 0.995 |
| 2 | 22 | 0.22 | 0.99 |
| 3 | 22 | 0.58 | 0.974 |
| 4 | 22 | 1.22 | 0.947 |
| 5 | 22 | 2.75 | 0.889 |
| 6 | 22 | 11 | 0.667 |
| 7 | 22 | 22 | 0.5 |
| 8 | 22 | 44 | 0.333 |
| 9 | 22 | 88 | 0.2 |
| 10 | 22 | 1000 | 0.022 |

**Table 11. The Core Experiment Strategy for Determining Optimum fg at Constant Gas Flow Rate**

| CD concentration, mg/l | | | Flow rate, $cm^3/hr$ | | | fg |
|---|---|---|---|---|---|---|
| CWS | CSG | | Total | Gas | Liquid | |
| 0 | 500 | 2500 | 10 | 9 | 1 | 0.9 |
| 0 | 500 | 2500 | 10 | 7 | 3 | 0.7 |
| 0 | 500 | 2500 | 10 | 5 | 5 | 0.5 |
| 0 | 500 | 2500 | 10 | 3 | 7 | 0.3 |
| 0 | 500 | 2500 | 10 | 1 | 9 | 0.1 |

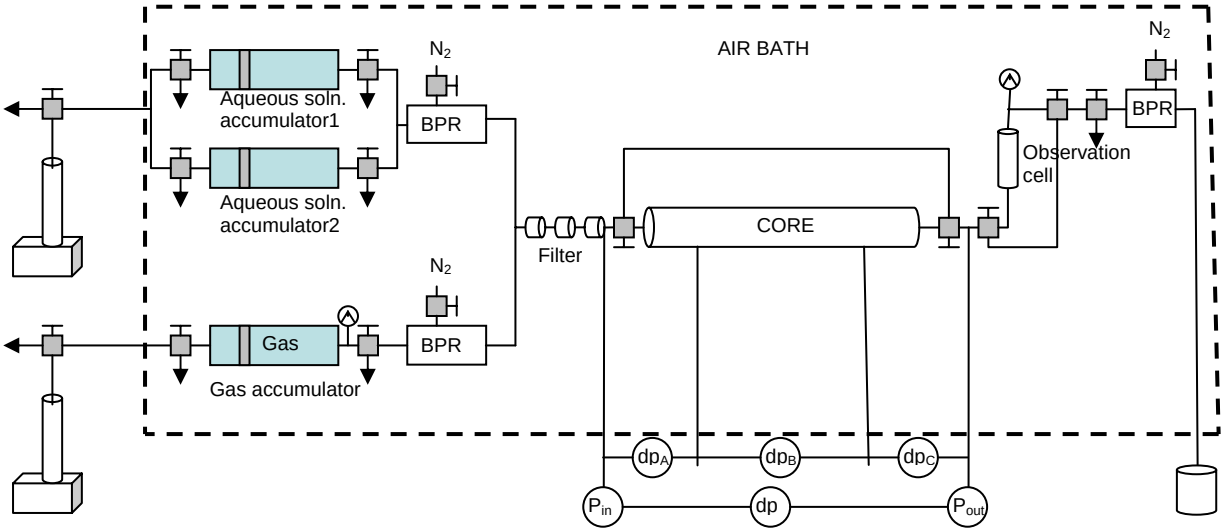


**Fig. 27. Schematic plot of core flooding setup.**

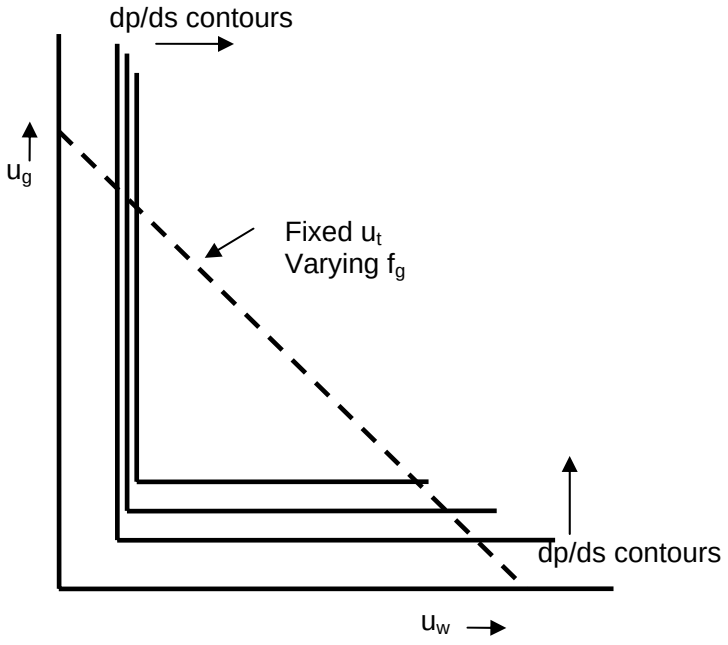


**Fig. 28. Two foam-flow regime.**[126,127]

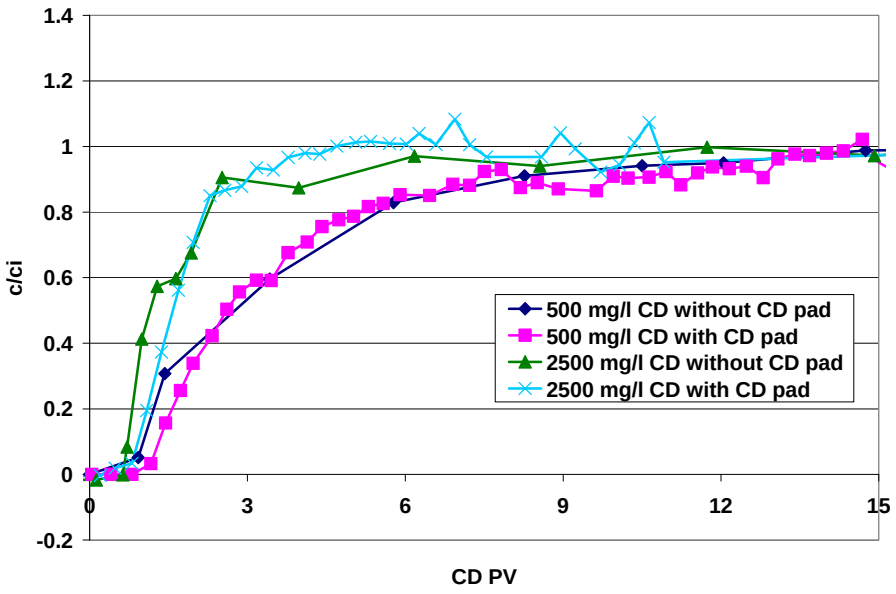


**Fig. 29. CD adsorption profile.**

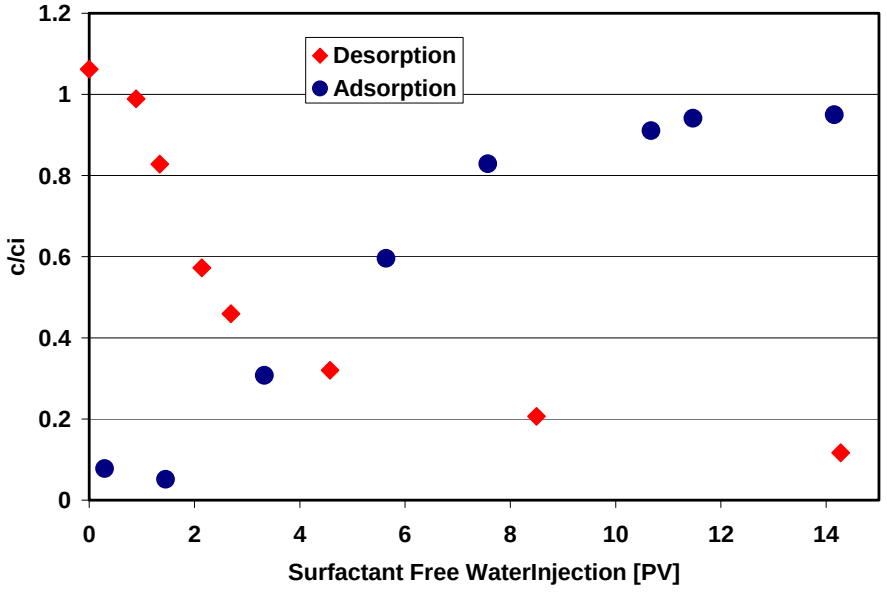


**Fig. 30. Comparison of CD adsorption and desorption profiles for 500 mg/l CD solution.**

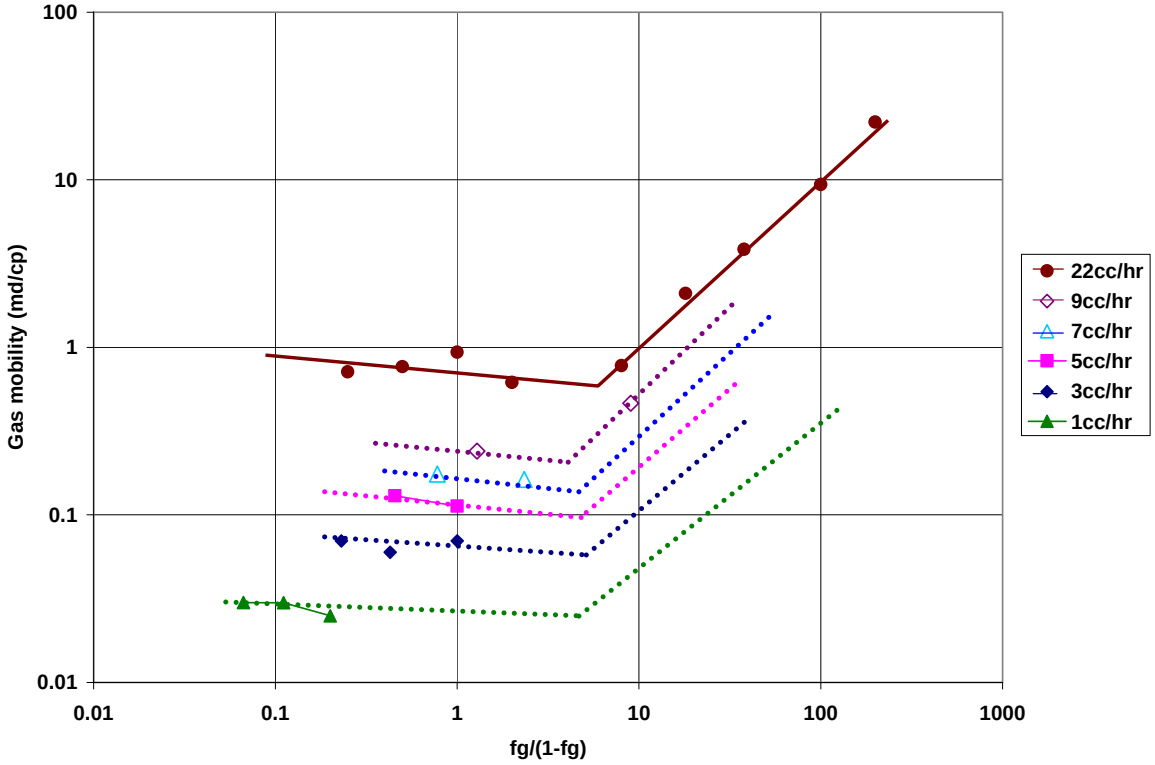


**Fig. 31. Determination of $f_g$* at constant $u_g$.**

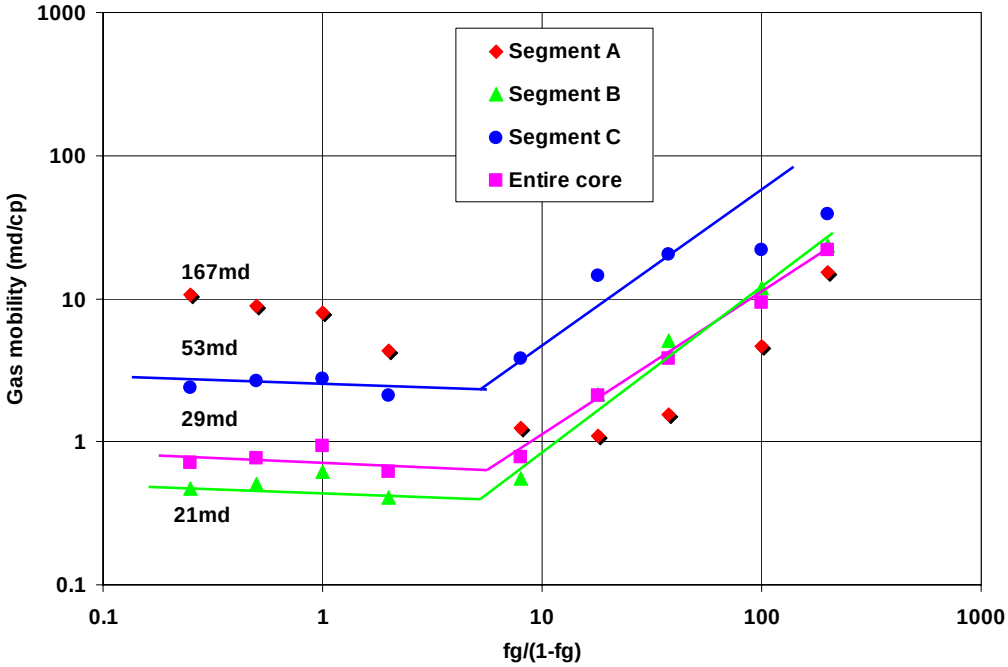


**Fig. 32. Permeability effect on $f_g$*.**

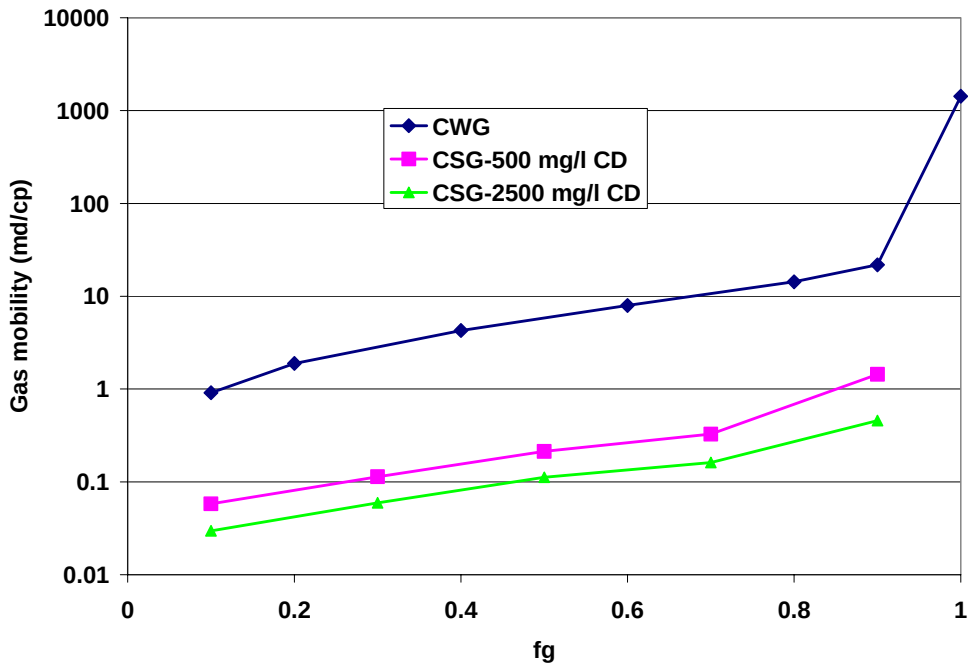


**Fig. 33. The relationship between foam quality and foam mobility at 10 $cm^3$/hr total flow rate as a function of surfactant concentration.**

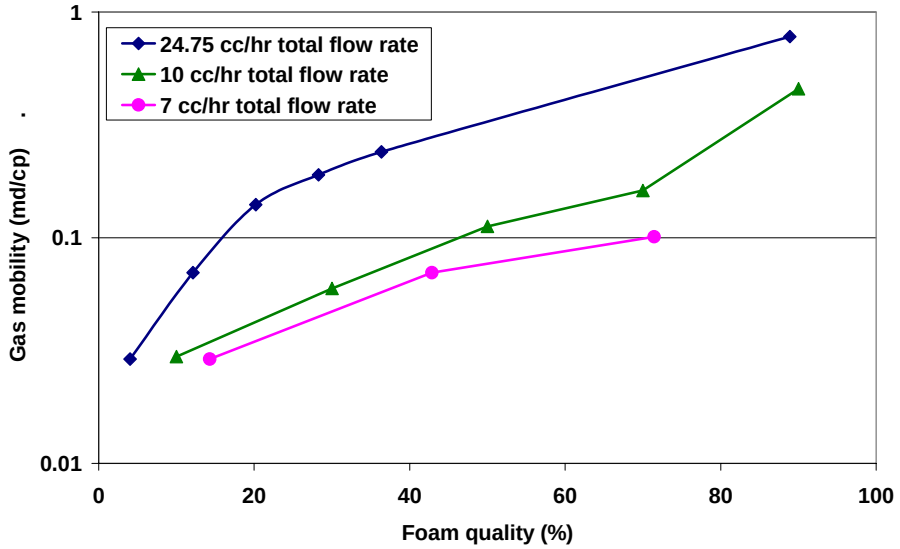


**Fig. 34. Comparison of mobility obtained for Fig. 31 at constant qt=7 and 24.75 $cm^3$/hr with mobility in Fig. 33 at qt=10 $cm^3$/hr at 2500 mg/l CD.**

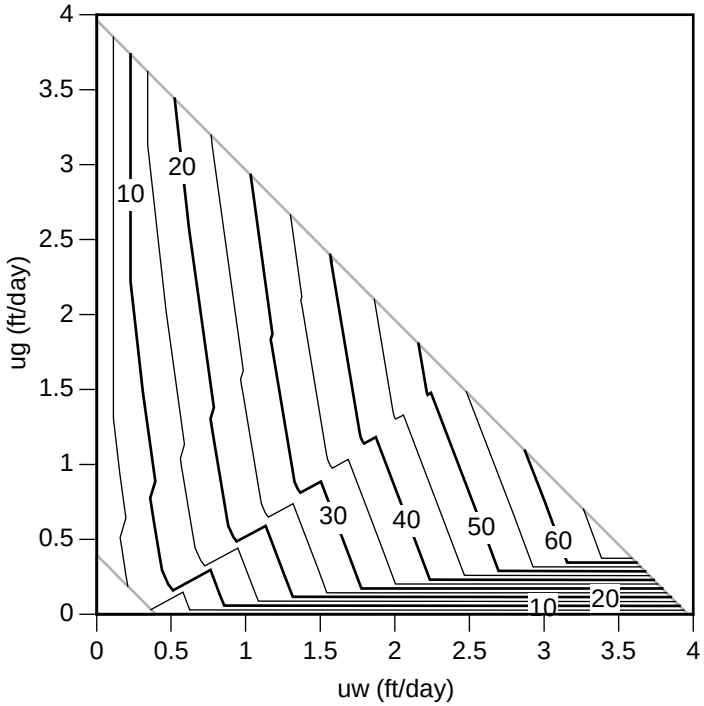


**Fig. 35. CWG dp/ds contours (psi/ft) vs aqueous and gas phases Darcy velocity (ft/day).**

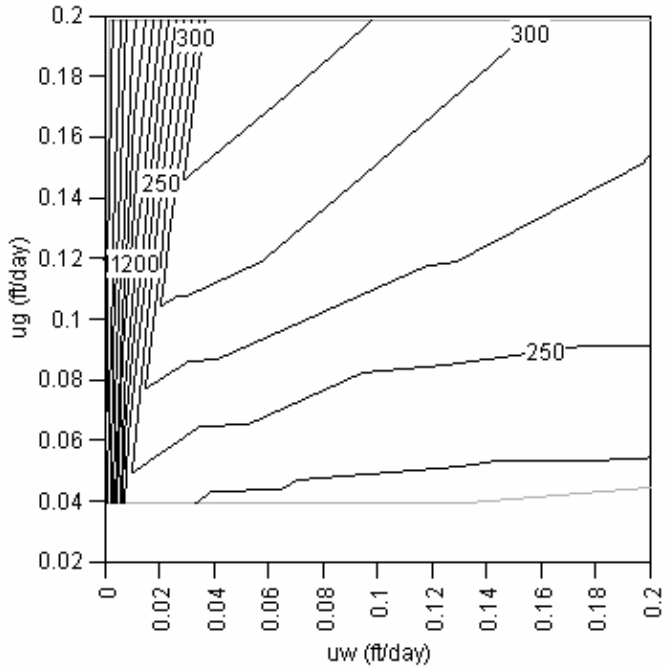


**Fig. 36. CSG dp/ds contours (psi/ft) vs. surfactant solution and gas phase Darcy velocity (ft/day).**

## Chapter 5: Partitioning of Surfactant in Oil and Aqueous Phases

### Introduction

Normally surfactant adsorption studies on surfaces have been performed in brine only or co-injection of surfactant and gas (CSG) mode without oil present. In the near future, our research project will focus on the foam behavior at reservoir condition in $CO_2$, surfactant solution and oil. To prepare for this, the partitioning analysis of the surfactant into the oil is required. In this paper, two series of experiments were performed with three different light oils and two types of surfactant.

Results from these experiments show that, if the mixture with surfactant and light oil is centrifuged the oil and emulsion phases are removed, the oil effect on the surfactant concentration is negligible. However, if the oil remains it will dissolve in the chloroform during concentration determination tests for the anionic surfactant and a significant effect of oil on reducing of the surfactant concentration will be observed. In addition, the more oil that is present, the more change in surfactant concentration. There are at least two mechanisms that will reduce surfactant concentration. The first is the adsorption of the surfactant on the rock surface, which is currently being studied. The second is the artitioning of the surfactant into an oil phase. This chapter presents the preliminary work in this study.

### Experimental Approach

**Chemicals.** Chaser$^{TM}$ CD1045 (CD) is the primary surfactant used in this study and was supplied by Chaser International as a 46.8 wt% active aqueous solution. The critical micelle concentration (CMC) of the CD is approximately 0.06 wt% (600 ppm). Calcium lignosulfonate (CLS), a weak foam-forming surfactant, was also used in the study and was obtained from the Georgia-Pacific Corporation. Calcium lignosulfonate is water soluble and is used as a sacrificial agent in $CO_2$ foam flooding to reduce the required primary-surfactant. Dimidium bromide-disulphine blue indicator, used for anionic surfactant determination, was supplied by BDH Laboratory Supplies. Chloroform, $CHCH_3$, HPLC grade, contains approximately 0.75% ethanol as a preservative and was used as a part of the process to determine CD concentration. The 2 wt% brine, used to prepare all surfactant solutions, was composed of 1.5 wt% NaCl, 0.5 wt% $CaCl_2$. Decane, obtained from Baker Analyzed Company, is a colorless light oil with chemical

formula of $C_{10}H_{22}$. Hexadecane, obtained through Aldrich Chemical Company, Inc., was 99+ wt% active solution; it is a colorless light oil with chemical formula of $C_{16}H_{34}$. O-xylene, obtained from Aldrich Chemical Company, Inc., is an aromatic light oil with a chemical formula of $C_8H_{10}$.

**Apparatus:** The spectrometer, model SPECTRONIC GENESYS™ 5, was used to measure the absorbance of the solution to determine surfactant concentration. The centrifuge, model IEC MODEL HN-SII, was used to separate phases.

**Experimental Procedure:** All the experiments were carried out at the room temperature (~77°F) and normal air pressure (~12.7 psia). Two series of experiments were performed in this study: series A and series B.

***Description of series A experiments:*** About 8.0 g of CD solution at concentrations of 1000 ppm and 500 ppm had from 1.0 to 24.0 g of decane added in 0.5 g increment. Each sample was shaken for 30 seconds to mix evenly. The sample was allowed to stand for at least 10 minutes for phase separation. The upper phase was a white, viscous emulsion. The lower phase was thought to be mostly the CD solution. The top phase was carefully removed until only the clear lower phase remained. The lower phase was then centrifuged for 10 minutes and then any remaining top phase was again removed. A sample of the lower phase was mixed with 7 ml of dimidium bromide-disulphine blue indicator, shaken 10 seconds, and then added to 7 ml of chloroform. This mixture was shaken vigorously for 30 seconds. This mixture was centrifuged for 10 minutes and the top phase removed. The absorbance of the bottom phase was determined using the spectrometer and tested at 295 nm. The absorbance values were compared to the calibration curve equation and the concentration of CD in the solution determined. The concentration of the initial decane-free CD solution was tested as the baseline.

This process was duplicated for two other light oils: hexadecane and o-xylene. Decane was also tested with 8.0 g of 2500 ppm CLS solution for each sample at various concentrations. Since CLS has a natural color it could be directly measured without adding the dye solution.

***Description of Series B experiments*:** In this series of tests 1.0 g of 500 ppm CD solution was used to incrementally add decane. The range of 0 to 24 wt% decane was used. At higher concentration absorption was too high. In each case, after decane was added the first stage to remove the oil phase was eliminated. Thus the dye and chloroform was added with free decane. The remaining procedure was identical to Series A.

**Results and Discussion**

Figure 37 illustrates the normalized CD initial and final concentration ratio versus the relative amount of decane in the decane-CD solution system. The results of Series A in Fig. 37 demonstrate that increasing decane into the 500 ppm or 1000 ppm CD solution, causes no dramatic change in CD concentration, but the concentration results seem to have a 10% scatter. This scatter is probably due to the additional steps and volatile components. However, in experimental Series B, as decane is increased the CD solution concentration appears to decrease. Due to the sensitivity of the spectrometer, CD absorbance could not be determined at high oil content. The plot in Fig. 37 shows that at the maximum percentage of decane tested, 24 wt%, the CD concentration decreased nearly 20%. Results indicate that there is interference when the decane phase is not removed before the indicator and chloroform are added. The more decane that is added, the more CD appeared to be lost from the aqueous solution.

To understand this behavioral interaction between the decane and CD solution, one additional experiment was performed with decane and chloroform. Ten samples were studied in total, among them; one sample was pure chloroform and another pure decane. The remaining eight samples were mixed with 8.0 g chloroform and each a different amount of decane. The samples were tested directly after each being shaken for 10 seconds. The results are shown in Fig. 38. From the plot, it can be seen that increasing of mass of decane, the absorbance of the chloroform-decane solution measured at 297 nm wavelength increased. However, the trend of the absorbance measured at 250 nm wave length was a decrease.

All the experimental procedures are similar for Series A and Series B except that the decane was removed in the former experiments but remained in the latter ones. Similar results were obtained in the experiments performed between CD and hexadecane or O-xylene (shown in Fig. 39) and for CLS and decane (shown in Fig. 40). Note that there are some points above the

base line. It is believe that this is the result of experimental scatter caused by the sensitivity of spectrometer and other factors such as human test errors.

Figure 40 illustrates that the scatter of the determined concentrations of CLS compared to the initial concentration was much less than that of CD. The procedure to test CLS is simpler and does not involve chloroform as does the procedure to determine the concentration of CD. Not having to use the indicator and volatile chloroform is probably the reason for the better precision.

## Conclusions

1. The evidence shows that the effect of light oil on partitioning of the CD solution can be negligible if the samples are centrifuged and the oil layer separated before adding the indicator and chloroform. However, the effect will be significant if the oil phase is not separated before adding the indicator and chloroform.
2. Future research will separate any oil phase before determining the surfactant concentration
3. The procedure for concentration determination of CLS is expected to be more accurate.
4. The method used in this study can be applied to sample analysis in the future oil recovery research.

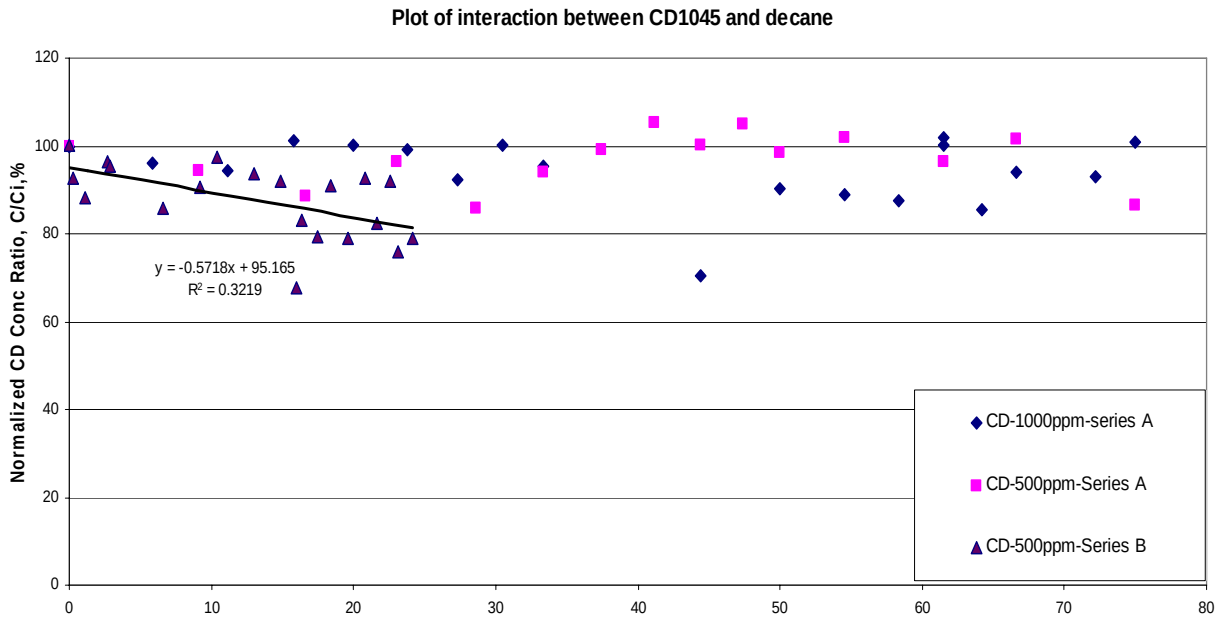


**Fig. 37. CD concentration normalized versus decane in the original system.**

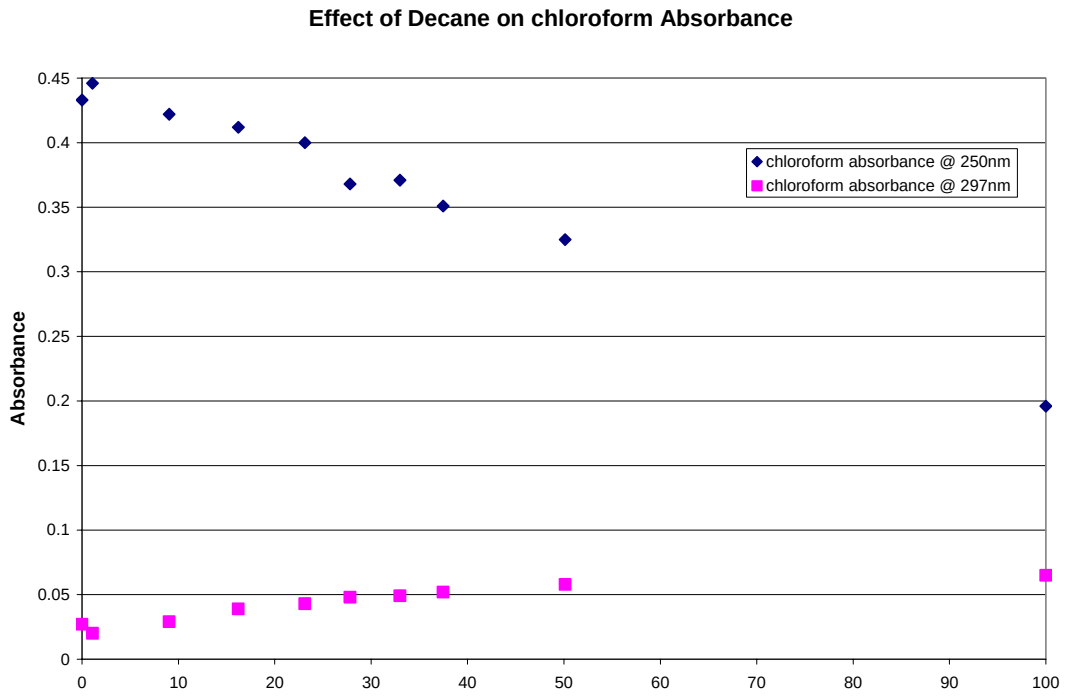


**Fig. 38. Absorption of chloroform at two wavelengths with dissolved decane.**

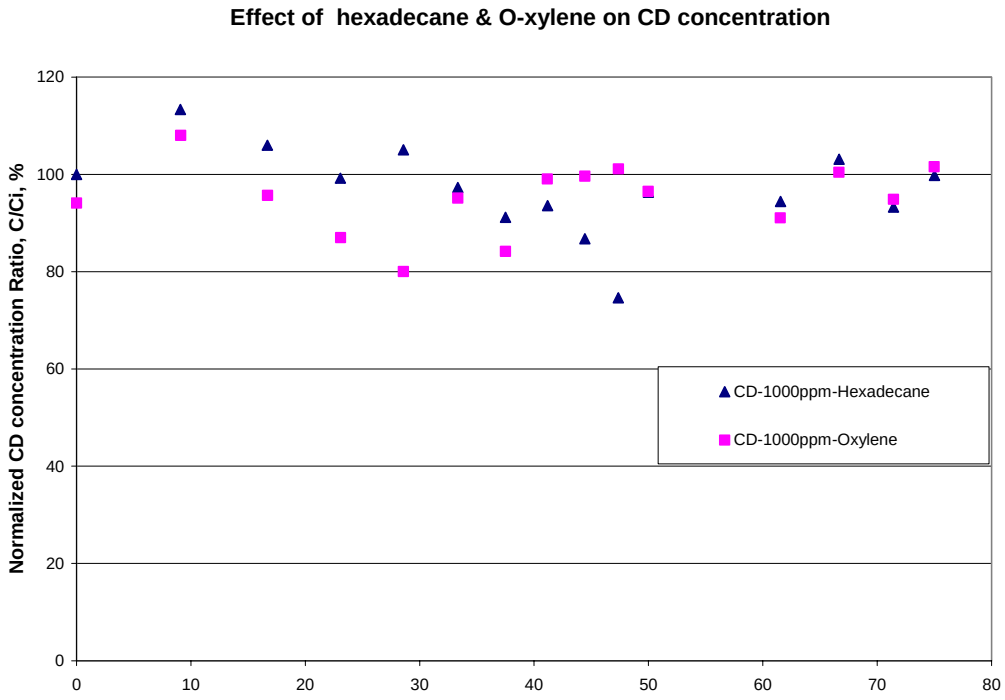


**Fig. 39. Normalized CD concentration with light oil in the original system.**

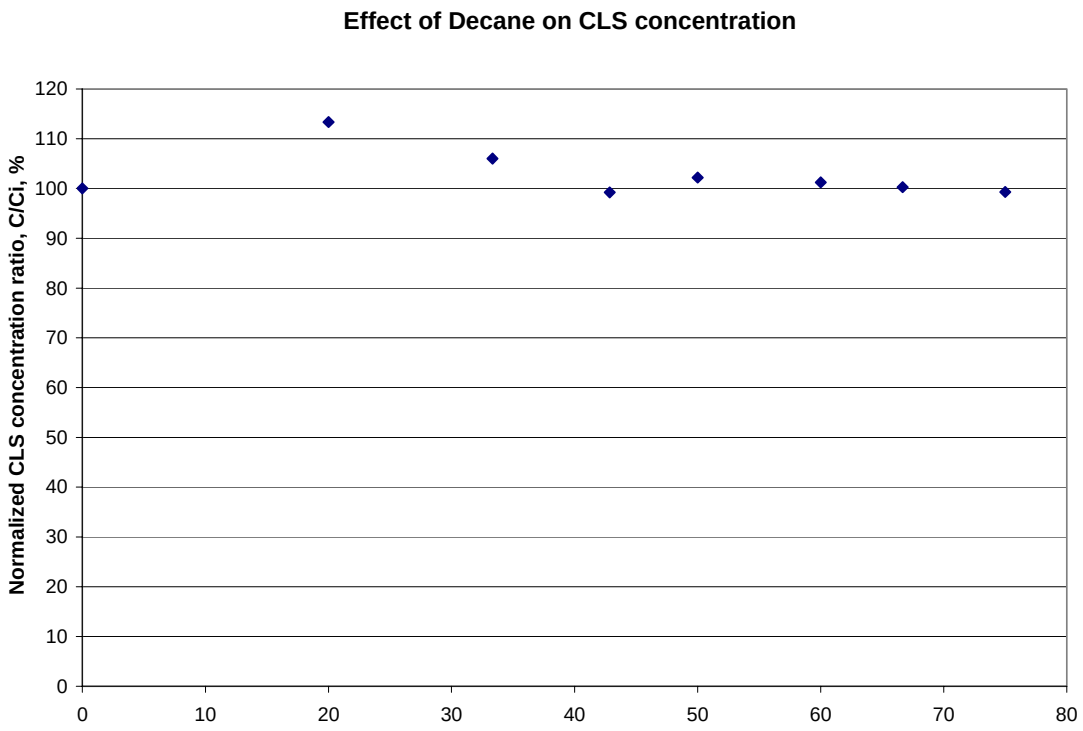


**Fig. 40. CLS concentration determinations with decane in the original mixture.**

## CONCLUSIONS

The conclusions achieved in the first year of research will be summarized by chapter in the following sections.

### Conclusions Chapter 1

Cores used in these experiments were relatively short (2.25 to 2.4 in.) and about 1.5 in. in diameter; therefore care must be taken when extrapolating results to reservoir scale. The conclusions:

1. A range of 0.2 to 0.3 PV fraction of $CO_2$ phase saturation was required to establish a $CO_2$ flow path, after which there was little brine production except through evaporation. $CO_2$ saturation can be increased by increasing flow rate, reducing pressure, and water evaporation.
2. At the end of $CO_2$ injection there was a relatively low $CO_2$ saturation and high brine saturation in the core, and no apparent reduction in $CO_2$ saturation was required to return to establish brine flow path. In the case of a water-wet system this and the previous conclusion are not surprising.
3. Brine is equilibrated with $CO_2$ in minutes over a relatively short distance.
4. In the systems tested, once $CO_2$ injection stopped, the $CO_2$ phase did not migrate and did not change except to the extent that unsaturated brine was available to dissolve $CO_2$.
5. The injection of brine into a 100% $CO_2$ phase required less than 0.3 PV fraction saturation to establish a brine flow path.

This is an ongoing work. We are presently looking at carbonate core and determining pore body and throat size distributions for each core type.

### Conclusions Chapter 2

1. CD adsorption onto Berea sandstone took several days to reach equilibrium. The adsorption process is characterized by a short period of fast adsorption followed by a long period of slow adsorption.
2. CD adsorption onto Berea sandstone can be described well by a pseudo-second-order adsorption kinetic model.

3. Increasing CD concentration increased CD adsorption density onto Berea sandstone. No plateau was found even when surfactant concentration is above its CMC, which indicates some other physical mechanisms may influence CD solution transport through Berea sandstone.
4. CD desorption from Berea sandstone can be fit well by a pseudo-second-order kinetic model.
5. At similar CD concentration, when compared with a CD solution before circulation, foam stability of CD solution after circulation decreased during adsorption, but remained similar level during desorption. This indicates a chromatographic separation when CD solution is transported through Berea sandstone, and the mechanisms for adsorption and desorption are different.

**Conclusions Chapter 3**

1. CD adsorption in porous media is obviously a diffusion-controlled process.
2. CD adsorption density depends on the total amount of CD available in the system rather than the initial CD concentration.

The next stage of this research is to study the effect of the addition of calcium lignosulphonate into the system on the equilibrium CD concentration and CD adsorption density.

**Conclusions Chapter 4**

1. At a constant gas flow rate, gas mobility slightly decreases with increasing foam quality when below the critical foam quality (fg*) and increases with increasing foam quality above $f_g$*.
2. Low gas mobility can be found over a wide range of foam qualities.
3. Increased surfactant concentration leads to the decrease of gas mobility. Comparing co-injected surfactant and gas (CSG) with co-injected water and gas (CWG) shows that the gas mobility of CSG is an order of magnitude lower than that of CWG.
4. Surfactant adsorption with gas present can be determined using surfactant solution alone, which lowers the expense due to simpler experimental setup and less time required.

**Conclusions Chapter 5**

1. The evidence shows that the effect of light oil on partitioning of the CD solution can be negligible if the samples are centrifuged and the oil layer separated before adding the indicator and chloroform. However, the effect will be significant if the oil phase is not separated before adding the indicator and chloroform.
2. Future research, will separate any oil phase before determining the surfactant concentration
3. The procedure for concentration determination of CLS is expected to be more accurate.
4. The method used in this study can be applied to the sample analysis in the future oil recovery research.

## ACKNOWLEDGEMENTS

Appreciation is expressed to the Department of Energy and the State of New Mexico for funding this work. Thanks to members of the New Mexico Petroleum Recovery Research center: Reid B. Grigg, Zhengwen Zeng, Baojun Bai, Yi Liu, Alexander Mikhalin, Guoqiang Yin, Ghislain E. Fai-Yengo, Peter Empey, Yusif Oni, Alvaro Nunez and Vignesh Proddaturi, who have contributed to this work. Also we would like to acknowledge Ms. Liz Bustamante for her assistance in editing this manuscript. For contributions from outside the PRRC we would like to acknowledge George Hirasaki at Rice University for his very helpful suggestions and Shinichi Sakurai, an Associate at the Bureau of Economic Geology, University of Texas at Austin.

## REFERENCES

1. Green, D.W. and White, G. P.: *Enhanced Oil Recovery*. (SPE Textbook Series), Midland, Society of Petroleum Engineers (1998).
2. Moritis, G.: "EOR Survey," *Oil & Gas Journal*, (15 April, 2002) 43-83.
3. Grigg, R.B. and Schechter, D.S., "State of the Industry in $CO_2$ Floods," paper SPE 38849, presented at the 1997 SPE Annual Technical Conference and Exhibition (ATCE), San Antonio, Oct. 5-8.

4. Dubois, M. K., et.al: "$CO_2$-Enhanced Oil Recovery, Co-Generation, Ethanol Production Linked," *The Class Act: DOE's Field Demonstration and Best Practices Newsletter* Vol. 8/2 (2002).
5. Grigg, R.B., et al.: "Improving $CO_2$ Efficiency for Recovering Oil In Heterogeneous Reservoirs," First Annual Technical Report, US DOE Contract No. DE-FG26-01BC15364 (2003).
6. Malik, Q.M. and Islam, M. R.: "$CO_2$ Injection in the Weyburn Field of Canada: Optimization of Enhanced Oil Recovery and Greenhouse Gas Storage with Horizontal Wells," paper SPE 59327 presented at the 2000 SPE/DOE Improved Oil Recovery Symposium, Tulsa, April 3-5.
7. Grigg, R.B., et al.: "Improved Efficiency of Miscible $CO_2$ Floods and Enhanced Prospects of $CO_2$ Flooding Heterogeneous Reservoirs," Final Technical Report, US DOE Contract No. DE-FG22-94BC14977 (1998).
8. Grigg, R.B., et al.: "Improved Efficiency of Miscible $CO_2$ Floods and Enhanced Prospects of $CO_2$ Flooding Heterogeneous Reservoirs," First Annual Technical Report, US DOE Contract No. DE-FG26-97BC15047 (1998).
9. Grigg, R.B., et al.: "Improved Efficiency of Miscible $CO_2$ Floods and Enhanced Prospects of $CO_2$ Flooding Heterogeneous Reservoirs," Second Annual Report, US DOE Contract No. DE-FG26-97BC15047 (1999).
10. Grigg, R.B., et al.: "Improved Efficiency of Miscible $CO_2$ Floods and Enhanced Prospects of $CO_2$ Flooding Heterogeneous Reservoirs," Final Report, US DOE Contract No. DE-FG26-97BC15047 (2001).
11. Grigg, R.B., et al.: "Improved $CO_2$ Efficiency for Recovering Oil in Heterogeneous Reservoirs," Second Annual Technical Report, DOE Contract No. DE-FG26-01BC15364 (2003).
12. Grigg, R.B.: "Improved $CO_2$ Efficiency for Recovering Oil in Heterogeneous Reservoirs," Third Annual Report for DOE contract no. DE-FC26-01BC15364 (2004).
13. Grigg, R.B.: "Improved $CO_2$ Efficiency for Recovering Oil in Heterogeneous Reservoirs," Final Report for DOE contract no. DE-FC26-01BC15364 (2005).
14. Rogers, J.D. and Grigg, R.B.: *SPE Reservoir Eval. & Eng.*, Vol. 5, No. 5.
15. Svec, R.K. and Grigg, R.B.: SPE 71496, 2001 SPE ATCE, New Orleans, October.

16. Grigg, R.B.: SPE 80228, 2003 International Symposium on Oilfield Chemistry (ISOC).
17. Grigg, R.B., et al.: The Second Annual DOE Sequestration Conference, Washington, D.C., 5-8 May 2003.
18. Grigg, R.B. and Svec, R.K.: SCA2003-19, 2003 International Symposium of the Society of Core Analysts, Pau, France, 21-24 September.
19. Grigg, R.B., Svec, R.K., Peter C. Lichtner, P.C., Carey, W., and Lesher, C.E.: "$CO_2$/Brine/Carbonate Rock Interactions: Dissolution and Precipitation," prepared and presented at the Fourth Annual Conference on Carbon Capture & Sequestration, Alexandria, 2-5 May 2005.
20. Svec, R.K. and Grigg R.B.: "Reservoir Characterization and Laboratory Studies Assessing Improve Oil Recovery Methods for the Teague-Blinebry Field," paper SPE 59550 presented at the 2000 SPE Permian Basin Oil and Gas Recovery Conference, Midland, March 21–23.
21. Westrich, H. R., et al.: "Sequestration of $CO_2$ in a Depleted Oil Reservoir: An Overview," paper presented at the U.S. DOE First National Conference on Carbon Sequestration, May 14-17, 2001, Washington D.C.
22. Zeng, Z., Grigg, R.B. and Ganda, S.: "Experimental Study of Overburden and Stress Influence on Non-Darcy Gas Flow in Dakota Sandstone," paper SPE 84069 presented at the 2003 ACTE, Denver, Oct. 5-8.
23. Grigg, R.B. and Hwang, M.K., "High Velocity Gas Flow Effects in Porous Gas-Water System," paper SPE 39978 presented at the 1998 SPE Gas Technology Symposium, Calgary, March 15-18.
24. Grigg, R.B., Zeng, Z. and Bethapudi, L.V.: "Comparison of Non-Darcy Flow of $CO_2$ and $N_2$ in a Carbonate Rock," paper SPE 89471 presented at the 2004 SPE/DOE IOR, Tulsa, April 17–21.
25. Zeng, Z., Grigg, R.B. and Gupta, D.B.: "Laboratory Investigation of Stress-Sensitivity of Non-Darcy Gas Flow Parameters," paper SPE 89431 presented at the 2004 SPE/DOE IOR, Tulsa, April 17–21.
26. Grigg, R.B. and Siagian, U.W.R.: "Understanding and Exploiting Four-Phase Flow in Low-Temperature $CO_2$ Floods," paper SPE 39790 presented at the 1998 SPE PBOGR, Midland, March 23–26.

27. Zeng, Z-W. and Grigg, R.: "A Criterion for Non-Darcy Flow in Porous Media," *Transport in Porous Media* (2006) **63**: 57-69.

28. Siagian, U.W.R. and Grigg, R.B.: "The Extraction of Hydrocarbons from Crude Oil by High Pressure $CO_2$," paper SPE 39684 presented at the 1998 SPE/DOE IOR, Tulsa, April 19–22.

29. Chang, S-H., et al.: "Characterization and Multiphase Equilibrium Prediction of Crude Oil Heavy Components," *Fuel Science and Technology Intl.*, (1996) 14(1&2) 179-201.

30. Taber, J.J.: "Technical Screening Guides for the Enhanced Recovery of Oil," paper SPE 12069 presented at the 1983 ATCE, San Francisco, Oct. 5-8.

31. Taber, J.J., et al.: "EOR Screening Criteria Revisited - Part 1: Introduction to Screening Criteria and Enhanced Recovery Field Projects," *SPERE*, (August 1997), 189-198.

32. Taber, J.J., et al: "EOR Screening Criteria Revisited—Part 2: Applications and Impact of Oil Prices," *SPERE*, (August 1997), 199-205.

33. Grigg, R.B., et al.: "Effect of Pressure on Improved Oilflood Recovery From Tertiary Gas Injection," *SPERE* (August 1997) 179-187.

34. Chang, S-H and Grigg, R.B.: "Effects of Foam Quality and Flow Rate on $CO_2$-Foam Behavior at Reservoir Temperature and Pressure," *SPERE* (June 1999) 2(3), pages 248-254.

35. Grigg, R. B., et al.: "Cost Reduction and Injectivity Improvements for $CO_2$ Foams for Mobility Control," paper SPE 75178 presented at the 2002 SPE/DOE IOR, Tulsa, April 13-17.

36. Tsau, J-S., et al.: "Smart Foam to Improve Oil Recovery in Heterogeneous Porous Media," paper SPE 39677 presented at the 1998 SPE/DOE IOR, Tulsa, April 19–22.

37. Syahputra, A.E., et al.: "Laboratory Evaluation of Using Lignosulfonate and Surfactant Mixture in $CO_2$ Flooding," paper SPE 59368 presented at the 2000 SPE/DOE IOR, Tulsa, April 3-5.

38. Tsau, J.-S., et al.: "Use of Sacrificial Agents in $CO_2$ Foam Flooding Application," paper SPE 56609 presented at the 1999 SPE ATCE, Oct. 3–6.

39. Tsau, J.S. and Heller, J.P.: "Evaluation of Surfactants for $CO_2$-Foam Mobility Control," paper SPE 24013 presented at the 1992 Permian Basin Oil and Gas Recovery Conference, Midland, March 18-20.

40. Tsau, J.-S., et al.: "Use of Mixed Surfactants to Improve Mobility Control in CO Flooding," paper SPE 39792 presented at the 1998 PBOGR, Midland, March 23–26.

41. Grigg, R.B. and Bai, B.: "Calcium Lignosulfonate Adsorption and Desorption on Berea Sandstone," Journal *of Colloid and Interface Science*, 279 (2004) 36-45.

42. Grigg, R.B. and Bai, B.: "Sorption of Surfactant Used in $CO_2$ Flooding onto Five Minerals and Three Porous Media," paper 93100 presented at the 2005 SPE International Symposium on Oilfield Chemistry, Houston, Feb. 2-4.

43. Bai, B. and Grigg, R.B.: "Kinetics and Equilibria of Calcium Lignosulfonate Adsorption and Desorption onto Limestone," paper 93098 presented at the 2005 SPE International Symposium on Oilfield Chemistry, Houston, Feb. 2–4.

44. Grigg, R.B., Bai, B., and Liu, Y.: "Competitive Adsorption of Hybrid Surfactant System onto Five Minerals, Berea Sandstone, and Limestone," paper SPE 90612 presented at the 2004 SPE ATCE, Houston, Sep. 26-29.

45. Grigg, R.B. and Bai, B.: "Calcium Lignosulfonate Adsorption and Desorption on Berea Sandstone," Journal *of Colloid and Interface Science*, 279 (2004) 36-45

46. Liu, Y., Grigg, R.B., and Svec, R.K.: "$CO_2$ Foam Behavior: Influence of Temperature, Pressure, and Concentration of Surfactant," paper 94307 presented at the 2005 SPE Production and Operations Symposium, Oklahoma City, 17-19 April.

47. Liu, Y., Grigg, R.B., and Bai, B.: "Salinity, pH, and Surfactant Concentration Effects on $CO_2$ Foam," paper 93095 presented at the 2005 SPE International Symposium on Oilfield Chemistry, Houston, Feb. 2-4.

48. Martin, F.D., et al.: "$CO_2$-Foam Field Verification Pilot Test at EVGSAU Injection Project Phase I: Project Planning and Initial Results," paper SPE 24176 presented at the 1992 SPE/DOE IOR, Tulsa, April 22-24.

49. Tsau, J.S., et al.: "$CO_2$ Foam Field Verification Pilot Test at EVGSAU: Phase IIIA—Surfactant Performance Characterization and Quality Assurance," paper SPE 27785, presented at the 1994 SPE/DOE IOR, Tulsa, April 17-20.

50. Stevens, J. E., and Martin, F. D.: "$CO_2$ Foam Field Verification Pilot Test at EVGSAU: Phase IIIB—Project Operations and Performance Review," paper SPE 27786 presented at the 1994 SPE/DOE IOR, Tulsa, April 17-20.

51. Harpole, K.J., et al.: "$CO_2$ Foam Field Verification Pilot Test at EVGSAU: Phase IIIC—

Reservoir Characterization and Response to Foam Injection," paper SPE 27798 presented at the 1994 SPE/DOE IOR, Tulsa, April 17-20.

52. Martin, F.D., et al.: "$CO_2$-Foam Field Test at the East Vacuum Grayburg/San Andres Unit," *SPERE* (November 1995) 10(4), 266-272.

53. Chang, S.-H. and Grigg R.B.: "History Matching and Modeling the $CO_2$-Foam Pilot Test at EVGSAU," paper SPE 39793 presented at the1998 SPE PBOGR, March 23–26.

54. Putra, E., et al.: "Reservoir Simulation of Waterflood Pilot in Naturally Fractured Spraberry Trend," paper SPE 54336 presented at the 1999 Asia Pacific Oil and Gas Conf. and Exhibition, April 20–22.

55. Schechter, D.S, et al.: "Wellman Unit CO2 Flood: Reservoir Pressure Reduction and Flooding the Water/Oil Transition Zone," paper SPE 48948 presented at the 1998 SPE ATCE, Sept. 27–30.

56. Sung, A.H., et al.: "An Application of Fuzzy Logic in Interpretation of Log Curves," In: *Proc*., 1999 IASTED Inter. Conf. on Artificial Intelligence and Soft Computing (ISC'99) 364–369.

57. Chang, S.H., et al.: "Use of MASTER Web to Improve History Matching," paper SPE 62617 presented at the 2000 SPE/AAPG Western Regional Meeting, Jun 19–22.

58. Rossen, W.R., "Foam in Porous Media," in Sadoc, J.F. and Rivier, N. ed., *Foams and Emulsions*, Kluwer Academic Publishers, 1999.

59. Rossen, W.R.: "Rheology of Foam in Porous Media at the 'Limiting Capillary Pressure'," *Revue de l'Institut Français du Pétrole* **47**, 68 (1992).

60. Rossen, W.R. and Zhou, A.H.: "Modeling foam mobility in porous media," *SPE Adv. Technol*. **3**, 146 (1995).

61. Kam, S. I., and Rossen, W. R.: SPE 77698, 2002 SPE ATCE, San Antonio, 29 Sept. - 2 Oct.

62. Rossen, W.R., et al.: *SPE Journal*, 4, 279-287 (Sept. 1999).

63. Zeilinger, S.C., et al.: "Simplified Mechanistic Modeling of Foam Processes for Improved Oil Recovery," In: *Proc.* 8th European Symposium on Improved Oil Recovery, Vienna, Austria, May 15-17 1995.

64. Shi, J.-X. and Rossen, W.R.: "Simulation and Dimensional Analysis of Foam Processes in Porous Media," *SPERE,* 1, 148-154 (April 1998).

65. Zhou, Z.H. and Rossen, W.R.: "Applying Fractional-Flow Theory to Foam Processes at the "Limiting Capillary Pressure"," *SPE Adv. Technol.* **3**, 154 (1995).

66. Rossen, W.R.: "Foams in Enhanced Oil Recovery," in Prud'homme, R.K. and Khan, S. ed., *Foams: Theory, Measurements and Applications*, Marcel Dekker, New York, 1996.

67. Hill, A.D. and Rossen, W.R.: "Fluid Placement and Diversion in Matrix Acidizing," paper SPE 27982 presented at the Proc. Tulsa/SPE Centennial Petroleum Engineering Symposium, Aug. 29-31, 1994.

68. Mamun, C. K., et al.: "Extending Foam Technology from Improved Oil Recovery to Environmental Remediation," paper SPE 77557 presented at the 2002 SPE ATCE, San Antonio, Sept. 29–Oct. 2.

69. Tanzil, D., et al.: "Mobility of Foam in Heterogeneous Media: Flow Parallel and Perpendicular to Stratification," *SPEJ*, 203-212 (June 2002).

70. Tanzil, D., et al.: "Conditions for Foam Generation in Homogeneous Porous Media," paper SPE 75176 presented at the 2002 SPE/DOE IOR, Tulsa, April 13-17.

71. Hirasaki, G. and Zhang, D.L.: "Surface Chemistry of Oil Recovery from Fractured, Oil-Wet, Carbonate Formation," paper SPE 80988 presented at the 2003 SPE ISOC, Houston, Feb. 5-8.

72. Hirasaki, G.J., et al.: "Surfactant/Foam Process for Aquifer Remediation," paper SPE 37257 presented at the 1997 SPE ISOC, Houston, Feb. 18-21.

73. Szafranski, R., et al: "Surfactant/Foam Process for Improved Efficiency of Aquifer Remediation," *Progr Colloid Polym Sci.* (1998) 111:162-167.

74. Enick, R.M., et al.: "Direct Thickeners for Carbon Dioxide," paper SPE 59325 presented at the 2000 SPE/DOE IOR, Tulsa, April 3-5.

75. Heller, J.P., et al.: "Field Test of $CO_2$ Mobility Control at Rock Creek**,"** paper SPE 14395 presented at the 1985 SPE ATCE, Las Vegas, Sept.22-25.

76. Jonas, T. M., et al.: "Evaluation of a $CO_2$ Foam Field Trial: Rangely Weber Sand Unit," paper SPE 20468 presented at the 1990 SPE ATCE, New Orleans, Sept. 23-26.

77. Chou, S. I., et al.: "$CO_2$ Foam Field Trial at North Ward-Estes," paper SPE 24643 presented at the 1992 SPE ATCE, Washington, DC, Oct. 4-7.

78. Hoefner, M. L., et al.: "$CO_2$ Foam: Results From Four Developmental Field Trials," paper SPE/DOE 27787 presented at the 1994 SPE/DOE IOR, Tulsa, April 17-20.

79. Holm, L.W. and Garrison, W.H.: "$CO_2$ Diversion with Foam in an Immiscible $CO_2$ Field Project**,"** *SPERE* (February 1988), Vol. 3, No. 1, 112-118.

80. Kuhlman, M. I., et al..: "Gas/Oil Lamellae and Surfactant Propagation in the Oil in Carbon Dioxide Foam," paper SPE/DOE 27788 presented at the 1994 SPE/DOE IOR, Tulsa, April 17-20.

81. Bernard, G.G., et al.: "Use of Surfactant to Reduce $CO_2$ Mobility in Oil Displacement," *SPEJ* (August 1980) 281-292.

82. Wellington, S.L. and Vinegar, H. L.: "CT Studies of Surfactant-induced CO2 Mobility Control," paper SPE 14393 presented at the 1985 SPE ATCE, Las Vegas, Sept. 22-25.

83. Lee, H.O., Heller, J.P., and Hoefer, A.M.W.: "Change in. Apparent Viscosity of $CO_2$ Foam with Rock Permeability," *SPERE* (Nov. 1991) 421-428.

84. Tsau, J.S. and Heller, J.P.: "Evaluation of Surfactants for $CO_2$-Foam Mobility Control," paper SPE 24013 presented at the 1992 SPE PBOGR, Midland, March 18-20.

85. Yaghoobi, H. and Heller, P. J.: "Laboratory Investigation of Parameters Affecting $CO_2$-Foam Mobility in Sandstone at Reservoir Conditions," paper SPE 29168 presented at the 1994 SPE Eastern Regional Conference and Exhibition, Charleston, Nov. 8-10.

86. Heller, J.P., Lien, C.L, and Kuntamukkula, M.S.: "Foamlike Dispersions for Mobility Control in $CO_2$ Floods," *SPEJ* (August 1985) 603-613.

87. Yaghoobi, H. and Heller, J.P.: "Effect of Capillary Contact on $CO_2$-Foam Mobility in Heterogeneous Core Samples," paper SPE 35169 presented at the 1996 SPE PBOGR, Midland, March 27-29.

88. Hanssen, J. E., and Dalland, M.: "Foams for Effective Gas Blockage in the Presence of Crude Oil," paper SPE 20193 presented at the 1990 SPE/DOE IOR, Tulsa, April 22-25.

89. Aarra, M. G., and Skauge, A.: paper SPE 18599 presented at the 1994 SPE ATCE, New Orleans, Sept. 25-28.

90. Hornof, V.: "Applications of Lignosulfonates in Enhanced Oil-Recovery," *Cellulose Chemistry and Technology*, (May–June 1990) vol. 24, no. 3, 407-415.

91. Hong, S. A., et al.: "An Evaluation of Lignosulfonate as a Sacrificial Adsorbate in Surfactant Flooding," *SPERE* (February 1987) 17-27.

92. Hong, S. A., and Bae, J. H.: "Field Experiment of Lignosulfonate Preflushing for Surfactant Adsorption Reduction**,** *SPERE* (November 1990) 467-474.

93. Kalfoglou, G., et al.: "Sacrificial Agents for Carbon Dioxide Foaming Agents," Canadian Patent 2,185,499.

94. Taber, J.J.: "Environmental Improvements and Better Economics in EOR Operations," *In Situ* (1990) 14(4), 345-404.

95. Stalkup, F. I.: "Miscible Displacement," SPE Monograph No. 8, New York (1983).

96. Cheng, L., et al.: "Simulating Foam Processes at High and Low Foam Qualities," paper SPE 59287 presented at the 2000 SPE/DOE IOR. Tulsa, April 2-5.

97. Shan, D. and Rossen, W.R.: "Optimal Injection Strategies for Foam IOR," paper SPE 75180 presented at the 2002 SPE/DOE IOR. Tulsa, April 13-17.

98. Tsau, J.-S. and Heller, J.P.: "Evaluation of Surfactants for $CO_2$-Foam Mobility Control**,"** paper SPE 24013, 1992 PBOGR, Midland, March 18-20.

99. Moritis, G.: "EOR/Heavy Oil Survey—Special Report" and "2006 Worldwide EOR Survey," *Oil & Gas Journal*, (April 17, 2006) **104:15**, 37-57.

100. Wiebe R. and Gaddy, V.L.: "The Solubility for Carbon Dioxide in Water at Various Temperatures from 12 to 40°C and at Pressure to 500 Atmospheres. Critical Phenomena," *J Amer. Chem. Soc.*, Vol. 62, 815-817, (April 1940).

101. Enick, R.M.: "$CO_2$ Solubility in Water and Brine under Reservoir Conditions," *Chem. Eng. Comm.* (1990), Vol. 90, pp 23-33.

102. Tsau, J.S., and Grigg, B.R.: "Assessment of Foam Properties and Effectiveness in Mobility Reduction for $CO_2$-foam Floods," paper SPE 37221 presented at the SPE international Symposium on Oilfield Chemistry, Houston, February 18-21, 1997.

103. Tsau, J.S. and Heller, J.P.: "Evaluation of Surfactants for $CO_2$-Foam Mobility Control," paper SPE 24013 presented at the Permain Basin Oil and Gas Recovery Conference, Midland, March 18-20, 1992.

104. Azizian, S.: "Kinetics Models of Sorption: a Theoretical Analysis," Journal of Colloid and Interface Science, 276(August 2004), p.1 47-52.

105. Rengaraj, S., et al.: "Removal of Copper from Aqueous Solution by Aminated and Protonated Mesoporous Aluminas: Kinetics and Equlibrium," *Journal of Colloid and Interface Science*, 273 (2004), 14-21.

106. Tsai, W.T., Lai, C. W., and Hsien, K.J.: "Adsorption Kinetics of Herbicide Paraquat from Aqueous Solution onto Activated Bleaching Earth," Chemosphere 55 (2004), p.829–837.

107. Ozcan, A.S. and Ozcan, A.: "Adsorption of Acid Dyes from Aqueous Solution onto Acid-Activated Bentonite," *Journal of Colloid and Interface Science*, 276(August 2004), No. 1, p.39-46.

108. Zhang, Z. and Bai, R.: "Mechanisms and Kinetics of Humic Acid Adsorption onto Chitosan-Coated Granules," *Journal of Colloid and Interface Science*, 264 (2003), p. 30-38.

109. Demirbas, E.: "Adsorption Kinetics for the Removal of Chromium (VI) from Aqueous Solutions on the Activated Carbons Prepared from Agricultural Wastes," *Water SA* 30(2004), 533-539.

110. Biswas, S.C. and Chattoraj, D.K.: "Kinetics of Adsorption of Cationic Surfactants at Silica-Water Interface," *Journal of Colloid and Interface Science,* 205 (1998), 12-20.

111. Pariani, G.J. et al.: "An Approach to Optimize Economics in a West Texas $CO_2$ Flood," *JPT* (September 1992) 984; *Trans*., AIME, 293.

112. Schramm, L.L.: *Foams: Fundamentals and Applications in the Petroleum Industry*, American Chemical Society, Washington, DC (1994).

113. Fried, A.N: "The Foam Drive Process for Increasing the Recovery of Oil," Report RI-5866, U.S. Bureau of Mines, Washington, DC (1961).

114. Bernard, G. G., Holm, L. W., and Jacobs, W. A.: "Effect of Foam on Trapped Gas Situation and on Permeability of Porous Media to Water," *SPEJ* (Dec. 1965) 295-300; *Trans.*, AIME, 234.

115. Heller, J.P. and Taber, J.J: "Mobility Control for $CO_2$ Floods-A Literature Survey," topical report, U.S. DOE Contract No. DE-AC21-79MC10689 Washington, DC (October 1980).

116. Marsden, S.S et al.: "Use of Foam in Petroleum Operations," *Proc*., Seventh World Pet. Cong., Mexico City (1966); Elsevier Press, Essex, England, 3, 235-242.

117. Marsden, S.S: "Foam in Porous Media," topical report, U.S. DOE Contract No. DE-AC03-81SF11564 (SUPRI TR-49) Washington, DC (May 1986)

118. Hirasaki, G.J.: "The Steam-Foam Process," *JPT* (May 1989) 449.

119. Hirasaki, G.J.: "Supplement to SPE 19505, The Steam-Foam Process-Review of Steam-Foam Process Mechanisms," paper SPE 19518, Richardson, TX (1989).

120. Bernard, G. G., Holm, L. W., and Harvey, C. P.: "Use of Surfactant to Reduce $CO_2$ Mobility in Oil Displacement," *SPEJ* (August 1980) 281-292.

121. Wellington, S.L. and Vinegar, H.L.: "CT Studies of Surfactant to Reduce $CO_2$ Mobility Control," paper SPE 14393 presented at the 1985 SPE Annual Technical Conference, Las Vegas, Sept. 22-25.

122. Dilgren, R.E., Deemer, A.R., and Owens, K.B.: "Laboratory Development and Field Testing of Steam Foams for Mobility Control in Heavy Oil Reservoirs," paper SPE 10774 presented at the 1980 SPE California Regional Meeting, San Francisco, March 24-26.

123. Holm, L.W. and Garrison, W. H.: "$CO_2$ Diversion Using Foam in an Immiscible $CO_2$ Field Project," *SPERE* (February 1988) 112-118; *Trans.*, AIME, 285.

124. Mohammadi, S.S. and McCollum, T.J.: "Steam-Foam Project in Guadalupe Field, California," paper SPE 15054 presented at the 1986 SPE California Regional Meeting, Oakland, and April 2-4.

125. Svec R.K. and Grigg, R.B.: "Physical Effects of WAG Fluids on Carbonate Core Plugs," paper SPE 71496 presented at the 2001 SPE Annual Technical Conference and Exhibition, New Orleans, Sep. 30–Oct. 3.

126. Holm, L.W.: "The Mechanism of Gas and Liquid Flow through Porous Media in the Presence of Foam," *SPEJ*. (1968) 8(4), 359-369.

127. Friedmann, F.: "Some Parameters Influencing the Formation and Propagation of Foams in Porous Media," paper SPE 15087 presented at the SPE 1986 California Regional Meeting, Oakland, April 2–4.

128. Sanchez, J.M., Schechter, R. S.; Monsalve, A.: "The Effect of Trace Quantities of Surfactant on Nitrogen/Water Relative Permeabilities," paper SPE 15446 presented at the 1986 SPE Annual Technical Conference and Exhibition, New Orleans Oct. 5–8.

129. Huh, D.G., Handy, L. L.: "Comparison of Steady- and Unsteady-State Flow of Gas and Foaming Solution in Porous Media," *SPEJ*, (1989) 4(1), 77-84.

130. De Vries, A.S., Wit, K.: "Rheology of Gas/Water Foam in the Quality Range Relevant to Steam Foam," *SPEJ*, (1990), 5 (2), 185-192.

131. Osterloh, W.T. and Jante, M. J.: "Effects of Gas and liquid Velocity on Steady-State Foam Flow at High Temperature," paper SPE 24179 presented at the 1992 SPE/DOE Enhanced Oil Recovery Symposium, Tulsa, Oklahoma, April 22-24.

132. Alvarez, J. M., Rivas, H. J. and Rossen, W. R.: "Unified Model for Steady-State Foam Behavior at High and Low Foam Qualities," *SPEJ* (September 2001) 325-333.

133. Khatib, Z.I., Ekserova, D.R., and Kruglyakov, P.M.: "Influence of Film Type on Foam Stability," *Colloid J. USSR* (1981)43, 80-84.

134. Khatib, Z.I., Hirasaki, G.J., Falls, A.H.: "Effects of Capillary Pressure on Coalescence and Phase Mobilities in Foams Flowing Through Porous Media," *SPERE*, (August 1988) 919-926.